ABSTRACT

Lithofacies Heterogeneity, Fluvial Style Variations, and Floodplain Vegetation Distributions: Deposition and Diagenesis of the Chinle Formation at Petrified Forest National Park, Arizona

Aislyn M. Trendell, Ph.D.

Committee Chairmen: Stacy C. Atchley, Ph.D., and Lee C. Nordt, Ph.D.

The Upper Triassic Chinle Formation in the Petrified Forest National Park (PFNP) was evaluated using sedimentologic, stratigraphic, paleopedologic and petrographic criteria. The study interval, which includes the Blue Mesa Member and overlying Sonsela Member, consists of paleosol-bearing alluvial strata whose characteristics vary markedly. The Sonsela Member is a fining upward succession that contains a higher proportion of coarse and conglomeratic sandstones than the Blue Mesa. Evidence is presented that suggests that the Sonsela was deposited within a mixed-load fluvial system that was influenced by tectonism. Sonsela sandstones have undergone an almost complete diagenetic loss of porosity due to the precipitation of authigenic clays that likely occurred at or immediately after burial and contemporaneous with the silicification of fossil logs in channel deposits.

The study succession from the Blue Mesa Member to the Sonsela Member records a progressive up-section increase in grain size, increase in channel depth and

width, increase in lateral and vertical connectivity of channel deposits, decrease in overbank preservation and crevasse-splay and/or sheetflood deposition, and increase in paleosol/ overbank drainage. Mean annual precipitation remained stable throughout deposition of the succession despite changing paleosol drainage. These features and an upsection decreasing sandstone mineralogic maturity are consistent with deposition within a progradational large fluvial fan system. Sediment accumulation rates within the study interval suggest decreased subsidence within the upper Blue Mesa Member that may have promoted progradation of the fluvial fan system.

The Sonsela Member contains few paleobotanical fossils other than abundant silicified conifer logs within channel sandstones and, as such, its ecosystem is poorly understood. Sonsela paleosols contain fossilized root traces that provide information regarding plant size and densities. Paleosol maturity suggests that the Sonsela fluvial system experienced high rates of lateral migration and cannibalization of overbank sediments. Fossilized root characteristics suggest that small-stature plants were living on channel-proximal paleosols while distal floodplain paleosols may have hosted herbaceous understory, small-stature shrubby and fewer arborescent plants. There is little evidence to suggest that Sonsela paleosols hosted a dense coniferous forest and conifer logs may have been sourced from uplands. Rhizohalos within the Sonsela Member appear diagenetic.

Lithofacies Heterogeneity, Fluvial Style Variations, and Floodplain Vegetation Distributions: Deposition and Diagenesis of the Chinle Formation at Petrified Forest National Park, Arizona

by

Aislyn M. Trendell, B.S.

A Dissertation

Approved by the Department of Geology

_____

Steven G. Driese, Ph.D., Department Chair

Submitted to the Graduate Faculty of
Baylor University in partial fulfilment of the
Requirements for the Degree
of
Doctor of Philosophy

Approved by the Dissertation Committee

_____

Stacy C. Atchley, Ph.D., Chairperson

_____

Lee C. Nordt, Ph.D.

_____

Steven G. Driese, Ph.D.

_____

Steve I. Dworkin, Ph.D.

_____

Joseph D. White, Ph.D.

Accepted by the Graduate School
December 2012

_____

J. Larry Lyon, Ph.D., Dean

Page bearing signatures is kept on file in the Graduate School.

TABLE OF CONTENTS

LIST OF FIGURES

LIST OF TABLES

ACKNOWLEDGMENTS

Primarily, I must thank my co-advisers, Drs. Stacy Atchley and Lee Nordt, who provided guidance and endured countless revisions with patience and persistence. Dr. Atchley is a highly-motivated, intelligent and on-task individual; leading by example, his high expectations pushed me to discover my potential. Working with such a knowledgeable, perceptive, and fun individual has both enriched and enabled my success. Dr. Nordt's passion for his work was very motivating; despite time constraints, he continues to publish at a rate that speaks to his commitment to his work. It has been a privilege to work with such a deeply intelligent, world-class researcher.

In addition to my advisors, I was lucky to work with many other faculty at Baylor, including my committee, Dr. Steven Driese, Dr. Stephen Dworkin, and Dr. Joseph White. Their thoughtful discussion and manuscript reviews enhanced the quality of my written work. Dr. Driese's classes provided me with much of the knowledge I needed for my dissertation. He is a patient and kind person whose thorough nature makes him a great educator. Dr. Dworkin has enthusiastically taught me in numerous classes and has supported me through countless impromptu discussions. His passion for his research is contagious, and his dynamic perspective was invaluable in the progression of my work. Dr. White, although not a geologist by trade, used his incredible critical-thinking skills to give me new perspective on all of my papers.

Nothing passes time (and digging) like great company: thanks to my two field assistants, Emyris E. Lane and Gaby I. Keeton for spending months in the Petrified

Forest National Park in extreme weather conditions and (sometimes) intimidating topography. Calibration of the study area to the most recent lithostratigraphic nomenclature was provided by William G. Parker and Jeffrey W. Martz of Petrified Forest National Park.

Paulette Penney, Erin Stinchcomb, Janelle Atchley and Jamie Ruth were the 'heart' of the department for all my tenure here. The department would grind to a halt without them. I cannot thank them enough for their friendships and support.

My father, Glenn Trendell, has always been a source of inspiration and support. His sacrifices have allowed me to pursue my goals without constraint. My mother, Jan Doyle, believed in me and when I lacked confidence, I simply had to call her. I thank my sisters, Karli, Sydney, and Caitlin, for their friendships and support. My friends and peers have enriched my life at Baylor both academically and socially. Together, we struggled through classes, writing, and revisions to keep each other on track.

Financial support for this study was provided by the Petroleum Research Fund administered by the American Chemical Society via grant PRF #45548-AC8, Southwest Section AAPG Graduate Student Scholarship (2008, 2010), Rocky Mountain Association of Petroleum Geologists(2010), Norman H. Foster Award (2010), Geological Society of America Graduate Research Grant (2008), Desk and Derrick Club Educational Trust Scholarship (2008), Fort Worth Geological Society Scholarship (2008), Baylor University Department of Geology Research Grant (2008) and the James W. Dixon Undergrad Field Assistant Scholarship (2008). Permission to conduct research was provided by permit # PEFO-2009-SCI-0007 as granted by the administration of Petrified Forest National Park.

"We shall not cease from exploration
And the end of all our exploring
Will be to arrive where we started
And know the place for the first time."

~ T.S. Eliot, *Four Quartets*

CHAPTER ONE

Introduction

The Upper Triassic Chinle Formation consists of continental strata deposited within predominantly fluvial environments and more minor lacustrine and palustrine settings (Stewart et al., 1972; Gubitosa, 1981; Blakey and Gubitosa, 1983; Dubiel et al., 1991; Dubiel, 1994). Chinle fluvial systems were highly variable and evolved between bedload and suspended-load transport through time, undergoing several periods of incision and aggradation (Stewart et al., 1972; Blakey, 1974; Kraus and Middleton, 1987; Demko, 1995; Dubiel et al., 1999; Woody, 2006; Beer, 2005). Discontinuous exposures (Stewart et al., 1972; Blakey and Gubitosa, 1983), geographically limited sediment packages (Kraus and Middleton, 1987; Demko et al., 1998; Dubiel et al., 1999; Dubiel and Hasiotis, 2011), and considerable missing strata that record time (Ramezani et al., 2011) have made regional correlations and interpretation of the mechanisms accounting for depositional variation difficult (Dubiel, 1994; Martz and Parker, 2010).

Chinle outcrops considered for this study include portions of the Blue Mesa through Sonsela Members of the Chinle exposed within the Petrified Forest National Park (PFNP). The study interval includes both mudrock-dominated intervals interpreted to represent deposition within high-sinuosity fluvial systems and sandstone-dominated intervals interpreted to have been deposited within low-sinuosity fluvial systems (Deacon, 1990; Demko, 1995; Woody, 2006). Detritus from this interval may have originated from a major source area to the south (Stewart, 1969; Stewart et al., 1972;

Blakey and Gubitosa, 1983; Stewart et al., 1986). Recent lithostratigraphic studies of the Chinle Formation within the Petrified Forest National Park (Martz and Parker, 2010) provide a geochronologically well-constrained record of fluvial deposition spanning 17 Ma (Ramezani et al., 2011) and well-exposed paleosols within the study succession provide information regarding the climatic regime that prevailed during deposition.

The overall objective of this research is to combine paleoclimatic (via paleosols), fluvial sedimentologic, petrographic and micromorphologic data to better understand the depositional processes and forcing mechanisms that may account for evolving fluvial deposition and floodplain environments throughout the study interval. This research focuses on three different aspects of this goal: 1) investigation of potential depositional and diagenetic forcing mechanisms that resulted in lithologic heterogeneity within the Sonsela Member; 2) determination of a depositional model that may account for fluvial, pedogenic, petrographic and climatic characteristics throughout the study interval (from the lower Blue Mesa Member through the lower Sonsela Member); and 3) investigation of Sonsela floodplain vegetation distributions, as determined from drab haloed root traces, and an exploration into environmental factors that resulted in these vegetation patterns.

Unlike the fine-grained floodplain deposits that characterize the majority of the Chinle Formation, the Sonsela includes a higher proportion of coarse and conglomeratic sandstones interpreted as mixed-load and/or low-sinuosity bedload fluvial deposits (Woody, 2006). Outcrops of the Upper Triassic Sonsela Member of the Chinle Formation at Petrified Forest National Park (PFNP) are ideal for investigation of depositional and diagenetic causes of lithologic variability because they are exceptionally

well-exposed, have undergone little structural deformation, and include interbedded paleosols that constrain the climatic conditions that prevailed during alluvial deposition. Additionally, sandstones of the Sonsela Member are mineralogically immature and have undergone several diagenetic phases which offer insight into the relationship between burial diagenesis and sandstone alteration. In Chapter Two, we use an interdisciplinary approach that includes sedimentologic, paleopedologic, and petrographic data to establish hypotheses that may explain depositional and diagenetic controls on Sonsela lithofacies and fluvial style variability.

Recent literature suggests that modern non-marine, low-relief alluvial plains in foreland basins similar to the Chinle Basin have been identified as containing 'large fluvial fans' (also referred to as megafans, large alluvial fans, wet alluvial fans, fluvial distributary systems, and distributive fluvial systems in the literature; Geddes, 1960; Wells and Dorr, 1987b; Singh et al., 1993; DeCelles and Cavazza, 1999; Shukla et al., 2001; Leier et al., 2005; Fisher et al., 2007; Hampton and Horton, 2007; Weissmann et al., 2010) in addition to alluvial fans (DeCelles and Cavazza, 1999; Horton and DeCelles, 2001) and tributary fluvial systems (DeCelles and Cavazza, 1999; Hartley et al., 2010; Weissmann et al., 2010; Weissmann et al., 2011). Large fluvial fans are distinct from alluvial fans and tributary fluvial systems in terms of their sizes, slopes, textural ranges, and depositional processes (Singh et al., 1993; Stanistreet and McCarthy, 1993; Shukla et al., 2001; Weissmann et al., 2011). With increased understanding of the variety of depositional systems and processes within continental basins, it is prudent to be aware of such models when examining continental successions such as the Chinle Formation. In Chapter Three, sedimentologic, paleopedologic, and petrographic data are used to

evaluate whether the study interval at the Petrified Forest National Park (PFNP) was deposited within distributary or tributary fluvial systems, determine potential controls on varying pedogenic (paleosol) characteristics, and discuss potential depositional models that can account for the fluvial succession.

The Sonsela Member within PFNP contains abundant, spectacularly preserved silicified logs within fluvial channels (Daugherty, 1941; Ash, 1972; Demko, 1995; Ash and Creber, 2000; Creber and Ash, 2004). From this, some authors have interpreted that coniferous forests inhabited the Sonsela floodplain ecosystem (Demko, 1995) and that paleosol characteristics may have been similar to modern Alfisols (Retallack, 1997). Conifers, however, are only very rarely preserved *in-situ* within the lower Sonsela (W. Parker, personal communication, 2012), and channel logs rarely have roots and branches preserved, suggesting that logs may have been abraded during transportation for an undeterminable distance from an upstream source area (Demko, 1995). Contrary to previous interpretations, paleosol characteristics within this research suggest that paleosols are more similar to modern Vertisols and Inceptisols. Other than conifer logs, no other plant remains are preserved within the Sonsela Member (Demko et al., 1998) and as such, the Sonsela plant ecosystem is not well understood. Because plant populations are both influenced by and alter soil characteristics (Brady and Weil, 2001), it follows that plant size, growth habits and lateral distributions may be inferred from paleosols. Chapter Four is an investigation into Sonsela floodplain vegetation that uses detailed paleosol morphological, geochemical, and micromorphological characteristics analyzed in conjunction with paleobotanical data, allowing potential reconstruction of plant formations and distributions on the Sonsela paleo-landscape.

CHAPTER TWO

Depositional and diagenetic controls on reservoir attributes within a fluvial outcrop analog: Upper Triassic Sonsela Member of the Chinle Formation, Petrified Forest National Park, Arizona

This chapter published as: Trendell, A.M., Atchley, S.C., and Nordt, L.C., 2012, Depositional and diagenetic controls on reservoir attributes within a fluvial outcrop analog: Upper Triassic Sonsela Member of the Chinle Formation, Petrified Forest National Park, Arizona: AAPG Bulletin, v. 96, no. 4, p. 679–707.

Abstract

The Upper Triassic Sonsela Member of the Chinle Formation in the Petrified Forest National Park (PFNP) was evaluated using sedimentologic, stratigraphic, paleopedologic and petrographic criteria along a continuous 0.5 km outcrop. The study interval consists of interbedded sandstones and mudstones and is composed of a two-tiered hierarchy of cyclic alluvial deposits with bounding paleosols. The succession is composed of 15 fluvial aggradation cycles (FACs) that comprise two fluvial aggradational cycle sets (FAC-Sets). FAC-Sets are composed of architectural elements suggestive of a mixed-load fluvial system that is alternately dominated by bedload deposits and suspended load deposits. A thinning and fining stacking pattern within FAC-Sets is accompanied by an upward increase in pedogenic modification that suggests cycles systematically stack in response to a longer-period decrease in the rate of accommodation gain. Sandstones are classified as litharenites, feldspathic litharenites, and lithic sub-arkoses, and occur within recycled orogen, dissected arc, and transitional arc provenance fields. Sandstone compositional maturity increases upwards through the FAC-Sets. Point-counts of intergranular volume (as a proxy for primary porosity) within

channel facies and subsequent transform to syndepositional permeability provide a 2D depiction of the lateral variability in reservoir quality. Paleosols are weakly to moderately developed and have little stratigraphic variation. These characteristics suggest that climatic fluctuations are not responsible for evolving fluvial depositional style or associated reservoir quality. Trends in sandstone compositional maturity suggest that fluvial stacking patterns and depositional style are related to pulses of tectonism. Sandstones are volcanogenic-rich, and have undergone an almost complete diagenetic loss of porosity due to the precipitation of authigenic clays. Paragenetic reconstruction suggests that porosity loss occurred contemporaneous with the silicification of fossil logs in channel deposits. Log compaction at the time of silicification averaged 9.1% suggesting that log silicification and porosity loss occurred soon after deposition.

Introduction

Outcrops of the Upper Triassic Sonsela Member of the Chinle Formation at Petrified Forest National Park (PFNP) are ideal as subsurface fluvial analogs because they are reservoir-scale (0.5 km long by 25 m thick), have lateral facies relationships that are exceptionally well-exposed, have undergone little structural deformation, and include interbedded paleosols that constrain both chronostratigraphic correlations and the climatic conditions during alluvial deposition. Additionally, sandstones of the Sonsela Member are mineralogically immature and have undergone several diagenetic phases which offer insight into the relationship between burial diagenesis and sandstone alteration. Stratigraphic nomenclature is after Martz and Parker (2010).

Considering the attributes of the Sonsela Member, the objectives of this study are to: 1) evaluate the spatial variability of fluvial facies, architectural elements and paleosols

and relate them to their potential extrinsic and intrinsic controls; 2) determine how these controls relate to corresponding porosity and permeability distributions; 3) determine paragenetic history and timing; and 4) determine the relationship between immature sandstones and the timing and depth of diagenetic porosity reduction.

Previous studies have highlighted the relationship between fluvial sediment supply and base level and how their changes affect the stacking of fluvial deposits (Wright and Marriott, 1993; Shanley and McCabe, 1994). Alluvial successions have been documented to be composed of a three-tier cyclic hierarchy of meter-, decameter-, and hectometer-scale fining-upward deposits with paleosols commonly weathered into their upper boundaries (Beerbower, 1964; Allen, 1978; Bridge, 1984; Kraus, 1987; 2002; Kraus and Aslan, 1999; Atchley et al., 2004; Prochnow et al., 2006; Cleveland et al., 2007). Both intrinsic (individual and sequential avulsion events) and extrinsic (climatic, orogenic, and eustatic) processes have been interpreted to account for this hierarchy (Beerbower, 1964; Allen, 1978; Bridge, 1984; Kraus, 1987; 2002; Wright and Marriott, 1993; Shanley and McCabe, 1994; Kraus and Aslan, 1999; Atchley et al., 2004; Prochnow et al., 2006a; Cleveland et al., 2007).

The characterization of fluvial reservoirs oftentimes utilizes modern and ancient analogs to calibrate numerical models (Miall, 2006). Outcrop analogs are invaluable because they constrain fluvial facies and architectural element geometries, and may provide corollary distributions of porosity and permeability (Aigner et al., 1996; Bridge et al., 2000; Dalrymple, 2001; Miall, 2006; Pranter et al., 2007; Donselaar and Overeem, 2008).

Stratigraphic, paleogeographic and paleoclimatic overview

Upper Triassic deposits of the Chinle Basin are well exposed in badlands across the southwest United States (Figure 2.1). Outcrops within PFNP in north-eastern Arizona include the Upper Carnian Mesa Redondo Member through the Rhaetian Rock Point Formation (Parker, 2006; Woody, 2006; Martz and Parker, 2010; Figure 2.2). This study focuses on the lower portion of the Norian Sonsela Member, including (from base to top) the Camp Butte Beds, the Lot's Wife Beds, and the Jasper Forest/Rainbow Forest Beds (stratigraphic nomenclature after Martz and Parker, 2010; Figure 2.2). Unlike the fine-grained floodplain deposits that characterize the majority of the Chinle Formation, the Sonsela includes a higher proportion of coarse and conglomeratic sandstones interpreted as mixed-load and/or low-sinuosity bedload fluvial deposits (Woody, 2006).

The Chinle Formation is composed of alluvial, lacustrine and eolian strata that were deposited during the Late Triassic in a broad alluvial plain within a large retro-arc basin (Figure 2.3). The Chinle Basin was bounded to the west and southwest by the Cordilleran Magmatic Arc (associated with convergent margin tectonism), to the south by the Mogollan Highlands (related to magmatic-volcanic arc tectonism), and to the northeast and east by the Paleozoic Uncompahgre, Front Range, Pedernal and Amarillo-Wichita foreland uplifts (Figure 2.3; Dickinson, 1981; Marzolf, 1993; Lawton, 1994; DeCelles and Giles, 1996; Dickinson and Gehrels, 2008). Sediments provided to the northwest-trending paleoriver system within the Chinle basin included volcaniclastics that were likely derived from the magmatic arc located to the west or southwest.

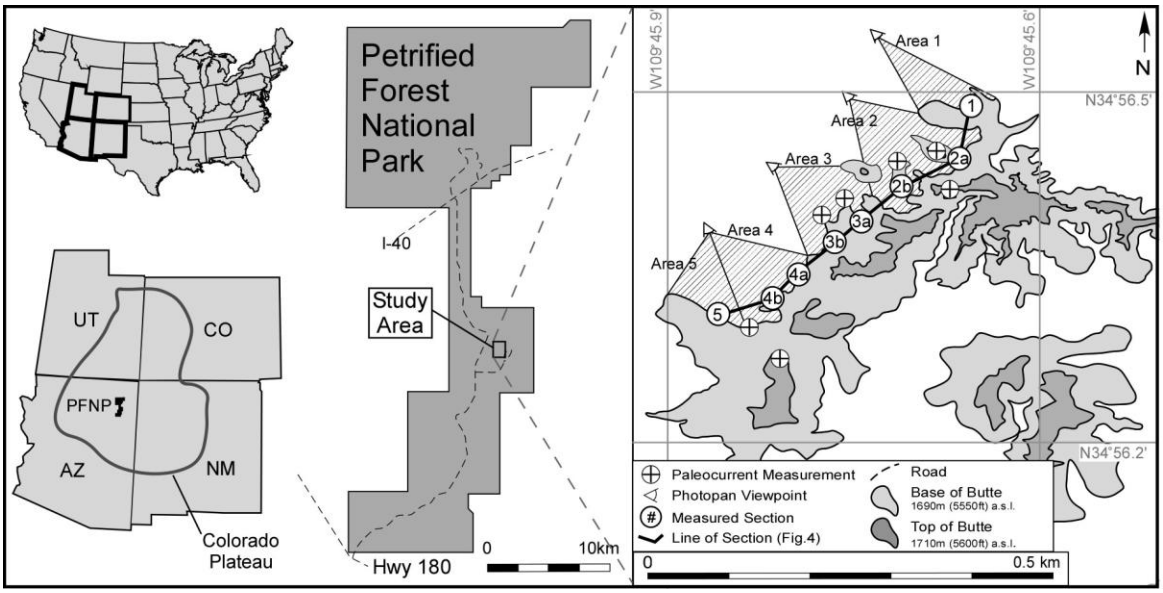

Figure 2.1. Topographic map of the Blue Mesa Overlook study area within Petrified Forest National Park. Elevation contours constrain the outcrop base (1690m [5550ft] above sea level) and top (1710m [5600ft] above sea level). Also highlighted are the location of measured sections (numbers in circles), and viewpoint of photopanoramas (compare with Figures 2.4 and 2.8).

Contributions of sedimentary, metamorphic and igneous rock fragments were likely derived from the Uncompahgre and Front Range uplifts to the northeast and Paleozoic uplifts to the east (Stewart et al., 1972; Bilodeau, 1986; Riggs et al., 1993; 1996; 2003 2009; Dickinson and Gehrels, 2008).

Chinle deposition was likely influenced by climatic, orogenic and potentially eustatic forcing. Climate at PFNP during the Late Triassic was subtropical and strongly seasonal with increasing aridity throughout Chinle deposition (Dubiel, 1987; Kutzbach and Gallimore, 1989; Dubiel et al., 1991; Dubiel and Skipp, 1992; Driese and Mora, 2002; Tanner, 2003; Prochnow, Nordt, et al., 2006; Tanner and Lucas, 2006; Cleveland et al., 2008). Forcing mechanisms such as Milankovitch orbital cyclicity (Olsen and Kent, 1996; 1999), a Pangean mega-monsoon (Kutzbach and Gallimore, 1989; Dubiel et al., 1991), and the gradual drift of present-day North America away from the paleo-equator

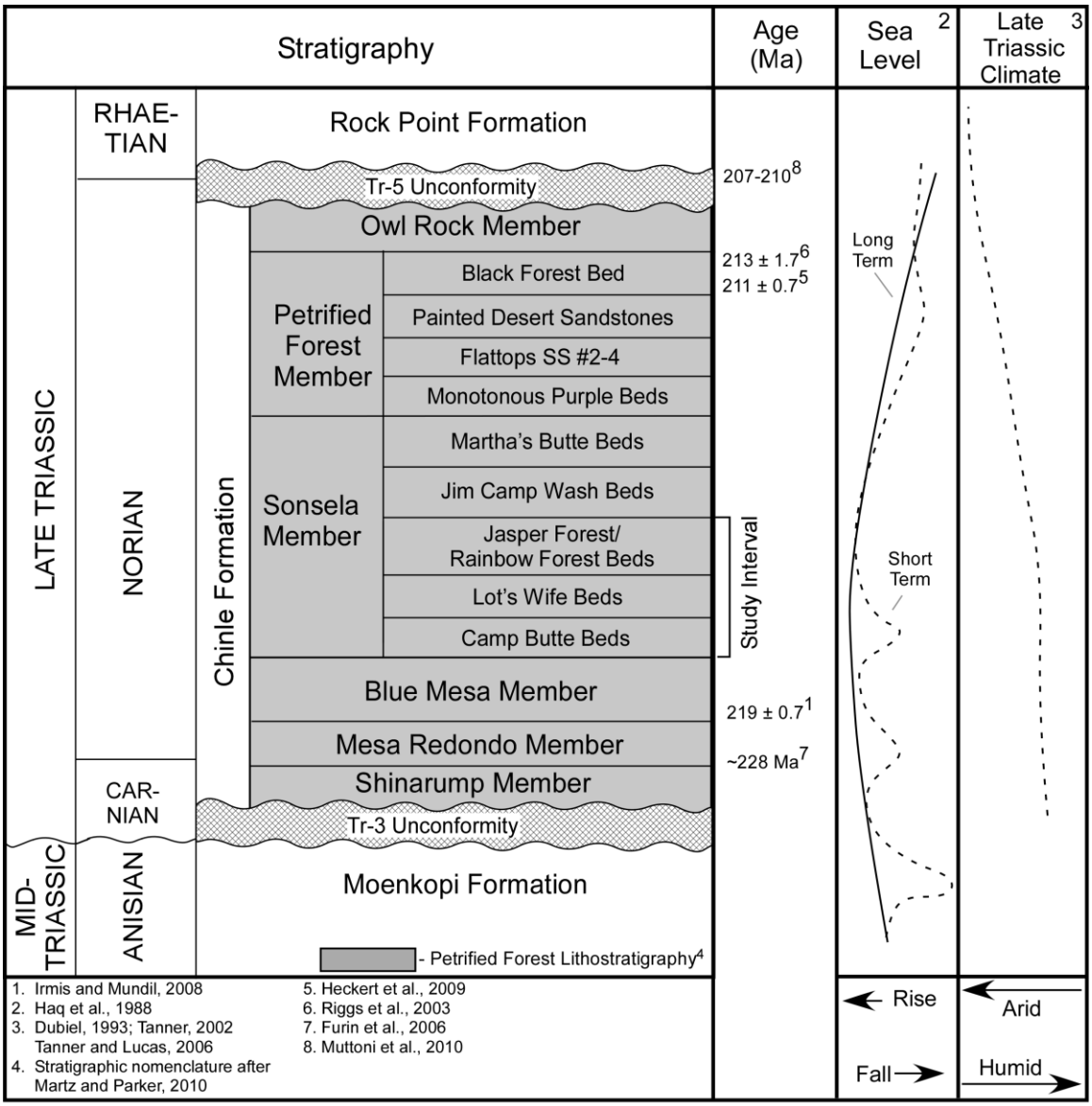

Figure 2.2. Stratigraphic correlation chart of the Petrified Forest National Park (study interval indicated). Information adjacent to the stratigraphic chart summarizes Late Triassic sea level and climate during deposition of the Petrified Forest strata. Stratigraphic nomenclature is after Martz and Parker (2010).

(Kent and Muttoni, 2003; Tanner and Lucas, 2006) created complex climatic conditions. Chinle deposition was also influenced by Cordilleran magmatism and volcanism, basin subsidence, and uplift of surrounding highlands (Riggs et al., 2003). Potential eustatic fluctuations during Sonsela deposition include the composite interference of 2nd and 3rd-order sea-level oscillations (Haq et al., 1988; Figure 2.2).

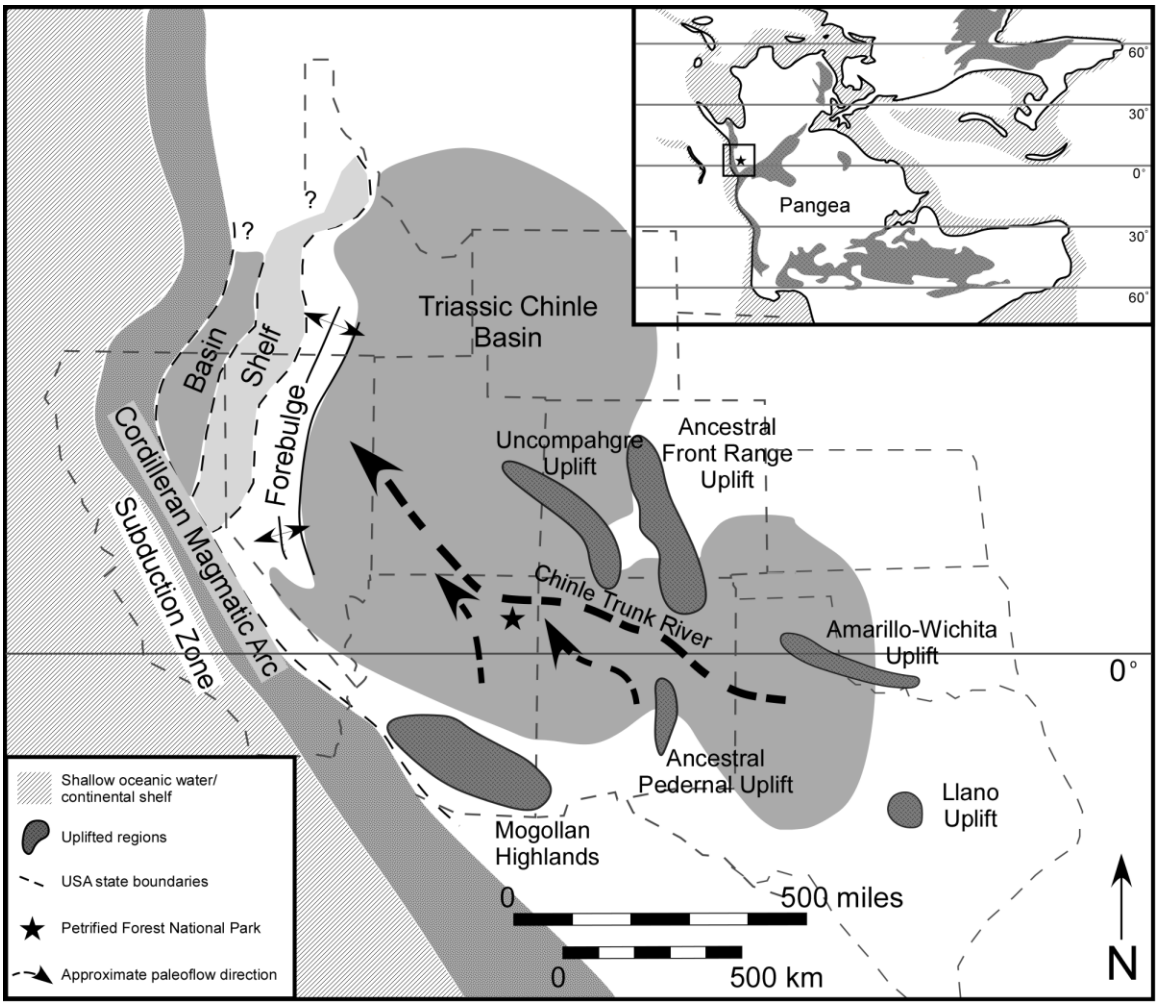

Figure 2.3. Paleogeographic map of the south-western United States showing the location of the study area relative to the Chinle Basin, Chinle Trunk River and major Late Triassic structural features (modified from Riggs et al., 1996; Scotese, 2007).

Methods

Stratigraphic Correlation

The Sonsela outcrop at the PFNP Blue Mesa Overlook is divided into five adjacent areas. The geographic extent of areas 1 to 5 is provided on Figure 2.1. Stratal relationships were traced on photopanoramas of each area and walked-out on outcrop to establish lateral continuity.

Eight outcrop sections were measured. These include documentation of grain size, stratal thickness, sedimentary and biological structures, lithostratigraphic contacts and the stratigraphic location of paleosols (Figures 2.1 and 2.4). Meter-scale fluvial aggradational cycles (FACs) and decameter-scale FAC-sets were identified based on the methodology of Atchley et al. (2004) and Cleveland (2007) (Figure 2.4). Within each measured section, fresh sandstone samples were collected for petrographic analysis by digging down to unaltered rock. Samples represent material from downstream accretion, lateral accretion, massive channel and thin sandy bedform architectural elements (Table 2.1). Correlation of stratal relationships between sections is constrained by laterally extensive paleosol surfaces. At locations where paleosol surfaces are not continuous, a hand-level was used to project surfaces between areas. Surfaces were subsequently walked-out. Through this process, paleosols and facies were interpolated across the entire study area.

Paleosol Description

Within this study, paleosols are used to identify the surfaces of fluvial cycles, characterize relative floodplain aggradation rates and drainage, and interpret climatic variability within the Sonsela succession. Paleosol horizon descriptions follow the standard guidelines of the Soil Survey Staff (1999), Retallack (1988; 2001) and Schoenberger et al. (2002) and include field observations of thickness, matrix color, structure, texture, horizon boundaries, root traces and abundance, size, and type of carbonate, slickensides, and iron concentrations and depletions (Figure 2.5).

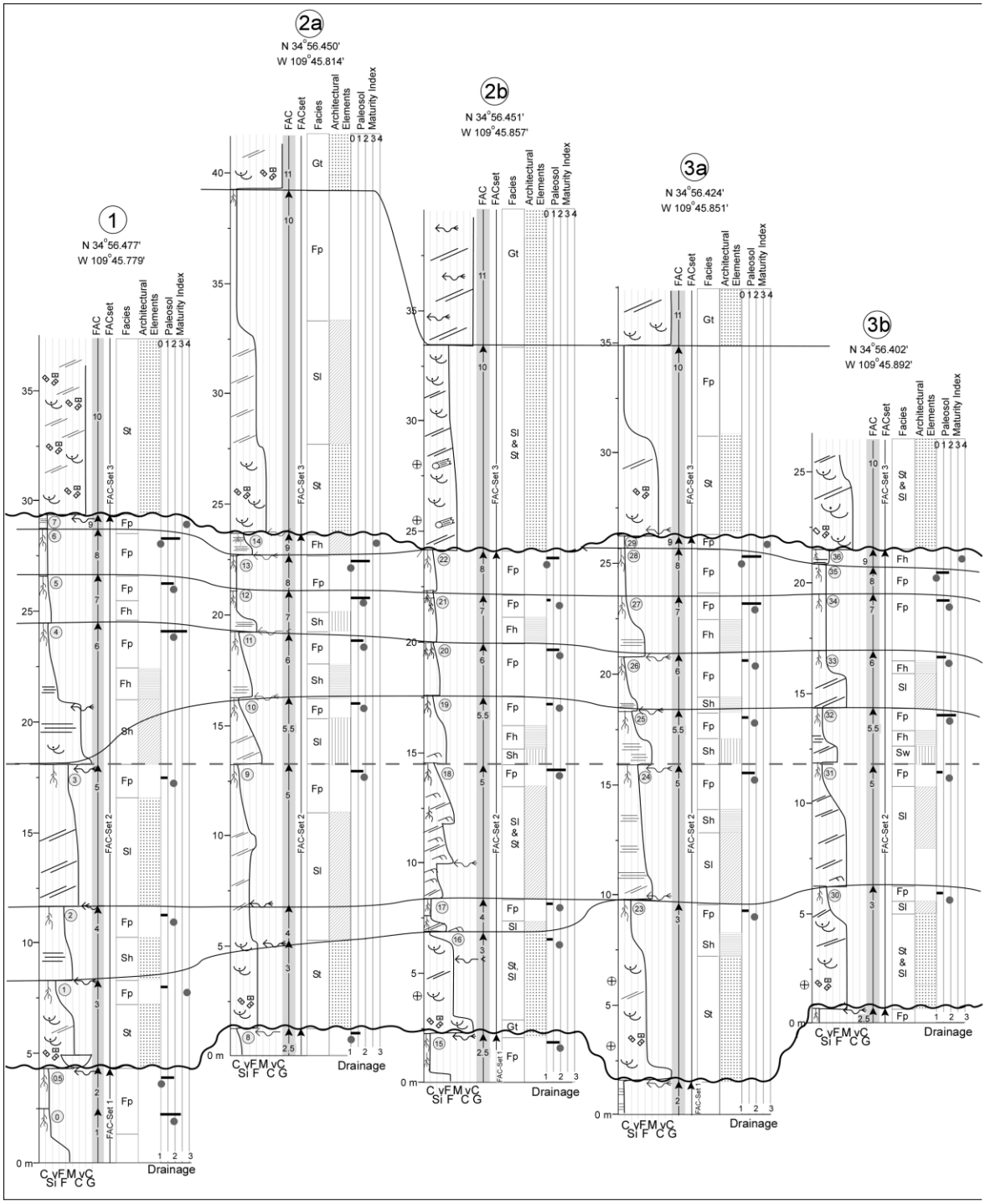

Figure 2.4. Stratigraphic cross-section of the study area (compare to Figure 2.1). The stratigraphic datum is the conspicuously flat-lying and laterally continuous FAC 5 paleosol. The status of paleosol maturity (bars) and drainage (dots) are provided at paleosol locations adjacent to measured sections. Approximate lithostratigraphic boundaries of Martz and Parker (2010) are shown in gray adjacent to measured section 5.

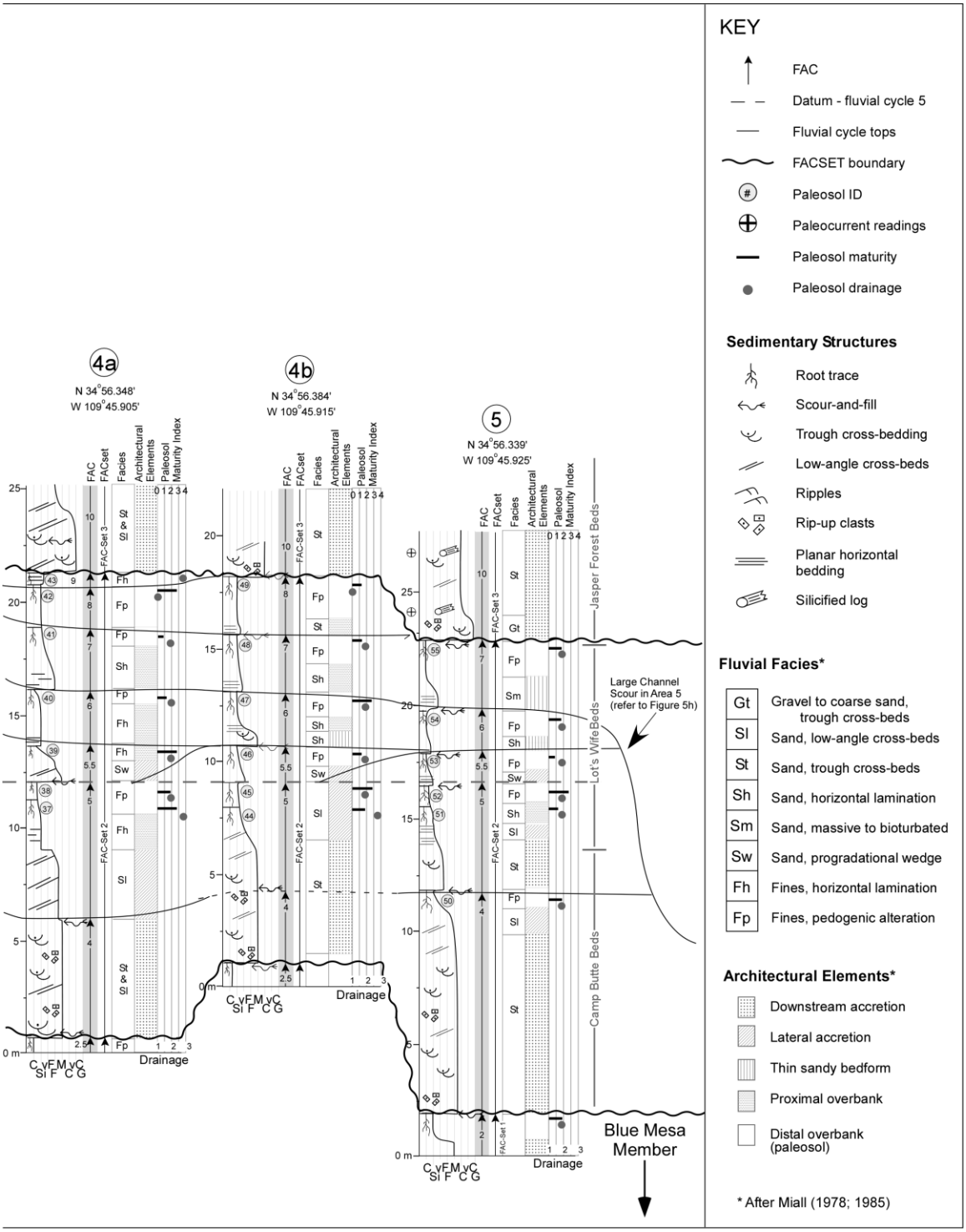

Figure 2.4. Continued.

Table 2.1. Diagnostic attributes of fluvial facies and architectural elements (modified from Miall, 1978; 1985).

Facies	Lithology	Features	Interpretation	Architectural Element
Gt	Gravel	trough cross beds; poorly-sorted gravels to coarse sands; clast supported with abundant matrix	minor channel filling deposit	Downstream accretion
St	Sandstone	trough cross beds; poorly-sorted coarse to medium sand	upper flow regime channel fill deposit, dunes	Downstream accretion; Lateral accretion
Sl	Sandstone	large-scale, low-angle cross beds; coarse to fine sand; fining upwards along beds	point-bar deposit from fluvial migration	Lateral accretion
Sh	Sandstone	horizontally bedded	crevasse splay or non-pedogenically altered overbank deposit	Lateral accretion; Proximal overbank
Sr	Sandstone	ripple laminated	lower flow regime; often found in upper portions of Sl facies	Lateral accretion; Thin sandy bedforms
Sw	Sandstone	progradational wedge with pedogenic alteration along bedding planes; poorly sorted medium to very fine sands	progradational sediment wedge within a channel	Thin sandy bedforms
Fh	Mudstone	laminated and horizontally bedded; very fine sands, silts, and clays; has minor to abundant drab root halos that overprint sedimentary structure.	overbank deposition	Proximal overbank; Thin sandy bedforms
Fp	Mudstone	unstratified; silts and clays; evidence of pedogenic alteration	paleosol	Distal Overbank

Paleosol maturity and drainage are used to evaluate the relative rate and conditions of fluvial aggradation (Atchley et al., 2004). Paleosol maturity and associated landscape stability is qualitatively evaluated by paleosol thickness and polypedogenesis (welding of successive paleosols). Paleosols are assigned a maturity index modified from Retallack's (1988) categorization (Figure 2.6). Color and hydromorphic features are used to evaluate paleosol drainage (Table 2.2). Although some, if not all, colors are a result of

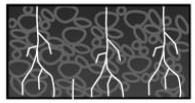	**A**	Ped structure is fine to medium granular and subangular blocky. Has a darker color than other horizons indicating higher organic matter content. Abundant to rare drab root halos. Is the uppermost horizon in a profile, and is commonly truncated, and therefore, poorly preserved.
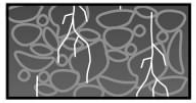	**Bw**	Ped structure is medium to coarse subangular block to angular blocky. Has few to abundant drab root halos. Color is brighter (higher chroma and value) than the overlying and underlying horizons; no other distinguishing characteristics.
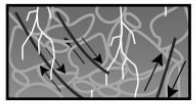	**Bss**	Ped structure is fine to very coarse angular blocky to wedge-shaped. Few to common grooved slickensides are present. Rare to many root traces.
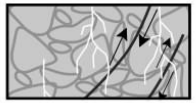	**Bssg**	Fine to very coarse angular blocky to wedge-shaped ped structure. Dominated by drab colors. Has red, purple and blue iron mottles ranging from 2 to 10 cm in diameter. Root traces are rare.
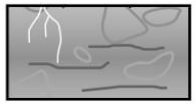	**BC**	Structure is medium to coarse subangular blocky; however, bedding and laminations are present. Root traces are rare to common.
	**C**	All original sedimentary structures are preserved and there is no evidence of pedogenic alteration.

Figure 2.5. Diagnostic attributes of paleosol horizons with illustrations of horizon characteristics.

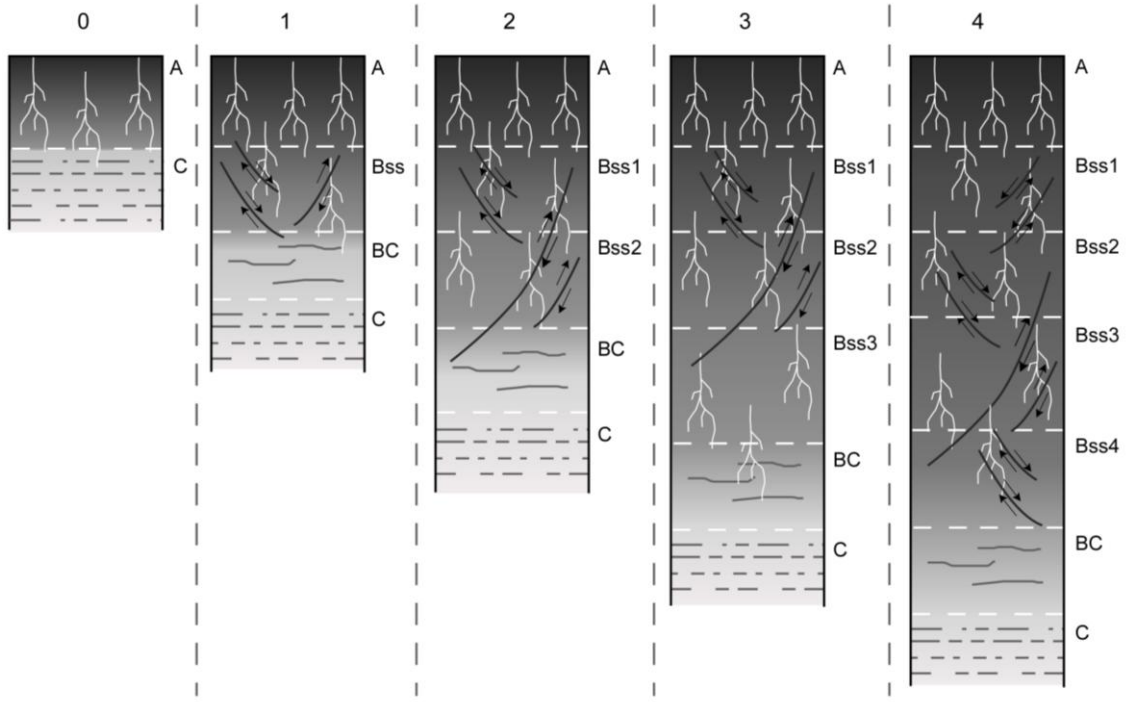

Figure 2.6. Paleosol profiles that represent degrees of pedogenic maturity that are assigned to Sonsela paleosols. Paleosol maturity is based on paleosol thickness and degree of pedogenic alteration of parent material through the study interval. Although paleosols containing Bss horizons are shown here, it should be noted that Bss, Bw and Bg horizons require equal pedogenesis for formation and so the maturity index applies to all paleosols in the study area. It is assumed that welded paleosols with n subhorizons have undergone more pedogenic modification than two single-stacked paleosols, each with n/2 subhorizons, and are assigned a value of n.5. Paleosol maturity is shown on Figure 2.4 as bars adjacent to paleosol locations on measured sections.

diagenetic recrystallization of iron oxides (Retallack, 1991; Blodgett et al., 1993), all paleosols underwent the same diagenetic history, and therefore the presence of several matrix colors in Sonsela paleosols suggests that depositional soil drainage may have influenced resultant diagenetic paleosol color (PiPujol and Buurman, 1994).

Sandstone Petrography

Sandstone petrography was utilized to evaluate possible provenance changes, depositional controls on porosity and permeability, and to reconstruct the timing of diagenetic events.

Thin sections were prepared from twenty-one sandstone specimens and two silicified logs and were point-count analyzed (300 to 500 counts) under plane-polarized and cross-polarized light to determine composition and intergranular volume as a proxy for pre-cementation porosity. Thin sections were stained for potassium and sodium feldspar identification following the methodology of Houghton (1980). The framework compositional classification is after Dickinson and Suczek (1979) and McBride (1963). Thin sections were also examined under UV fluorescence to determine organic matter content (Smith, 1984). Pre-cementation permeability is estimated using the porosity-permeability transform function of (Pape et al., 1999; Pape and Clauser, 2000).

Table 2.2. Paleosol drainage index*

Paleosol Drainage Index	Color Description	Drainage Interpretation	Interpretation Reference
1	Red Munsell colors with chroma >2, 5R 5/3 (weak red), 7.5R 4/3 (weak red), 7.5R 4/4 (weak red), 7.5R 5/3 (weak red), 10R 4/3 (weak red)	Well drained	Soil Survey Staff, 1999
2	Purple Munsell colors with chroma ≤2, 5R 3/1 (dark reddish gray), 5R 4/1 (dark reddish gray), 5R 5/1 (reddish gray)	Moderately drained	Kraus and Hasiotis, 2006
3	Blue 5PB with color chroma = 1 (bluish black)	Poorly drained	Vepraskas, 1992, 2001

* Paleosol drainage is shown in Figure 4 as dots adjacent to paleosol locations on measured sections.

Results

Depositional Facies

Depositional facies observed within the outcrop were classified based on grain size and mechanical and biological structures (Table 2.1; classification after Miall, 1978; 1985). Strata consist of interbedded sandstones and mudstones. Trough-cross stratified (St) and large-scale low-angle horizontal cross stratified (Sl) sandstones are most common (Figures 2.4 and 2.7). Fine-grained facies are horizontally bedded (Sh, Fh) or

structureless due to pedogenic overprint (Fp; Figure 2.7). The basal portion of the succession across the study area is dominated by a thick, amalgamated, laterally-extensive complex of charcoal-bearing sandstone beds (multi-story sandbodies) that include Gt, St and Sl facies with abundant reactivation and scour surfaces (Figure 2.4). Mudrocks are not present within 8 m (~25 ft) of the section base. Overlying strata have increasing proportions of mudrock and decreasing proportions of sandstone (Figures 2.4 and 2.7c). Within the upper portion of this fining-upward succession, sandstones are single-story, thinner and predominantly composed of the Sh and Sl facies (Figure 2.4).

Facies are grouped into downstream- and lateral-accretion, proximal and distal overbank, thin sandy bedform and massive channel architectural elements that are interpreted as channel fill and overbank deposits (Table 2.1; Miall, 1985). The succession of architectural elements within the study interval gradually transitions from downstream and lateral accretion dominated multi-story sandbodies with minimal overbank at the base to thin sandy bedform and overbank at the top (Figure 2.4). This suggests that fluvial style evolved from a bedload system at the section base to a suspended load system at the section top. Channel deposits are uncommon in the upper portion of the section and when present are composed of thin sandy bedform and lateral accretion deposits (Figure 2.4). This pattern is disrupted in the uppermost portion of the section by a truncation surface overlain by bedload (Gt, St) downstream accretion deposits (Figure 2.4).

Paleocurrent data obtained from channel deposits at the base and top of the succession were plotted on rose-diagrams to evaluate flow direction. Average paleocurrent direction at the section base is 104˚E, and 93˚E at the section top.

Paleocurrent observation locations are provided on Figure 2.1. Paleocurrent data suggest that a significant change in flow direction between the section base and top likely did not occur. Previously published paleocurrents from the Sonsela similarly indicate northeastward to southeastward flow (Woody, 2006).

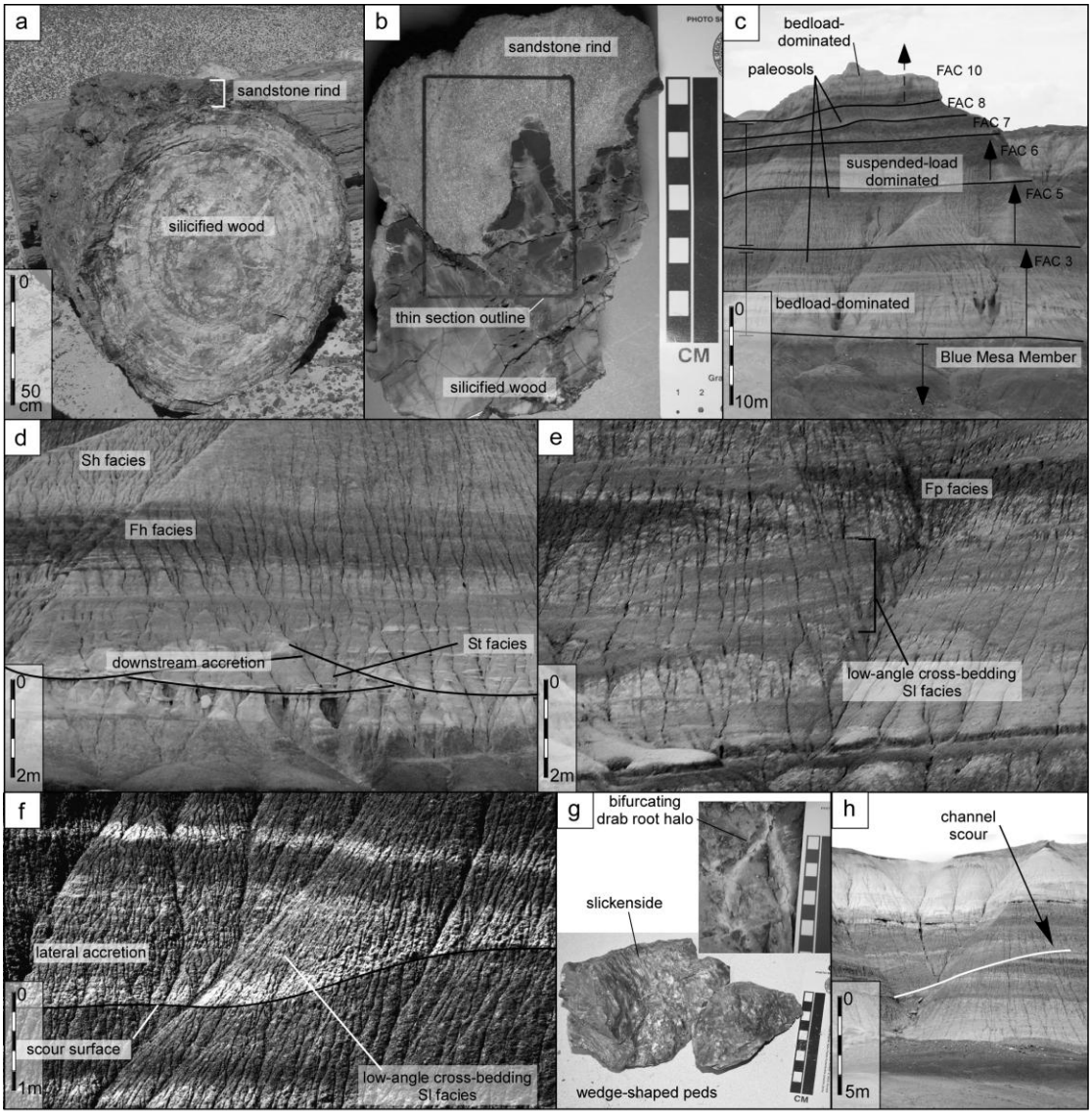

Figure 2.7. Photographs of sedimentary features: a) Silicified log with sandstone rind; b) Hand sample of sandstone rind and silicified wood. Thin section outline is shown by a black rectangle. Photomicrographs of this thin section are shown in Figure 2.10; c) Sonsela interval showing the stratigraphic distribution of depositional features and paleosols; d) St, Fh and Sh facies and downstream accretion architectural element; e) Sl and Fp facies; f) Sl facies and lateral accretion architectural element; g) Wedge-shaped peds and drab root halos from Sonsela paleosols; H) Sonsela Interval at Area 5 with large channel scour within FAC 7 truncating several underlying FACs.

Paleosols

In contrast to findings from previous studies of Sonsela paleosols at PFNP, no horizons with stage II through IV calcretes (Tanner and Lucas, 2006) or illuviated clay enrichment (Retallack, 1997) in subsurface horizons are observed. The most common features include ped structure, root traces and slickensides (Figure 2.7g). Root traces range in diameter from 1mm to 5cm and have morphologies that vary from downward and bifurcating traces that taper with depth to those that follow ped-boundaries. Root density and size are variable, but do not display systematic trends related to paleosol stratigraphic position. Slickensides range from few to many and include small to master slickensides. Grain size ranges from silty clay to clay, with decreasing silt upwards through a paleosol.

Pedogenic features that require significant periods of time to form, such as carbonate nodules or clay cutans (Retallack, 2001; 2005), are not present within these paleosols and suggest relative immaturity and high floodplain aggradation rates or rapid lateral channel migration and overbank cannibalization. Variations in paleosol maturity are reflected primarily in paleosol thickness, horizonation, and ped structure. Paleosol thicknesses range from <1m to 2m, with increasing thickness and polypedogenesis upwards in the section (Figure 2.4). The most commonly observed subsurface horizons are Bw and Bss (Figure 2.5), both of which require a similar degree of pedogenesis to form. The Bw horizons, however, form in more silty sediments with less shrink-swell potential. Paleosols increasingly have Bss horizons upwards in the section. Ped structure in these paleosols include subangular blocky, angular blocky, and wedge-shaped peds (Figure 2.7g). Morphological characteristics suggest they may be similar to modern well-

and poorly-drained non-calcareous Entisols (have original bedding and no subsurface horizons), Inceptisols (have subsurface horizons) and Vertisols (have subsurface horizons, high shrink-swell capacity, and slickensides) that formed within a subhumid to humid climate (Soil Survey Staff, 1999). Paleosol maturity varies along each paleosol surface (FAC surface); however, there is an overall trend of increasing paleosol maturity upward through the study interval (Figures 2.4).

Paleosols are predominantly purple in color, with lesser red and blue paleosols, suggesting variability in paleosol drainage (Figure 2.4; Table 2.2). Colors vary within texture classes, suggesting no relation between color and paleosol grain size. Purple matrix colors are interpreted as post-burial diagenetic color alteration from an unknown soil color, inasmuch as purple is not a modern soil matrix color (Retallack, 1991; Soil Survey Staff, 1999; Kraus and Hasiotis, 2006). Paleosols in proximal overbank positions are more commonly red (7.5R 5/2 and 10R 4/2 Munsell color), and are interpreted as moderately well-drained (Vepraskas, 1992; 2001). Paleosols in more distal overbank positions are commonly purple in color (5R 3/1, 4/1 and 5/1 Munsell color), which is interpreted to reflect moderate to poor drainage (Kraus and Hasiotis, 2006). Blue or drab paleosols occur only at the top of the succession. This color may indicate saturated, anoxic conditions and Fe reduction (Vepraskas, 1992; 2001).

Stratal Framework

Blue Mesa - Sonsela Member Contact and Characteristics. The Sonsela Member disconformably overlies fine-grained, pedogenically altered mudrocks of the Blue Mesa Member (FACs 1, 2 and 2.5; FAC-Set 1; Figure 2.4). The absence of upper soil horizons

in the Blue Mesa paleosols beneath the uneven surface of the Blue Mesa-Sonsela contact suggests erosional truncation. Above this abrupt contact, the succession consists of nine fining-upward FACs that stack into a longer-period fining-upward trend (Figures 2.4). From the basal to uppermost erosional contacts of the study interval, FACs exhibit an overall decrease in thickness, channel facies proportions and grain size, and increase in the proportion of fine-grained overbank deposits (Figure 2.4). This thinning- and fining-upward FAC succession above the Blue Mesa Member is classified as FAC-Set 2. FAC-Set 2 is erosionally truncated beneath FAC 10, which is the base of FAC-Set 3 (Figures 2.4).

FACs 2 and 2.5 (FAC-Set 1) are pedogenically modified overbank deposits of the Blue Mesa Member (Figure 2.4). Associated paleosols are relatively mature, with average maturity indices of 3, 2, and 1.8, respectively, and are blue in color. These attributes suggest iron reduction due to water saturation of the soil profile (Figure 2.4). The boundary between FACs 2.5 and FAC 3 marks the base of the Sonsela Member.

Sonsela Member Fluvial Aggradation Cycles. FACs 3 and 4 (Camp Butte Beds lithostratigraphic unit) are difficult to trace laterally due to amalgamation across intrachannel scour surfaces. FACs 3 and 4 have a high proportion of sand, i.e., 90% sand and 10% mud, and consist of fine to very coarse-grained sandstone. Deposits within FACs 3 and 4 include downstream accretion, lateral accretion, and discontinuous proximal overbank deposits (Figures 2.4 and 2.8). These FACs consist of approximately 85% downstream and lateral accretion sandstones that are thick and continuous across the outcrop. Paleosols weathered into the top of these FACs are discontinuous and truncated by adjacent channel facies (Figure 2.8). This suggests the paleosols were developed on

overbank deposits located adjacent to laterally migrating channels. Paleosols atop FACs 3 and 4 are 1 to 1.5 m in thickness and are classified as poorly developed (average maturity index of 1 and 1.3, respectively).

Above FAC 4, there is a notable change in architectural element proportions and decrease in inter- and intra-cycle erosion (Lot's Wife Beds lithostratigraphic unit; Figure 2.8). FACs 5, 5.5 and 6 are dominated by lateral accretion, thin sandy bedform, proximal overbank and distal overbank deposits (Figures 2.4 and 2.8). The succession of architectural elements from FACs 4 to 5 suggests that fluvial style changed from bedload to suspended load. FACs 5, 5.5 and 6 have a lower proportion of sand (40% sand and 60% mud), and sandstones are finer-grained and more thinly bedded (Figure 2.8). Paleosols atop these FACs are laterally continuous and more mature (average maturity index of 2.1, 1.7, and 2.1, respectively; Figures 2.4). Laterally within each of these FACs, the ratio of overbank to channel architectural elements varies inversely with channel sand thickness (Figure 2.4).

FAC 6 is overlain by a thin (approximately 35 cm thick), weakly stratified, poorly sorted, very fine grained sandstone that is interpreted as a thin sandy bedform at the base of FAC 7 (Figure 2.4). This continuous and invariant deposit is truncated by a channel scour that is filled with a 15 m thick, very fine, poorly-sorted, massive sand (Figures 2.4 and 2.7h). The margin of this channel occurs in Area 5 and truncates FACs 4 through 6. This is the only channel preserved within FACs 5 -9 and is filled with massive sand rather than downstream accretion and lateral accretion observed in FACs 3-4. The paleosol weathered into the top of FAC 7 also extends across this channel within Area 5. The paleosol atop FAC 7 is more poorly developed (average maturity index of 1.88) than

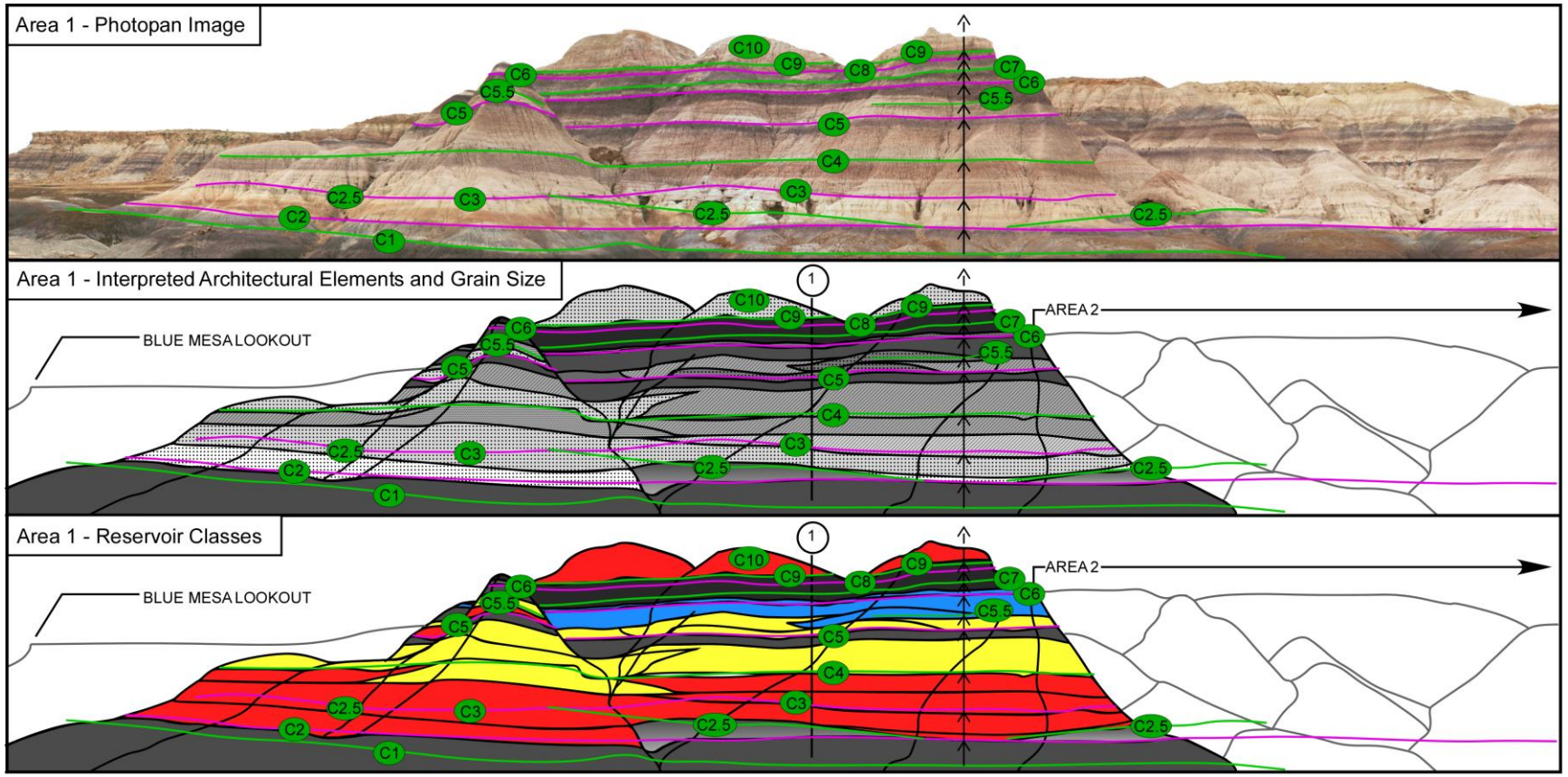

Figure 2.8A. Photopanoramas of area 1, highlighted with reservoir quality classes. FAC surfaces are labeled across outcrop.

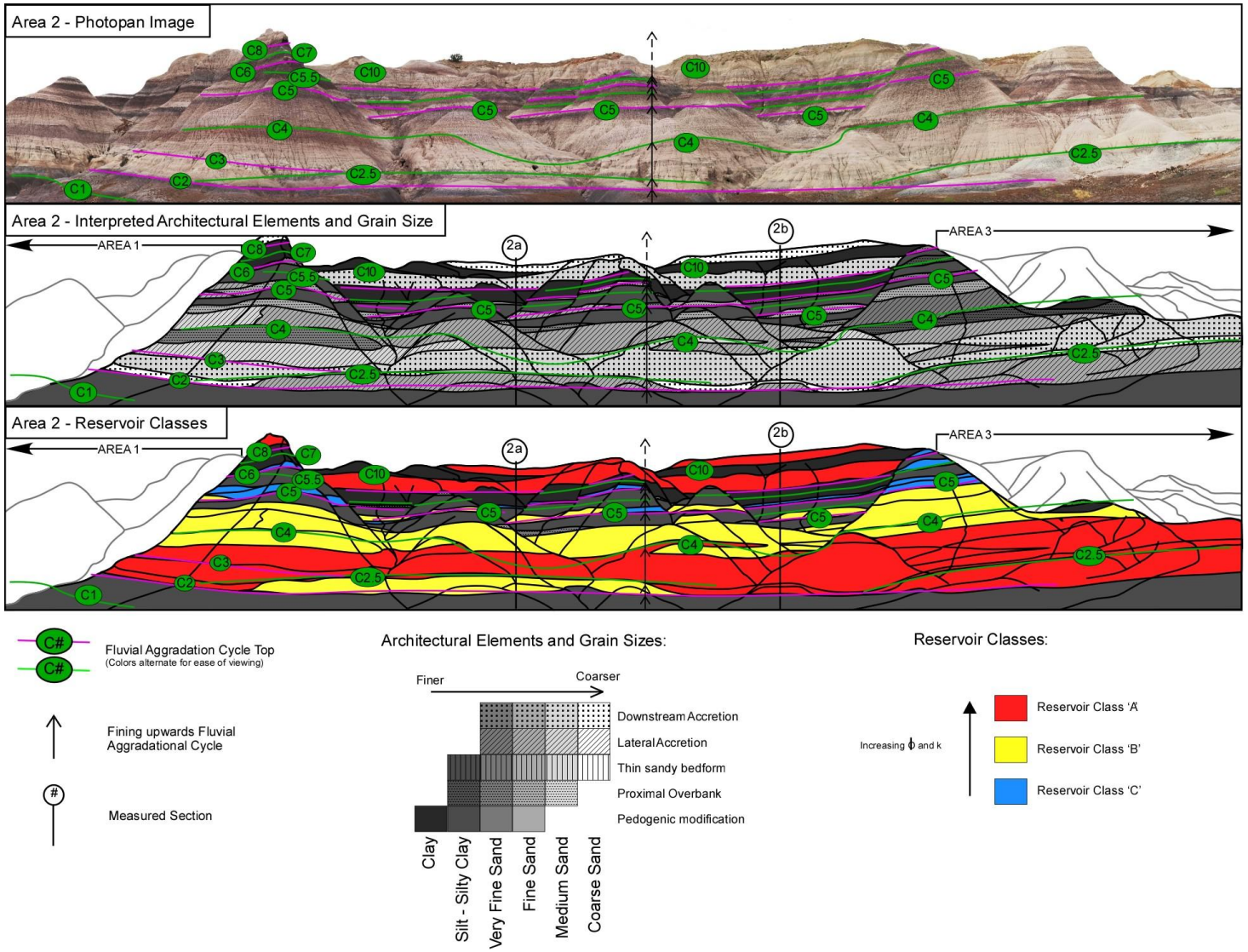

Figure 2.8.B. Photopanoramas of area 2, highlighted with reservoir quality classes. FAC surfaces are labeled across outcrop.

paleosols above both FAC 6 and 8 due to its proximity to a paleochannel. FAC 8 is composed of pedogenically modified silty claystone to claystone welded into FAC 7 and is recognized by a pronounced change in paleosol color from purple (FAC 7) to blue (FAC 8; Figure 2.8). The paleosol atop FAC 8 has well-developed prominent slickensides, wedge-shaped peds, and abundant drab root halos and is the most mature and continuous of the paleosols weathered into FACs in this succession (average maturity index of 2.8). The blue color suggests iron reduction due to poorly-drained hydromorphic conditions (Vepraskas, 1992; 2001).

FAC 9 is predominantly composed of laminated fine to very fine sandstone with abundant drab root halos and is interpreted as proximal overbank deposits with minor pedogenic overprint (Figure 2.4). FAC 10 is similar to FACs 3 and 4 (Jasper Forest Beds lithostratigraphic unit; Figures 2.4 and 2.8). FAC 10 has an erosional base, approximately 85-90% sandstone and consists of downstream accretion deposits with discontinuous overbank mudrock and paleosols.

Sandstone Petrography

Of the twenty-one thin-sections that were point-counted, eleven were sampled from downstream accretion sandstones, six from lateral accretion sandstones, three from thin sandy bedforms and one from a massive channel sandstone. Quartz-Feldspar-Lithic (QFL) modal percentages were used to determine sandstone composition and to evaluate provenance (Table 2.3; Figure 2.9; Dickinson and Suczek, 1979). Petrographic data are plotted by the stratigraphic position of samples to evaluate trends in composition, and therefore provenance, through time (Figure 2.9). Sandstones are classified as litharenites, feldspathic litharenites, and lithic sub-arkoses (*sensu* McBride, 1963), and occur within

the recycled orogen, dissected arc, and transitional arc fields of Dickinson and Suczek (1979; Figure 2.9). QFL values are consistent with previous published Sonsela sandstone compositions (Dickinson and Gehrels, 2008). Sandstones have high proportions of quartz and lithic grains (altered volcanogenic sediments and hydrated volcanic glass, metamorphic and plutonic igneous lithic grains), and include abundant authigenic clay within the intergranular volume (Figures 2.10 and 2.11). Sandstone compositional maturity increases upwards through FACs 3-7 where the base of FAC-Set 2 is characterized by feldspathic litharenites and the top is characterized by lithic sub-arkoses and subarkoses (Figure 2.9). Mineralogical maturity abruptly decreases to litharenite within FAC 10 (base FAC-Set 3; Figure 2.9). Sandstones at the base of both FAC-Set 2 and FAC-Set 3 have between 40-60% lithic grains, whereas sandstones within FAC 7 (the upper portion of FAC-Set1) have only 10-30% lithic grains. A sandstone from the FAC 7 channel in Area 5 is coarser-grained and exhibits relative compositional maturity similar to other finer-grained FAC 7 sandstones (Figure 2.9). This suggests maturity trends may be independent of grain size.

Diagenesis

Strata within Petrified Forest National Park have been buried beneath a minimum of 2.5 to 2.8 km of sediment (AAPG, 1988). Petrographic evaluation of Sonsela sandstone thin sections indicates at least eight diagenetic events (Figure 2.12).

Table 2.3. Point-count data and permeability values of all sandstone thin sections.

Diagenetic products include pervasive authigenic clays, several zeolite phases, sericitized feldspars, silica cement and minor calcite, chlorite, and hematite cements (Figures 2.10 and 2.11). Sandstone porosity is completely occluded by diagenetic products. The

Table 2.2. Paleosol drainage index (Paleosol drainage is shown in Figure 4 as dots adjacent to paleosol locations on measured section).

Paleosol Drainage Index	Color Description	Drainage Interpretation	Interpretation Reference
1	**Red** Munsell colors with chroma >2 5R 5/3 (weak red), 7.5R 4/3 (weak red), 7.5R 4/4 (weak red), 7.5R 5/3 (weak red), 10R 4/3 (weak red)	Well drained	Soil Survey Staff, 1999
2	**Purple** Munsell colors with chroma ≤ 2 5R 3/1 (dark reddish gray), 5R 4/1 (dark reddish gray), 5R 5/1 (reddish gray)	Moderately drained	Kraus and Hasiotis, 2006
3	**Blue** 5PB with color chroma = 1 (Bluish black)	Poorly drained	Vepraskas, 1992; 2001

* Row contains average and median (permeability) values for each architectural element. Note that the first nine columns contain data, and the last column contains interpreted values.
**Estimation is based on an empirical formula developed by Pape et al. (1999, 2000).

dominant pore-occluding diagenetic phase is authigenic clay (Figure 2.11). Authigenic characteristics (Figure 2.11). Authigenic clays have two crystallographic forms. Most commonly, they are identified by their high-order yellow colors in cross-polarized light, aligned book-like crystallet orientation, and growth on grain surfaces and in available pore spaces (Figure 2.10g and 2.11). Less commonly, authigenic clays are very fine grained, have sweeping extinction and low-order gray colors (Figure 2.11-1). Devitrified volcanic rock fragments, on the other hand, have clear, definable boundaries (most obvious in plane-polarized light; Figures 2.11-1c and 2.11-2c) with fine-grained internal fabrics that are disorganized and blotchy and contain ghosts or laths of feldspars and quartz (Figure 2.11). Authigenic clay volume (from point-count analysis) ranges from 16 – 41% (average 30%), values consistent with the intergranular volume of unconsolidated sands (Beard and Weyl, 1973; Nagtegaal, 1978), and suggesting minimal burial compaction prior to early cementation. X-ray diffraction indicates that Sonsela sandstone authigenic clays consist of montmorillonite and interlayer illite (Sigleo, 1979).

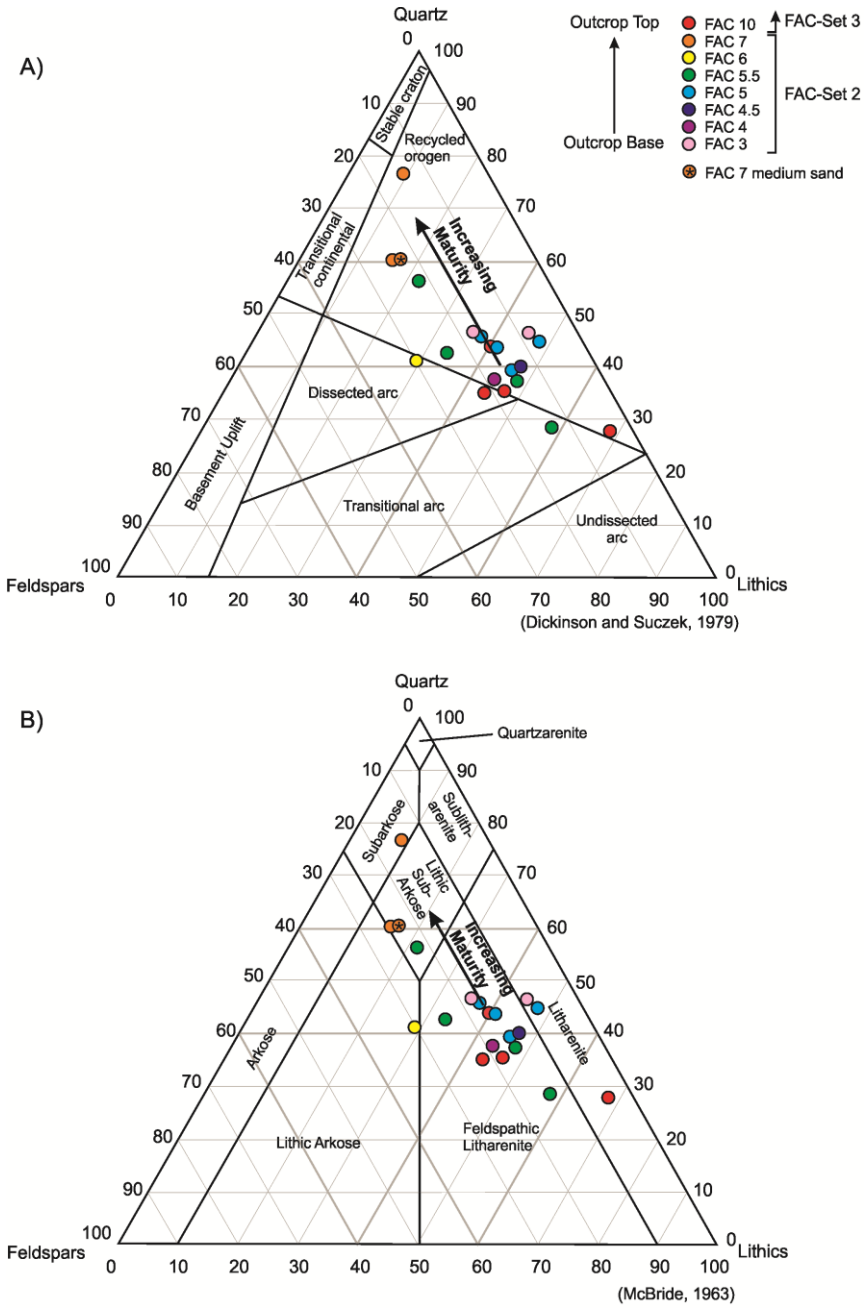

Figure 2.9. Sandstone compositional ternary diagrams for A) provenance (Dickinson and Suczek, 1979), and B) sandstone classification (McBride, 1963). Data are sorted by FAC. Data indicate that FAC compositional maturity increases upsection within FAC-Set 2 and abruptly decreases at the base of FAC-Set 3.

Volcanogenic devitrification processes result in the formation of montmorillonite and illite clay and excess silica (Murata, 1940; Sigleo, 1979). Devitrification of volcanogenic sediments in Sonsela sandstones likely resulted in the precipitation of authigenic clays

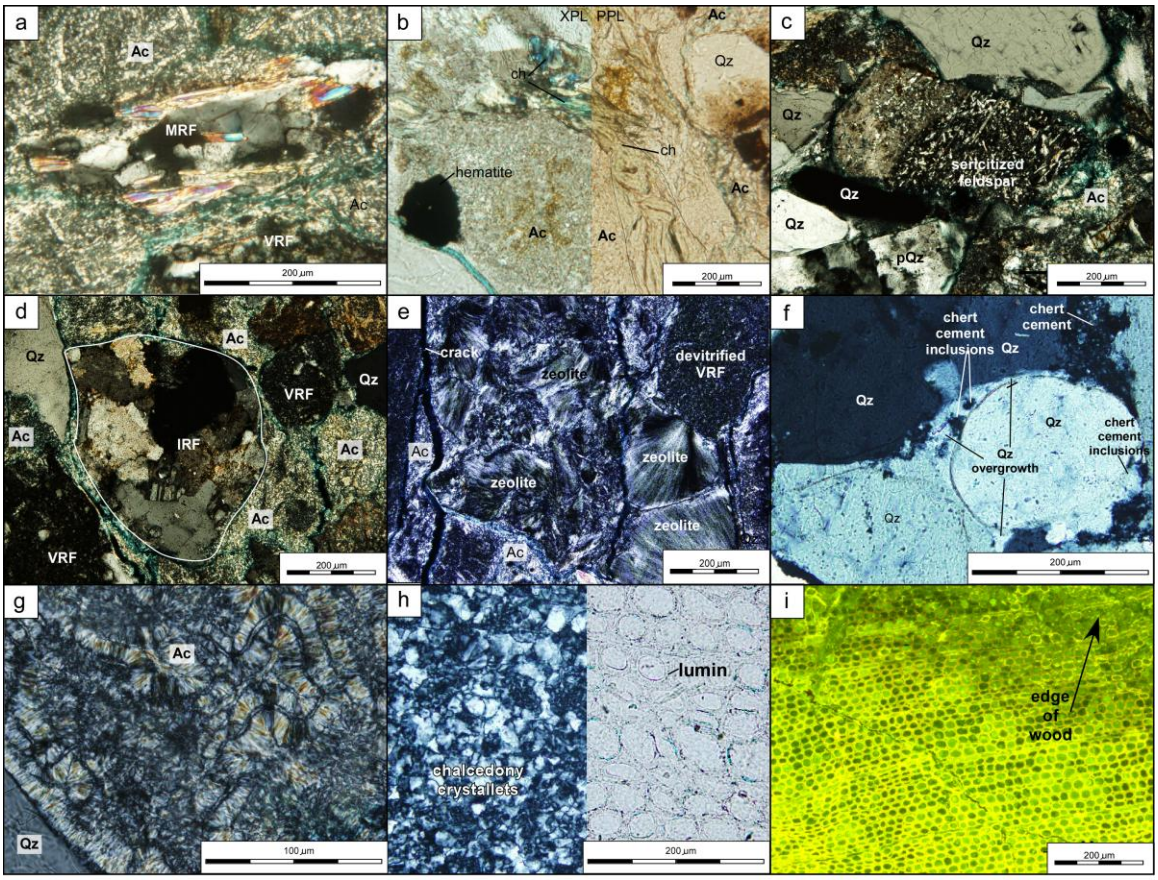

Figure 2.10. Thin section photomicrographs of Sonsela sandstones and silicified wood. XPL = cross-polarized light; PPL = plane-polarized light; VRF = volcanic rock fragment; MRF = metamorphic rock fragment; IRF = igneous rock fragment; AC = authigenic clay; Qz = quartz; pQz = polycrystalline quartz; ch = chlorite cement; ca = calcite. a) Metamorphic rock fragment surrounded by authigenic clay; b) Photomicrographs display the same viewpoint in both XPL (left) and PPL (right). Chlorite cement with ultra-blue extinction (XPL) and green pleochroism (PPL); c) Sericitized feldspar grain along with polycrystalline quartz, quartz, and authigenic clays. d) Igneous rock fragment surrounded by authigenic clays, volcanic rock fragments and quartz grains; e) Zeolite crystals that have replaced grains surrounded by authigenic clays; f) Quartz grains surrounded by quartz overgrowths and chert cement. Quartz overgrowths have chert inclusions; g) High magnification view of authigenic clays showing growth on the edge of a quartz grain and aligned "book-like" orientations of clay; h) Photomicrographs display the left and right sides of the same viewpoint in XPL (left) and PPL (right). Silicified wood in cross polarized light is replaced by chalcedony crystals (left). Outlines of log lumin can clearly be seen in PPL (right); i) Silicified wood has organic matter (bright areas) within lumin viewed under blue fluorescent light. Image has increasing disarticulation of log lumin with proximity to log edge.

and provided the silica responsible for wood silicification (Sigleo, 1979). If so, then the precipitation of authigenic clay and silicification of wood were concurrent events.

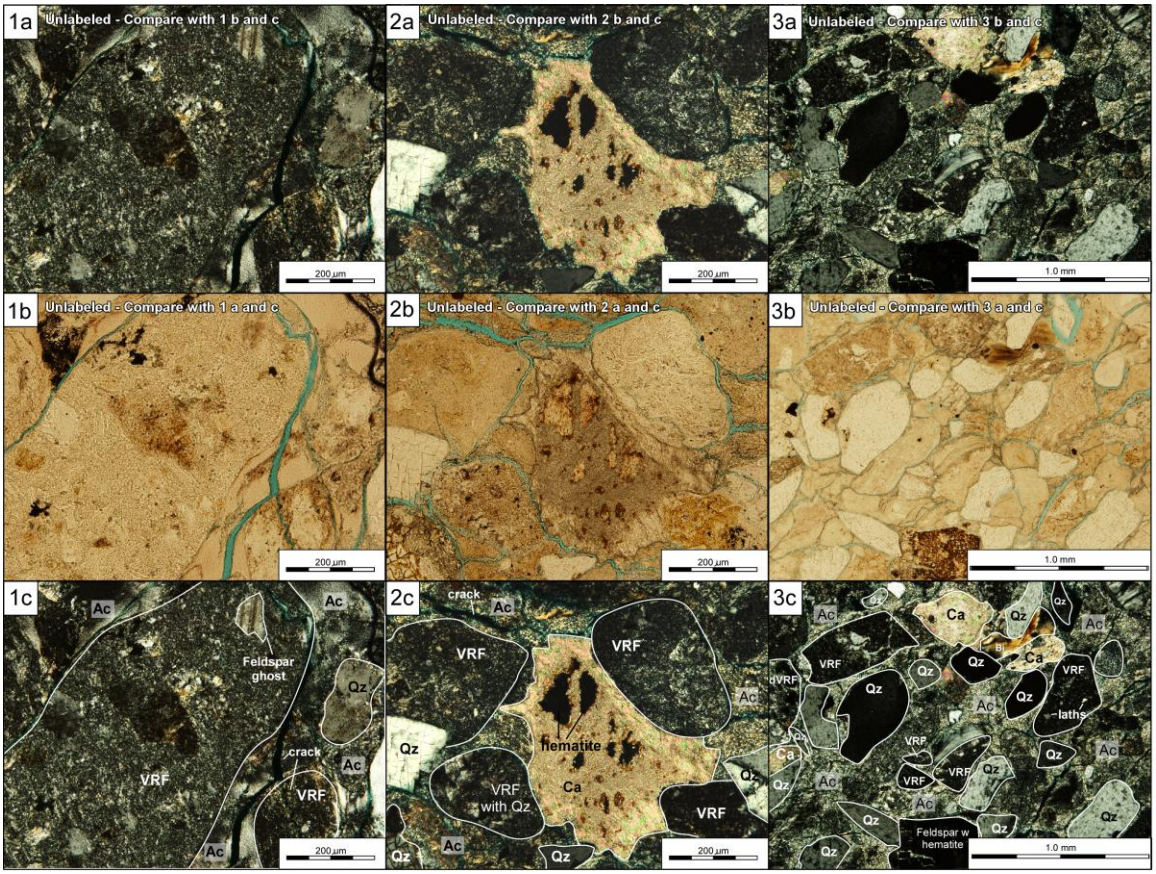

Figure 2.11. Thin section photomicrographs of Sonsela sandstones showing three different views of volcanic rock fragments surrounded by authigenic clays (columns 1, 2 and 3). Row 'a' is cross-polarized light and unlabeled, row 'b' is unlabeled plane polarized light view, whereas row 'c' is labeled with interpretations. Figure illustrates characters by which authigenic clays are distinguished from devitrified volcanic rock fragments. Compare with Figure 10g to see authigenic clay fabrics at high magnifications. AC = authigenic clay; Qz = quartz; VRF = devitrified volcanic rock fragment; ca = calcite. The column 1 view (photos 1a, 1b, and 1c) has a large devitrified VRF with disorganized or patchy internal texture. The outline of the grain can be clearly seen in both XPL and PPL. Ghosts and laths of feldspar and quartz are within the grain. The column 2 view (photos 2a, 2b, and 2c) has calcite grain replacement with a hematite nucleus and includes abundant VRF grains. The VRF grain to the bottom left of the calcite cement shows ghosts of feldspar or quartz. VRF grains are easy to distinguish from authigenic clays by texture in PPL view. In XPL authigenic clays have much brighter high-order yellow colors than VRFs. The column 3 view (photos 3a, 3b, and 3c) is at lower magnification, as such, VRFs are more difficult to distinguish. However, the grain boundaries are clearly distinguishable from clay matrix in PPL.

Authigenic clay precipitation was followed by the alteration of mineral grains (plagioclase?) to zeolites and minor quartz and calcite cementation/grain replacement (Figures 2.10e and 2.11-2). The divergence in precipitation from authigenic clay to

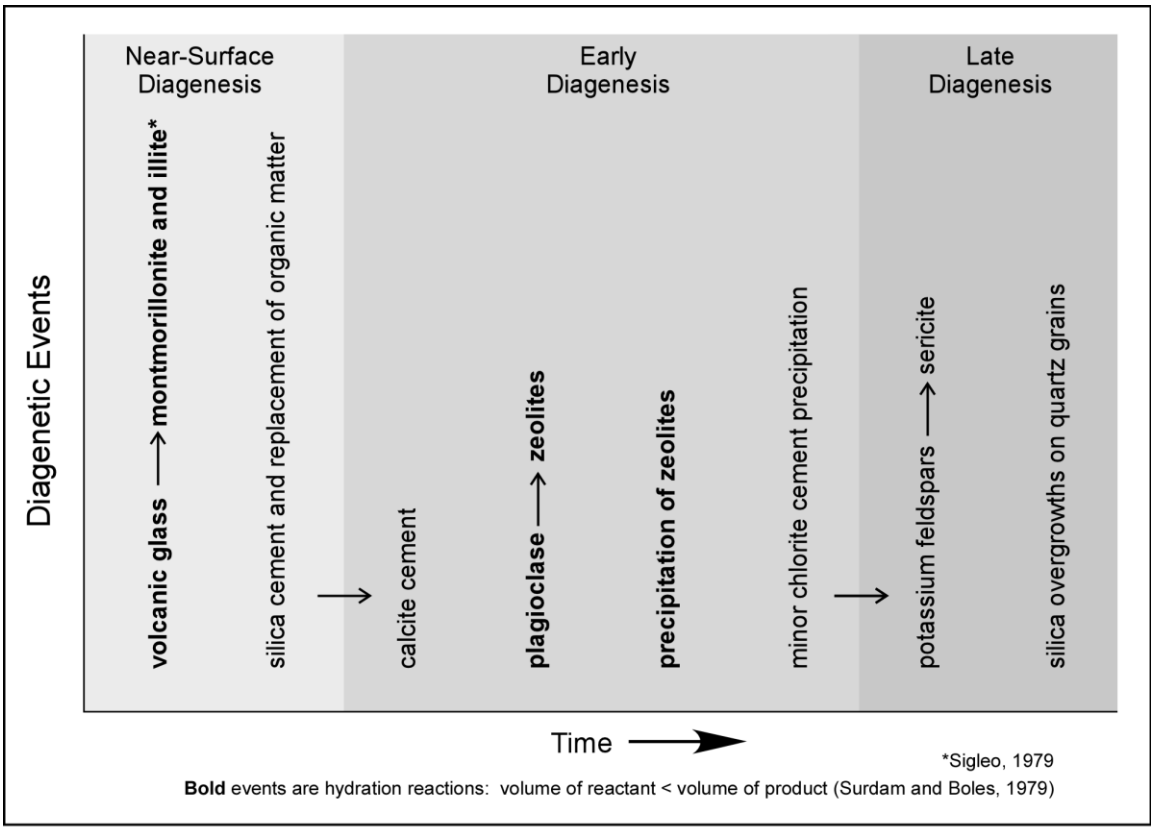

Figure 2.12. Sonsela sandstone paragenetic history. Events listed within "near-surface", "early" and "late" diagenesis fields are either concurrent or their relative timing is ambiguous.

zeolites suggests a change in fluid chemistry from fresh (pH <8) to alkaline (pH >8; Surdam and Parker, 1972). Calcite and chlorite cement precipitation was likely limited because of porosity destruction during earlier cementation events (Surdam and Boles, 1979; Figures 2.10b, 2.11-2 and 2.11-3). The final diagenetic phases include quartz overgrowth and feldspar sericitization (Figure 2.10 c, f). The paragenetic reconstruction provided here is similar to previously published interpretations within similar volcanogenic basins (Surdam and Boles, 1979).

Thin sections of permineralized wood show superb preservation of cellular structure and wood lumin replaced by spherical chalcedony crystallets (Figure 2.10h, i). Cell structure located on the exterior of silicified logs appears to have undergone

decomposition inasmuch as lumin are slightly disarticulated (Figure 2.10i). Decomposition only affects cells within 1 cm (0.4 in) of the log perimeter (Figure 2.10i), indicating limited time to silicification. The bright fluorescence of lumin within petrified logs indicates preserved wood organic matter (Smith, 1984; Figure 2.10i).

Compaction

To estimate the approximate depth and timing of silicification, burial compaction is calculated using the methodology of Stout and Spackman (1989) from aspect ratios measured from 200 silicified logs observed within the Jasper Forest Bed (base of FAC-Set 3). From this, burial compaction prior to silicification ranges from 0 - 25.7%, and averages 9.1% (Figure 2.13A). Based upon observations of Holocene peat, Bloom (1964) determined that peat is compacted to 20% of its original thickness within 11m of burial. A transform created from this relationship is applied to silicified logs within the Jasper Forest Bed and indicates a burial of 0.6m at 9.1% compaction (Figure 2.13B). High water content and the soft organic matter of peat likely allow it to more readily compact than logs. As such, this value provides a minimum depth of burial prior to log silicification. Nonetheless, these findings suggest that log silicification and pore occlusion by diagenetic products occurred soon after deposition (Figure 2.13B).

Modern studies of logs submerged in hot springs suggest that wood silicification begins in as little as a few years and takes only tens to hundreds of years to occur (Akahane, 2004). Consistent with these findings, Sigleo (1979) found that the sediment mineral and trace element contents of clay mineral components indicate precipitation took place within the chemical and pH range of most surface waters. To our knowledge, this is the first study to document complete primary porosity destruction at such shallow

depths of burial. Consistent with these findings, Sigleo (1979) found that the sediment mineral and trace element contents of clay mineral components indicate precipitation took place within the chemical and pH range of most surface waters. To our knowledge, this is the first study to document complete primary porosity destruction at such shallow depths of burial.

Reservoir Parameters

Sandstone grain size varies through time and between architectural elements. In general, sandstone grain size decreases upwards through the succession with coarse- to fine-grained sandstones near the section base and medium- to very fine-grained sandstones within upper portions of FAC-Set 2 (Figures 2.4). Coarse conglomeratic sandstones and/or sandy conglomerates of FAC 10 abruptly overlie this otherwise fining-upward succession. Grain size also varies between architectural elements. Downstream accretion deposits range from gravel and very coarse sand to fine sand (average size of coarse sand), lateral accretion deposits from coarse to very fine sand (average size of medium sand), thin sandy bedform deposits from medium sand to silt (average size of fine sand), and overbank deposits from fine sand to clay (average size of silt to very fine sand). Sandstone depositional sorting is difficult to estimate due to abundant interstitial authigenic clay, but likely range from well to moderately sorted.

Sandstone porosity is completely occluded in Sonsela sandstones. As such, depositional porosity is estimated by using intergranular volume as a proxy. Porosity is estimated to have ranged from 16 – 41% (average 30%) and decreased up-section from FAC 3 to FAC 7 (no thin-sections were obtained from FACs 8 and 9 as there were no sandstones) and abruptly increased within FAC 10 (Table 2.3). Sandstones from FACs

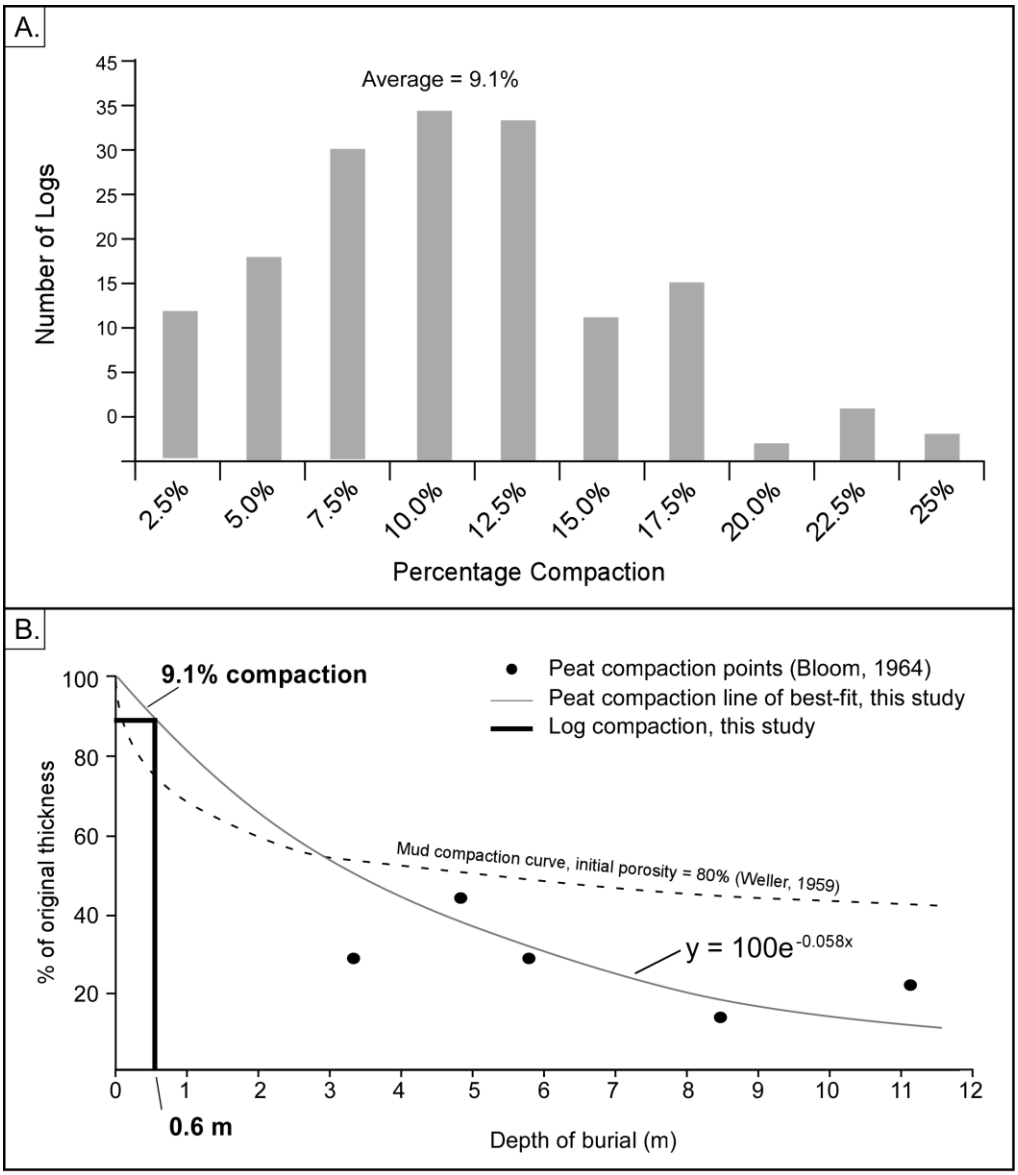

Figure 2.13. A) Histogram of log compaction data for 200 silicified logs from the Jasper Forest Bed at the "Crystal Forest" area of Petrified Forest National Park (FAC 10). B) Scatterplot of Holocene peat compaction with depth (modified from Bloom, 1964). Line-of-best-fit was created using Bloom's compaction data in order to determine depth of log burial at silicification. An average compaction of Sonsela logs of 9.1% suggests that silicification occurred under less than 1m of burial. Mud compaction curve is shown as a reference (Weller, 1959).

3-5 had an average porosity of 31%, sandstones from FACs 5.5 and 6 had an average of 29% and sandstones from FAC 7 had an average of 19%. Porosity within FAC 10 averaged 34%. Porosity also varied between and within architectural elements (Table 2.3). Downstream accretion (33%, n = 11) and lateral accretion (32%, n = 6) deposits had

the highest porosity. Thin sandy bedforms had an average porosity of 19% (n =3), and massive channel fill sandstone 18% (n = 1).

Values of sandstone depositional permeability, i.e., prior to diagenetic reduction, are estimated using the transform function of Pape et al. (1999, 2000). This empirical formula estimates permeability using a fractal dimension, *D*, which models the relationship between pore effective radius, tortuosity and porosity, a relationship which is difficult to quantify. As such its use has limitations including: a) determination of the *D* value is dependent upon lithology (initial sorting) and diagenetic compaction and cementation of sandstones, which are characteristics unique to each sandstone; b) Pape et al. (1999, 2000) define equations appropriate for use with sandstones of specific lithologies, however, these lithologies are qualitative classes; c) permeability and porosity data sets used to calibrate equations consisted of well log and core data, not point count data; d) equations are only applicable to porosity values which fall within the range of data used for equation definition (within which Sonsela sandstone values fall). Sandstone permeability ranged from 25 millidarcys to 250 darcys (Table 2.3). Corresponding with porosity, sandstone permeability decreased up section from FAC 3 to FAC 8, and abruptly increased within FAC 10 (Table 2.3). Sandstones from FACs 3-5 had a median permeability of 12 darcys, sandstones from FACs 5.5 and 6 had a median of 13 darcys, and sandstones from FAC 7 had a median of 0.1 darcys. Median permeability within the FAC 10 sandstones is estimated to have been 135 darcys. Permeability also varied by architectural elements (Table 2.3). The highest median permeabilities were associated with downstream accretion (32 darcys, n = 11) and lateral accretion (13 darcys, n = 6) deposits. Thin sandy bedforms had a median permeability of 0.1 darcys (n =3), and the

massive channel fill sandstone had a permeability of 0.07 darcys. The lowest permeability was associated with an overbank sandstone that had a permeability of 0.02 darcys.

Paleosols are likely low permeability owing to their silty-clay to clayey-silt texture. Paleosols in FACs 3-4.5 are discontinuous and poorly-developed, and would likely serve as baffles to fluid flow in similar subsurface reservoirs. Paleosols in FACs 5-6 are continuous and thicker, and would more likely behave as either barriers or baffles to fluid flow. FACs 7 and 8 are almost completely composed of welded paleosols developed on fine-grained overbank deposits that are continuous across the outcrop (Figure 2.8). These paleosols would likely serve as barriers to fluid flow within subsurface counterparts.

A scatterplot of primary porosity versus permeability indicates that sandstones cluster into discrete reservoir classes (Figure 2.14). Downstream and lateral accretion deposits of reservoir class A have the highest values with porosity ranging from 37 - 41% and permeability from 90 - 250 darcys (Figure 2.14). Reservoir class B ranges in porosity from 26 - 34% and permeability from 3 – 33 darcys, and also consists of downstream and lateral accretion deposits. Reservoir class C ranges from 16 - 21% porosity and 0.02 – 0.35 darcys of permeability and consists predominately of thin sandy bedform and massive channel fill. The reservoir classes are partitioned stratigraphically (Figure 2.8). Sandstones of reservoir class A occur at the base of FAC-Set 2 (FACs 3, 4) and FAC-Set 3 (FAC 10; Figure 2.8). Sandstones of reservoir class B occur within FACs 5, 5.5 and 6 and sandstones of reservoir class C within FACs 6 and 7 (Figure 2.8).

Mechanism(s) for Evolving Fluvial Deposition

FACs and FAC-Sets in this study are consistent with autogenic depositional mechanisms attributed to similar-scale fluvial cycles by Bridge (1984), Kraus (1987), Kraus and Aslan (1999), Atchley et al. (2004) and Cleveland et al. (2007). FACs are interpreted to record deposition during episodes of channel migration and avulsion that are punctuated by periods of channel stability and pedogenesis across floodplains (*sensu* Kraus and Aslan, 1999; Atchley et al., 2004; Prochnow et al., 2006a; Cleveland et al., 2007). FAC-Sets are interpreted to be produced by successive episodes of avulsion and channel drift back and forth across an alluvial valley (Kraus, 1987; Atchley et al., 2004; Prochnow et al., 2006a; Cleveland et al., 2007), e.g. the increasing proportion of overbank deposits and increasing paleosol maturity from base to top in FAC-Set 2 may reflect avulsive channel drift away from a fixed reference point within the alluvial valley of deposition (Bown and Kraus, 1987; Kraus and Aslan, 1999; Atchley et al., 2004; Prochnow et al., 2006a; Cleveland et al., 2007). In contrast to the FAC-Set model, FAC-Set 2 is abruptly overlain by the coarse, basal bedload deposits of FAC-Set 3 rather than a gradually coarsening succession of alluvial deposits that suggests the channel is migrating across the valley back to a proximal position. The abrupt nature of this change may reflect an allogenic event superimposed upon otherwise autogenic processes. Possible explanations include a shift in climate, sea level change, and/or an orogenic/volcanogenic pulse.

Climate Shift

The abrupt truncation of FAC-Set 2 beneath the coarse, bedload deposits of FAC-Set 3 may suggest a climatically-induced change in either sediment supply or fluvial

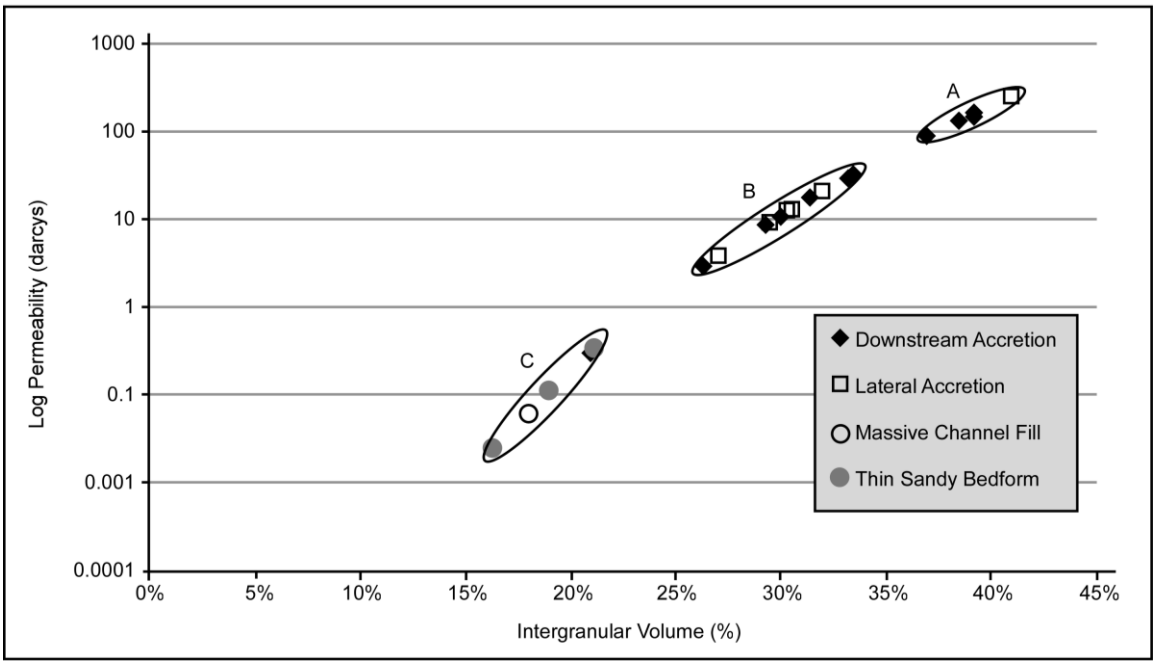

Figure 2.14. Scatter plot of porosity and permeability for sandstone samples with data points discriminated by architectural element, and sorted by reservoir class. Reservoir class A has porosity ranging from 37 - 41% and permeability from 90 - 250 darcies. Sandstones within this class coincide with downstream and lateral accretion deposits. Reservoir class B ranges in porosity from 26 - 34% and permeability from 3 – 33 darcies, and also consists of downstream and lateral accretion deposits. Reservoir class C ranges from 16 - 21% porosity and 0.02 – 0.35 darcies of permeability and coincides with thin sandy bedform, massive channel fill and downstream accretion deposits. Sandstone reservoir class distributions are plotted on photopanoramas (compare with Figure 2.8).

competence and capacity (Bull, 1991; Blum and Törnqvist, 2000; Vandenberghe, 2002; 2003). Climate forcing may have increased precipitation and associated stream power, or decreased precipitation and denuded overbank areas with loss of stabilizing vegetation (*sensu* Bull, 1991; Blum and Törnqvist, 2000; Millar, 2000). Within the study interval, however, paleosol macromorphology is relatively invariable and provides little to no evidence for changing climate. Similarly, fauna within the study interval include abundant unchanging aquatic forms which further suggest that climate remained humid to subhumid throughout Sonsela deposition (Martz and Parker, 2010). Major climate change within the source region of the Chinle basin could have altered stream erosive power downstream without being recorded within the study area. Although this study

indicates that local changes in climate are not likely responsible for the aforementioned truncation surface, regional climate variability cannot be ruled out.

Sea Level Fluctuation

Fluctuations in base level and adjustment of the fluvial equilibrium profile may also account for the abrupt truncation surface between FAC-Set 2 and 3. The influence of eustatic sea level change on fluvial systems is likely limited to tens of kilometers from the shoreline for typical fluvial systems along modern passive continental margins (Schumm, 1993; Wright and Marriott, 1993; Shanley and McCabe, 1994; Catuneanu, 2006) and up to 300 to 400 km for low-gradient, high sediment supply fluvial systems (Blum and Törnqvist, 2000). Eustatic sea level change does not likely account for Sonsela FAC-Set characteristics, inasmuch as the contemporaneous shoreline is thought to have been 500-800 km from the study area (Dickinson, 1981; Marzolf, 1993; Lawton, 1994).

Orogenic/Volcanogenic Pulse

High abundance of volcanic lithics within the Sonsela sandstones suggests either a volcanic source region or contemporaneous volcanism. The volcanic source, however, is controversial and authors have suggested both a basinal or external (eolian input) source (Stewart et al., 1986; Riggs et al., 1993; Riggs et al., 2003; Barth et al., 1997). Despite source location, the influx of high amounts of volcanic detritus could have influenced Sonsela fluvial style. Sediment load may have increased due to a rapid influx of pyroclastic material and a resultant associated decrease in overbank stability due to loss of vegetation (Millar, 2000; Paredes et al., 2007). Within the Sonsela, however,

there is a lack of volcanic ash beds associated with bedload channel sandstones. This is unlike the Cretaceous Matasiete Formation, in which bedload fluvial deposits and correlative ash beds were attributed to an influx of pyroclastic sediments (Paredes et al., 2007).

Beyond the landward limit of eustatic influence, fluvial systems are influenced by tectonic uplift and/or subsidence (Wright and Marriott, 1993; Shanley and McCabe, 1994; Catuneanu, 2006). Base level fall associated with uplift steepens the fluvial equilibrium profile resulting in initial incision and transport and deposition of immature sediments within higher competence and capacity bedload-prone fluvial systems (Wright and Marriott, 1993; Shanley and McCabe, 1994; Holbrook and Schumm, 1999; Catuneanu, 2006). Following the uplift, the gradual denudation of the source area due to erosion and basin fill reduces the fluvial equilibrium gradient, and the system evolves to a more suspended-load fluvial style characterized by relatively more reworking of sediments (Johnsson and Stallard, 1989; Johnsson and Meade, 1990; Johnsson et al., 1991). Fluvial deposits of Sonsela FAC-Sets are characterized by compositionally immature, bedload sediments at their base and increasingly mature, finer-grained suspended load sediments at their top. FAC-Sets within the Sonsela are perhaps most likely the result of punctuated orogenic uplift and/or pulses of basin subsidence as suggested by the corresponding cyclic changes in fluvial style and immature sediment abundance. The fluvial source region, and in particular the source of volcanic detritus, remains enigmatic (Bilodeau, 1986; Stewart et al., 1986; Riggs et al., 1993, 2003; Barth et al., 1997).

Applications

The primary stratigraphic factors that influence recovery efficiency are reservoir continuity and associated permeability heterogeneity (Larue and Friedmann, 2005). The outcrop dimensions of the study interval (20-30 m thick by 0.5 km long) are approximately equivalent to a subsurface, production-scale well spacing of 80 acres. From an analog reservoir continuity perspective, reservoir flow units are partitioned within a hierarchy of meter-scale FACs that in turn stack into decameter-scale FAC-Sets. This two-tier stratal hierarchy accounts for vertical "reservoir" heterogeneity produced by the cyclic interbedding of relatively coarser-grained sandstones and finer-grained paleosols (Figures 2.4 and 2.8). Trends of porosity and permeability between sandstones, i.e., as reservoir Class A, B, and C, are controlled by sediment textures unique to specific fluvial environments (Figures 2.8 and 2.14). Lateral continuity within flow units is controlled by the spatial distribution of fluvial architectural elements and associated facies. The most continuous, and highest porosity and permeability sandstones coincide with bedload channel complexes concentrated in the lower portion of FAC-Sets, whereas relatively lower quality, more discontinuous sandstones are associated with suspension-load channel complexes (within the upper portion of FAC-Sets; Figure 2.8). Within similar subsurface reservoirs, waterflood or enhanced recovery initiatives should account for the likelihood that hierarchical reservoir partitioning will preferentially sweep the lowermost, bedload-prone portion of FAC-Sets.

Perhaps the most significant finding in the study is that mineralogically immature sandstones similar to those observed within the Sonsela may pose high exploration risk due to the early effects of diagenesis. Although previous studies confirm the increased

risk of porosity reduction associated with the diagenetic alteration of compositionally immature volcaniclastic sandstones, significant reductions in porosity are documented to occur below burial depths of 1 km (e.g., Nagtegall, 1978). Within the subhumid to humid paleoequatorial climates within which the Sonsela study interval accumulated, complete reservoir destruction associated with vadose diagenesis occurred at very shallow burial depths (Figure 2.13B). These findings have considerable implications for the exploration of mineralogically immature reservoirs.

Summary

1. The Upper Triassic Sonsela Member at Petrified Forest National Park accumulated as a bedload to suspended-load fluvial system, and includes interbedded overbank mudrock and channel sandstone. Overbank deposits contain paleosols of varying maturity and drainage. The overall immaturity of the paleosols indicates either a high rate of floodplain aggradation or a high rate of avulsion and overbank cannibalization.
2. The study interval consists of a two-tier hierarchy of meter-scale fluvial aggradational cycles (FACs) and decameter-scale fluvial aggradational cycle sets (FAC-Sets). Within a FAC-Set, FACs thin, fine and have increasing mineralogic maturity upsection. FACs are attributed to channel avulsion and ensuing periods of channel stability and soil development. FAC-Sets are interpreted to likely record autocyclic processes which are overprinted with pulses of orogenic uplift and/or subsidence.
3. Primary porosity within sandstones ranged from 16% to 41% and permeability from 90 to 250 darcys. The highest porosity and permeability values were associated with bedload sandstones at the base of FAC-Sets 2 and 3. These sandstones are also characterized by the highest lateral continuity.

4. Devitrification of volcanogenic sediments resulted in the silicification of wood as well as the precipitation of interparticle authigenic clays. The limited compaction of petrified logs (range from 0-26%, average 9%) suggests replacement cementation at very shallow burial depths.
5. To our knowledge, this is the first study to document the complete destruction of primary porosity in immature sandstones prior to burial. This has clear implications to the risk associated with the exploration of mineralogically immature sandstones.

CHAPTER THREE

Facies Analysis of a Probable Large Fluvial Fan Depositional System: the Upper Triassic Chinle Formation at Petrified Forest National Park, Arizona

This chapter published as: Trendell, A.M., Atchley, S. C., and Nordt, L.C., in press, Facies analysis of a probable large fluvial fan depositional system: the Upper Triassic Chinle Formation AT Petrified Forest National Park, Arizona: Journal of Sedimentary Research.

Abstract

The Upper Triassic Blue Mesa Member and overlying Sonsela Member of the Chinle Formation consist of paleosol-bearing alluvial strata whose characteristics vary markedly. Strata exposed within a 4km^2 study area at Petrified Forest National Park were evaluated using sedimentologic, stratigraphic, paleopedologic and petrographic criteria to formulate potential depositional models that may account for varying alluvial deposition. The study succession records a progressive up-section increase in grain size, increase in channel depth and width, increase in lateral and vertical connectivity of channel deposits, decrease in overbank preservation and crevasse-splay and/or sheetflood deposition, and increase in paleosol/ overbank drainage. Mean annual precipitation from the CALMAG paleosol weathering proxy suggests precipitation averages approximately 1300 mm/ yr (1.3 m/ yr) throughout the succession despite changing paleosol drainage. These features are consistent with deposition within a progradational fluvial system such as a large fan or splay complex. Sediment accumulation rates within the study interval suggest decreased subsidence within the upper Blue Mesa Member. Reduced rates of accommodation gain may have promoted progradation of the fluvial system. An up-section decrease in sandstone mineralogical maturity may be related to increasing

sediment bypass within proximal fan positions or increased rates of erosion and sedimentation. Increasingly better drained paleosols are attributed to deposition within more upland positions during fan or avulsion complex progradation, rather than changing climate.

Introduction

Fluvial sedimentologists rely on modern fluvial systems to assist in the interpretation of the sedimentary record. In the past, fluvial models were predominantly based on the tributary systems that dominate modern coastal fluvial deposition and account for the largest rivers in the world (Bridge, 1984; Miall, 2006; Weissmann et al., 2011; Fielding et al., 2012). Increasingly, modern non-marine, low-relief alluvial plains in foreland basins have been identified as containing 'large fluvial fans' (also referred to as megafans, large alluvial fans, wet alluvial fans, fluvial distributary systems, and distributive fluvial systems in the literature; (Geddes, 1960; Wells and Dorr, 1987b; Singh et al., 1993; DeCelles and Cavazza, 1999; Shukla et al., 2001; Leier et al., 2005; Fisher et al., 2007; Hampton and Horton, 2007; Weissmann et al., 2010). Within this study, the term 'large fluvial fan' is used as a generic descriptor that includes all large fluvial systems where rivers exit confinement from upland regions and debouch into open basins where the downstream reaches of the channel are free to migrate laterally resulting in a large-scale fan-shaped (or pseudo-fan-shaped) package of sediment (Geddes, 1960; Wells and Dorr, 1987a; Wells and Dorr, 1987b; Stanistreet and McCarthy, 1993). Large fluvial fans are distinct from alluvial fans and tributary fluvial systems in terms of their sizes, slopes, textural ranges, and depositional processes (Singh et al., 1993; Stanistreet and McCarthy, 1993; Shukla et al., 2001; Weissmann et al., 2011). Refinement of the

large fluvial fan facies model has promoted recognition of these systems in the sedimentary record (Cain and Mountney, 2009; Cain and Mountney, 2011; DeCelles and Cavazza, 1999; Horton and DeCelles, 2001). Continental basins containing large fluvial fans have laterally varying depositional systems and can also contain alluvial fans (DeCelles and Cavazza, 1999; Horton and DeCelles, 2001), and tributary fluvial systems (DeCelles and Cavazza, 1999; Hartley et al., 2010; Weissmann et al., 2010; Weissmann et al., 2011). With increased understanding of the variety of depositional systems and processes within continental basins, it is prudent to be aware of such models when examining continental successions such as the Chinle Formation.

The Upper Triassic Chinle Formation consists of continental strata composed of fluvial, lacustrine and palustrine deposits (Stewart et al., 1972; Gubitosa, 1981; Blakey and Gubitosa, 1983; Dubiel et al., 1991; Dubiel, 1994) that have been the subject of extensive sedimentological study. Chinle fluvial systems were highly variable and evolved between bedload and suspended-load systems through time, undergoing several periods of incision and aggradation (Stewart et al., 1972; Blakey, 1974; Kraus and Middleton, 1987; Demko, 1995; Dubiel et al., 1999; Woody, 2006; Beer, 2005). Discontinuous exposures (Stewart et al., 1972; Blakey and Gubitosa, 1983), geographically limited sediment packages (Kraus and Middleton, 1987; Demko et al., 1998; Dubiel et al., 1999; Dubiel and Hasiotis, 2011), and considerable missing time (Ramezani et al., 2011) have made regional correlations and interpretation of the mechanisms accounting for depositional variation difficult (Dubiel, 1994; Martz and Parker, 2010). Chinle outcrops considered for this study include portions of the Blue Mesa through Sonsela Members of the lower Chinle exposed within the "Tepees" and

"Blue Mesa" geographical areas of the Park (nomenclature following Martz and Parker, 2010; Figure 3.1). Within the Petrified Forest National Park (PFNP), the fine-grained dominated Blue Mesa Member has been interpreted to represent deposition within a high-sinuosity fluvial system (Demko, 1995; Woody, 2006; Martz and Parker, 2010). In contrast, the overlying Sonsela Member is sandstone-dominated and is interpreted to have been deposited within a low-sinuosity fluvial system (Deacon, 1990; Demko, 1995; Woody, 2006). Detritus from within this interval may have originated from a major volcanic source area to the south (Stewart, 1969; Stewart et al., 1972; Blakey and Gubitosa, 1983; Stewart et al., 1986). Recent lithostratigraphic studies of the Chinle Formation within the Petrified Forest National Park (Martz and Parker, 2010) provide a geochronologically well-constrained record of continental fluvial deposition spanning 17 Ma (Ramezani et al., 2011) and well-exposed paleosols within the study succession provide information regarding the climatic regime that prevailed during deposition.

Like many modern large fluvial fans (Stanistreet and McCarthy, 1993; DeCelles and Cavazza, 1999; Shukla et al., 2001; Horton and DeCelles, 2001; Hartley et al., 2010; Weissmann et al., 2010), the lower Chinle Formation (which includes the study succession) was deposited in an interior continental basin that was dominantly free of marine influence (Stewart et al., 1972; Blakey and Gubitosa, 1983; Dubiel et al., 1991; Dubiel et al., 1999) and subjected to monsoonal climatic conditions (Dubiel et al., 1991; Kutzbach and Gallimore, 1989; Leier et al., 2005). The objective of this research is to combine paleoclimatic data (via paleosols), fluvial architectural attributes and petrology to better understand the depositional processes and forcing mechanisms that may account for evolving fluvial deposition throughout the study interval. To this end, the research: a)

evaluates whether the study interval at the Petrified Forest National Park (PFNP) was deposited within a distributary or a tributary fluvial system; b) determines potential controls on varying pedogenic (paleosol) characteristics within the study interval; c) discusses potential depositional models that can account for the fluvial succession; d) proposes potential forcing mechanisms responsible for variations in fluvial depositional style; and e) discusses the limitations of recognizing large fluvial fans within outcrop successions of limited lateral extent (i.e., in studies where local and/or regional stratal geometries cannot be constrained due to discontinuous outcrop exposure).

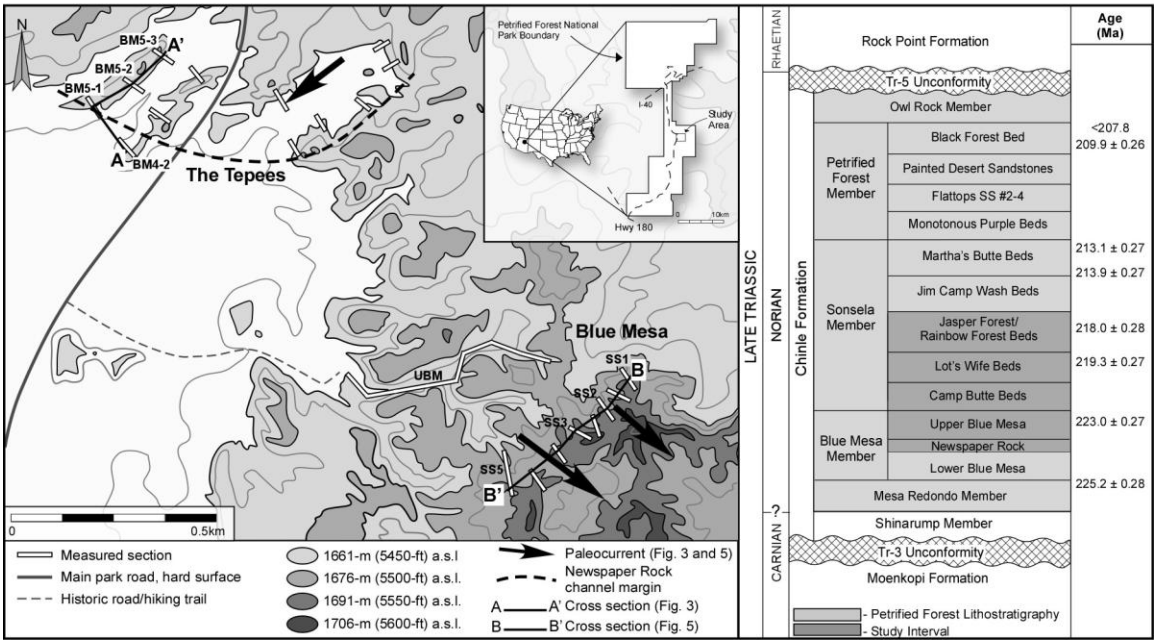

Figure 3.1. Topographic map of the study area in the Petrified Forest National Park (left) showing the location of all measured sections (white rectangles). Labeled measured sections and cross-sections A-A' and B-B' are illustrated in Figure 3.3 and 3.5. The A-A' cross-section was chosen to be perpendicular to the Newspaper Rock (NR) interval channel. The NR channel margin was traced in outcrop and is illustrated as a thick, dashed black line. Paleocurrent directions are indicated by large black arrows. Paleocurrent data and locations are shown in Figure 3.3 and 3.5. A lithostratigraphic chart for the Petrified Forest National Park with the study interval highlighted is shown on the right (nomenclature after Martz and Parker, 2010; absolute age dates from Ramezani et al., 2011).

Stratigraphic, Paleogeographic and Paleoclimatic Overview

Petrified Forest National Park in Arizona contains extensive exposures of the Upper Triassic Chinle Formation (Figure 3.1). The Chinle Formation is a continental succession deposited within the Upper Triassic Chinle Basin (Blakey and Gubitosa, 1983). The retro-arc basin formed on the eastern side of the Cordilleran volcanic arc on the western margin of equatorial Pangea (Figure 4.2; Dickinson, 1981; Blakey and Gubitosa, 1983; Marzolf, 1993; Dickinson and Gehrels, 2008). At the time of deposition, the present site of the Petrified Forest National Park was located at 5-15°N paleo-latitude (Van der Voo et al., 1976; Bazard and Butler, 1991) and was surrounded by Paleozoic uplifts (Blakey and Gubitosa, 1983; Dubiel, 1994; Dickinson, 2004; Dickinson and Gehrels, 2008). The basal Chinle contained a large northwestward-flowing trunk river system (Blakey and Gubitosa, 1983; Blakey and Gubitosa, 1984; Dubiel and Skipp, 1992; Dubiel, 1994) and, although no trunk channel deposits are found above the basal Chinle, it is likely that drainage connected present-day Texas to Nevada throughout deposition of the lower Chinle (Figure 3.2; (Blakey and Gubitosa, 1983; Blakey and Gubitosa, 1984; Good and Dubiel, 1992; Gehrels et al., 1993; Good, 1993; Riggs et al., 1996; Dickinson and Gehrels, 2008). Variable paleoflow directions within the various members of the Chinle Formation indicate more complexity within the drainage network than simple northwestward flow (Stewart et al., 1972; Beer, 2005; Woody, 2006; Trendell et al., 2012). Outcrops of the lower Chinle within the southern portion of the Colorado Plateau (which includes the study area) contain several indicators for a southern source area (Stewart, 1969; Stewart et al., 1972; Blakey and Gubitosa, 1983; Stewart et al., 1986). Paleocurrent data are consistently north to northwest trending and strata thicken to the

south (Stewart et al., 1972). Successions in the south have more common conglomeratic layers of which the clast sizes are larger (25 cm south; 5 cm north) than northern successions and volcanic cobbles and pebbles are almost exclusively found within the southern portion of the Colorado Plateau (Stewart, 1969; Stewart et al., 1972; Blakey and Gubitosa, 1983; Stewart et al., 1986). Remnants of the actual source area for the lower Chinle, termed the Mogollan Highlands, have not been identified (Stewart et al., 1986). It is hypothesized that the source area may have been sheared westward upwards of 700-800 km along the Mojave-Sonora megashear during the Jurassic (Stewart et al., 1986).

Although Chinle deposition was likely independent of eustatic influence (Stewart et al., 1972; Blakey and Gubitosa, 1983; Dubiel et al., 1991; Dubiel, 1994), deposition may have been influenced by climate and orogenesis. The Chinle Formation has been interpreted previously to have accumulated under a subtropical and strongly seasonal climate that became increasingly arid through time (Kutzbach and Gallimore, 1989; Dubiel et al., 1991; Dubiel and Skipp, 1992; Driese and Mora, 2002; Tanner, 2003; Prochnow, Nordt, et al., 2006; Tanner and Lucas, 2006; Cleveland et al., 2008; Dubiel and Hasiotis, 2011) due to a Pangean mega-monsoon (Kutzbach and Gallimore, 1989; Dubiel et al., 1991), and the gradual drift of North America northward away from the paleo-equator (Dubiel, 1994; Kent and Muttoni, 2003). During Chinle deposition the Chinle Basin underwent subsidence and was potentially influenced by Cordilleran magmatism and uplift of surrounding highlands (Riggs et al., 2003).

Methods

The study interval is informally subdivided into the lower Blue Mesa Member (below the Newspaper Rock interval), Newspaper Rock interval (strata filling a large

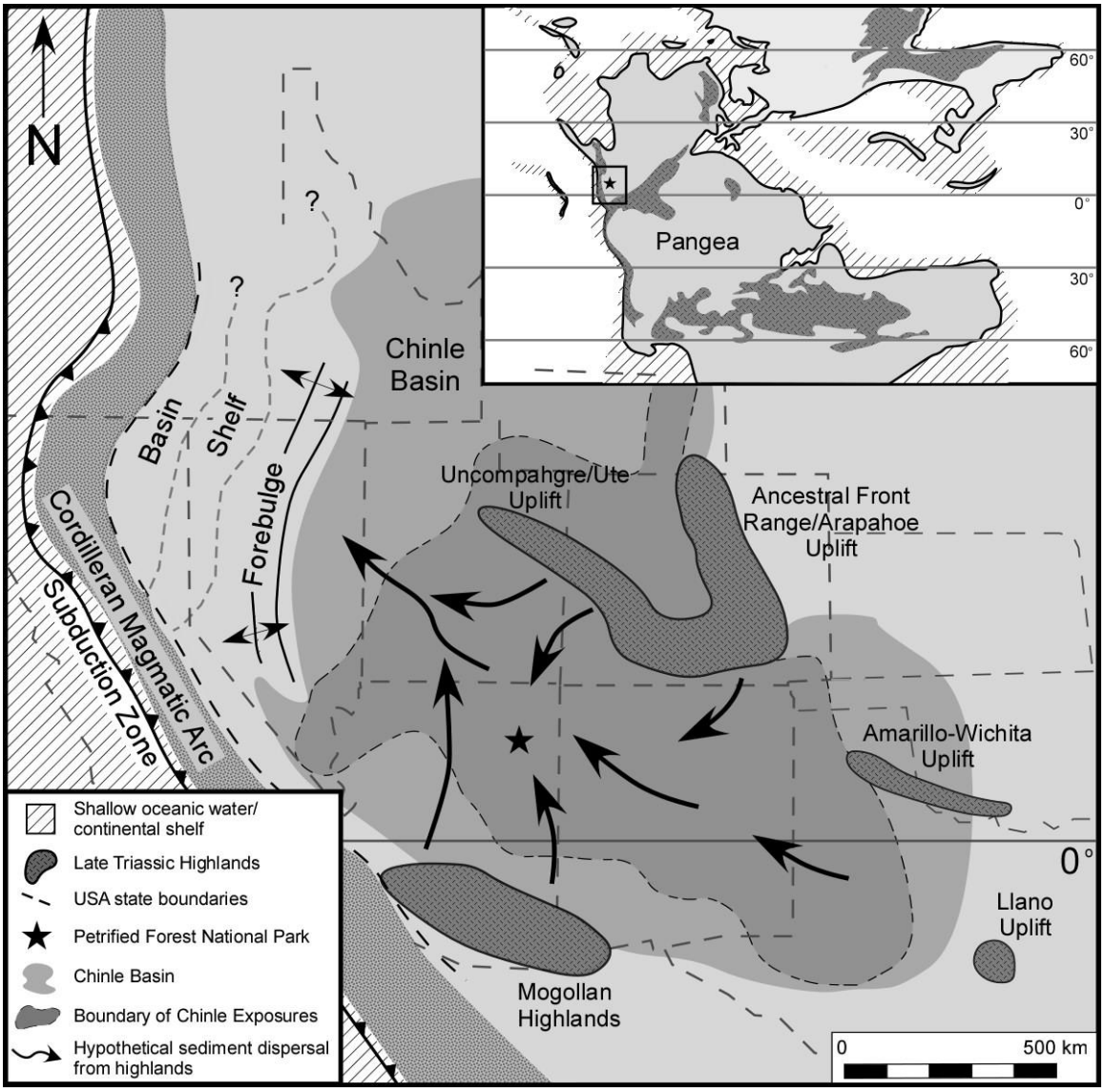

Figure 3.2. Paleogeographic map of the southwestern United States showing the location of the study area relative to the Chinle Basin and major Late Triassic structural features (Blakey and Gubitosa, 1983; Dubiel et al., 1991; Dubiel, 1994; Trendell et al., 2012; Riggs et al., 1996). Solid arrows represent hypothetical sediment dispersal patterns in alluvial systems in the lower Chinle (Dickinson, 1981; Blakey and Gubitosa, 1983; Dubiel, 1987; Dubiel, 1989; Dubiel et al., 1991). The boundary of present-day Chinle Exposures is shown within the Chinle Basin. The inset global paleogeographic map highlights the position of Petrified Forest National Park along the western margin of equatorial Pangea (Scotese, 2007).

channel), upper Blue Mesa Member (Blue Mesa strata above the Newspaper Rock interval), and lower Sonsela Member (Sonsela strata from the Blue Mesa-Sonsela contact up to and including the Jasper Forest Beds; nomenclature follows Martz and Parker, 2010 and references therein). Twenty stratigraphic sections were measured within the Tepees

and Blue Mesa areas of Petrified Forest National Park (Figure 3.1). Of these, 11 were selected to capture facies variability (Figures 3.3, 3.4 and 3.5).

Thin-sections were prepared from forty-two sandstone specimens and each sample was point-counted (300 to 500 counts dependent upon grain size) to determine proportional composition of framework grains. Paleocurrent measurements were collected from trough cross-stratification axes (rib and furrow structures), ripple foresets, and in-situ petrified logs that were transported and deposited within fluvial channels and appear to be aligned with paleoflow direction (when compared with trough cross-stratification axes).

Paleosols encountered within each measured section were described in detail following the standard guidelines of the Soil Survey Staff (1999), Retallack (1988; 2001), and Schoeneberger et al. (2003), and include field observations of thickness, matrix color, structure, texture, horizon boundaries, root trace abundance and size, carbonate type, slickensides, and iron concentrations and depletions. Paleosol colors are described using the Munsell® Soil Color Book. Paleosols were decompacted following the methods of Sheldon and Retallack (2001). Bulk samples of paleosol horizons were collected and analyzed for elemental compositions by ALS Laboratories in Reno, Nevada. Paleosol molecular oxides from the uppermost B horizon of each paleosol are used to estimate mean annual precipitation (MAP) using the CALMAG weathering index (Nordt and Driese, 2010b).

Zircon age dates established by Ramezani et al. (2011) were used to establish a chronostratigraphy between which paleosol ages were interpolated. In order to determine approximate paleosol ages between absolute ages, paleosols were assigned a relative

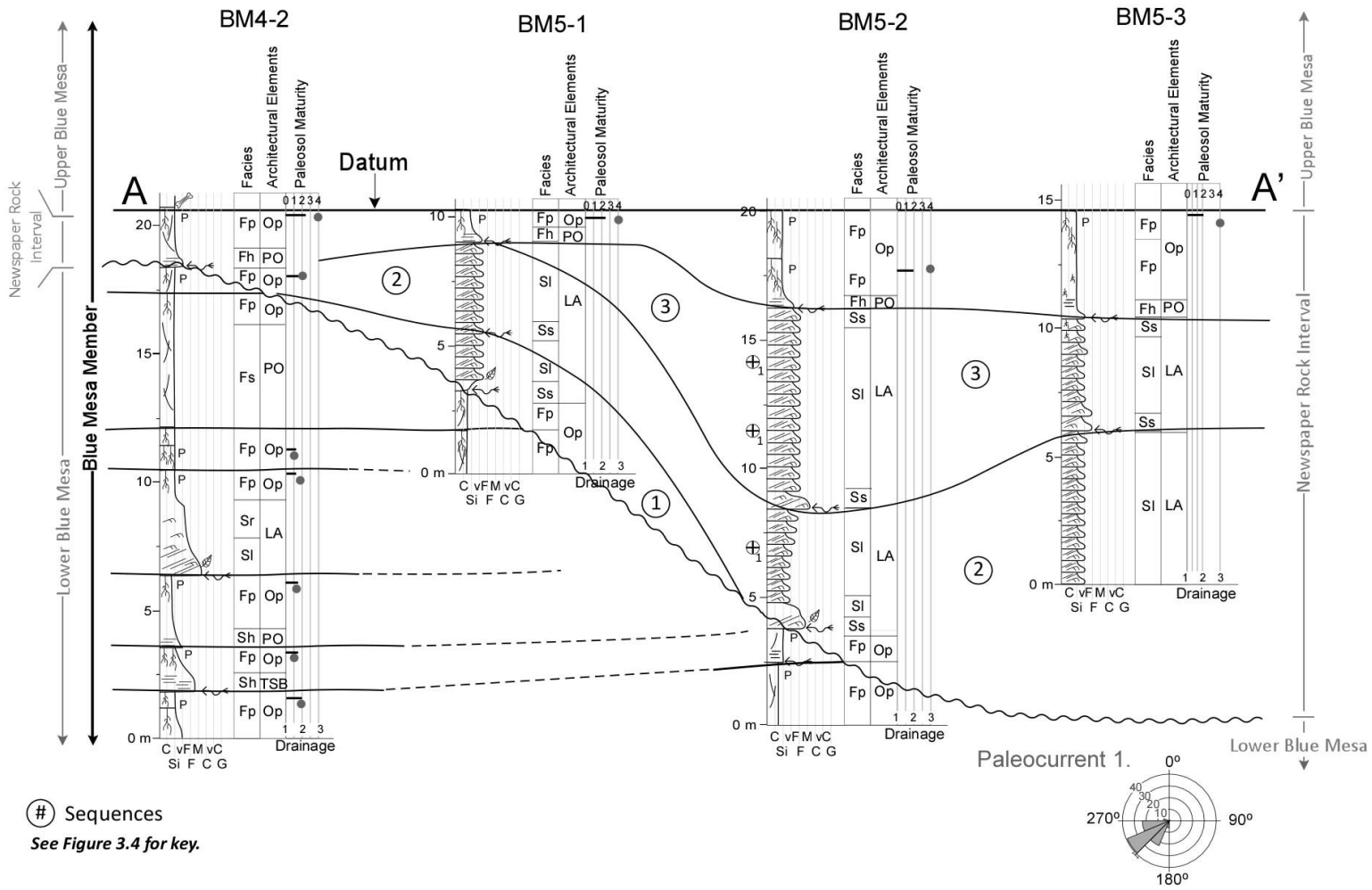

Figure 3.3. Western measured stratigraphic sections (BM4-2, BM5-1, BM5-2, and BM5-3) and cross-section (A-A'; Figure 3.1) of the Newspaper Rock (NR) interval. Lithostratigraphy (after Martz and Parker, 2010) is shown adjacent to measured sections. Cross-section spans the channel perpendicular to the channel margin (Figure 3.1). Stratigraphic datum is the NR paleosol, which is laterally correlative to the NR paleosol in Figure 3.4. Paleocurrent data are depicted in the rose diagram 'Paleocurrent 1'. Sequence boundaries and sequences (#1-3) are identified within the channel. Outcrop photographs of this interval are shown in Figure 3.6a-f.

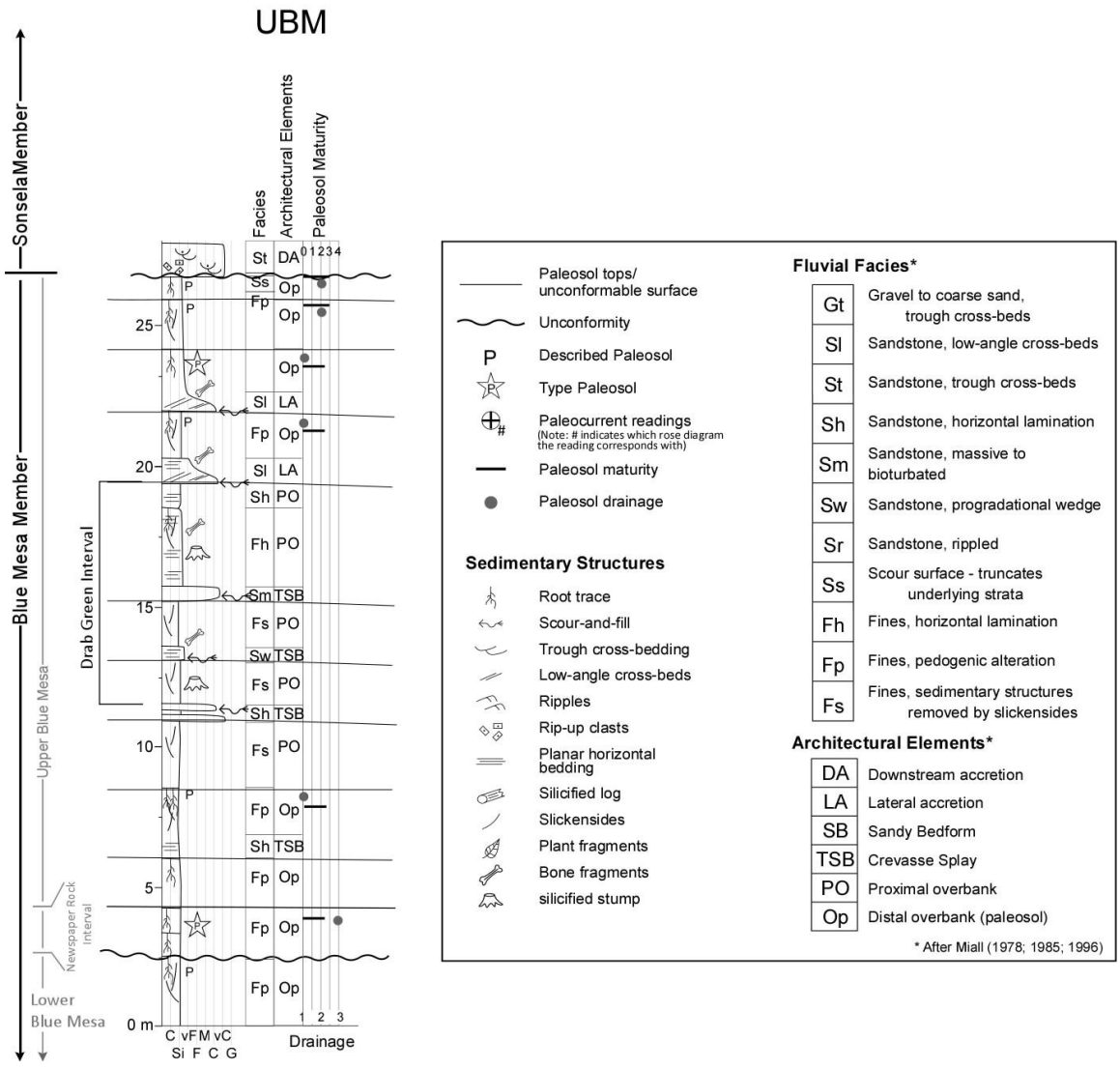

Figure 3.4. Measured stratigraphic section (BMQ) of the upper Blue Mesa Member and the key for measured sections in Figures 3.3, 3.4, and 3.5. The Newspaper Rock (NR) interval is laterally correlative to the NR paleosol in Figure 3.3. The contact between the Blue Mesa and Sonsela Member is laterally correlative to the contact in Figure 3.5. Outcrop photographs of this interval are shown in Figure 3.6g, 3.7b and c.

degree of maturity (as suggested by each paleosol's morphologic features; see bars adjacent to paleosol locations in measured sections, Figures 3.3, 3.4 and 3.5). Paleosols were then assigned a temporal fraction that was calculated by dividing individual paleosol maturities by the cumulative paleosol maturities between the bracketing absolute zircon age reference points. This fraction represents the proportion of formation time for

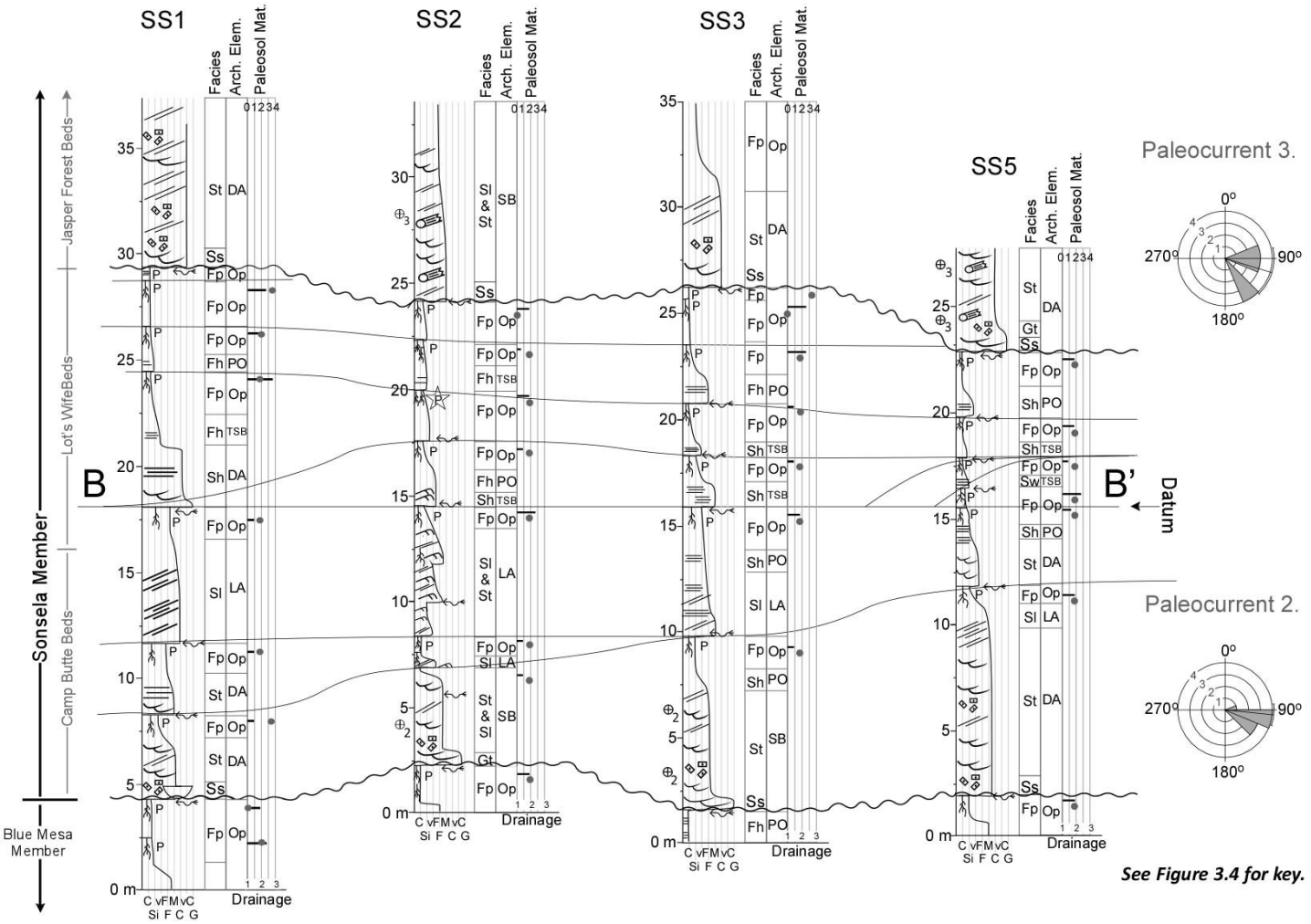

Figure 3.5. Measured stratigraphic sections (SS1, SS2, SS3, and SS5) and cross-section (B-B';Figure 3.1) of the lower Sonsela Member. Stratigraphic datum is a flat-lying paleosol in the middle of the study succession. The contact between the Blue Mesa and Sonsela Members is correlative to the contact in Figure 3.4. Paleocurrents were obtained from the base (Paleocurrent 2) and top (Paleocurrent 3) of the outcrop and are shown in rose diagrams. Outcrop photographs of this interval are shown in Figure 3.7a, d-g.

each paleosol occurring between absolute age dates. The fraction was multiplied by the total time between those absolute ages to determine individual time of formation (*sensu* Nordt et al. 2003). This method assumes that most of geologic time is recorded as non-deposition and weathering in alluvial successions. Although the base of the study succession does not have an absolute age date, strata underlying the study succession have been dated (SS-28 of Ramezani et al., 2010). An approximate date for the oldest paleosol in the study succession was determined by using stratal thicknesses, absolute age dates of older strata, and sediment accumulation rates from Ramezani et al. (2011). Paleosol ages were then determined for the portion of the study interval older than the youngest absolute age date within the study succession (Newspaper Rock to Green Lacustrine beds). The rate of sediment accumulation for that interval reflects the rates determined by Ramezani et al. (2011). From this age model, an apparent 'sediment accumulation' curve was generated based upon the current cumulative stratal thicknesses between temporal pinning points. Thicknesses were decompacted following the methodology of Sheldon and Retallack (2001) and an actual 'sediment accumulation' curve was also generated for comparison.

Results

Depositional Characteristics

Depositional facies observed within each outcrop succession were documented and classified following the scheme of Miall (1978; 1985; 1996; Table 3.1). Depositional facies observed were then used for interpretations of architectural elements (specific

depositional environments) using associated facies, stratigraphic relationships and scale following the methods of Miall (1978; 1985; 1996); Table 3.1).

Lower Blue Mesa Member. Three measured sections (BM4-2, BM5-1, and BM5-2 in Figure 3.3) document the portion of the lower Blue Mesa Member immediately below the Newspaper Rock interval. The Newspaper Rock fills a channel scoured into the lower Blue Mesa. Total stratal thickness of the lower Blue Mesa Member study interval ranges from approximately 5 m beneath the channel to 18 m within interfluve areas adjacent to the channel. Lower Blue Mesa strata consist of interbedded fine-grained mudrocks (85 %) and interbedded sandstones (15 %; Figures 3.3 and 3.6c). Mudrocks consist of thick successions of light-blue, beige- or gray-laminated (Fh) and light-blue slickensided (Fs) rocks interpreted as proximal and distal overbank architectural elements (Table 3.1; Figures 3.3 and 3.6c). Tabular sandstones fine-upwards and include low angle cross-stratification (Sl) or are thin (<0.6 m), lenticular beds containing ripple and horizontal lamination (Sr, Sh; Figures 3.3 and 3.6c). Sandstones are classified as lateral-accretion and thin sandy bedform architectural elements based on their facies associations and lateral relationships to each other and overbank deposits (Table 3.1; Figures 3.3 and 3.6c).

Newspaper Rock Interval. Eleven outcrop sections were described across the Newspaper Rock interval within the Tepees area (Figure 3.1) of Petrified Forest National Park (four are shown in Figure 3.3). The Newspaper Rock interval consists of inclined heterolithic strata deposited within a large channel that is up to 20 m deep (Figures 3.3 and 3.6a). Inclined large-scale, low-angle cross-stratified (Sl; 3 m to 10 m vertical

Table 3.1. Diagnostic attributes of fluvial facies and architectural elements (modified from Miall, 1978; 1985; 1996).

Facies	Lithology	Features	Interpretation	Architectural Element*	Outcrop photos
Gt	Gravel	Trough cross beds; poorly-sorted gravels to coarse sands; clast supported with abundant matrix	Minor channel filling deposit	DA	
St	Sandstone	Trough cross beds; poorly-sorted coarse to medium sand	Upper flow regime channel fill deposit, dunes	DA, LA, SB	Figure 3.7a, g
Sl	Sandstone	Large-scale, low-angle cross beds; coarse to fine sand; fining upwards along beds	Point-bar deposit from fluvial migration	LA	Figure 3.6a, c, d, g and 3.7a, e, f
Sh	Sandstone	Horizontally bedded	Crevasse splay or non-pedogenically altered overbank deposit	LA, PO, SB	Figure 3.7a, g
Sr	Sandstone	Ripple laminated	Lower flow regime; often found in upper portions of Sl facies	LA, TSB	Figure 3.6e, f and 3.7b
Sw	Sandstone	Progradational wedge with pedogenic alteration along bedding planes; poorly sorted medium to very fine sands; border channels and are topographically higher than the adjacent floodplain facies	Crevasse splay	TSB	Figure 3.7b
Sm	Sandstone	Contains no observable sedimentary structures; border channels and are topographically higher than the adjacent floodplain facies	Crevasse splay	TSB, SB	Figure 3.7b
Ss	Sandstone	Scour surface that truncates sedimentary structures within underlying strata	Channel scour	DA, LA, SB	Figure 3.6a, d and 3.7a, e, g
Fh	Mudrock	Laminated and horizontally bedded; very fine sands, silts, and clays; minor to abundant drab root halos that overprint sedimentary structure.	Overbank deposition	PO, TSB	Figure 3.7g
Fp	Mudrock	Unstratified; silts and clays; evidence of pedogenic alteration	Paleosol	Op	Figure 3.6a, c, d, f, g and 3.7a, e, f
Fs	Mudrock	Unstratified; silts and clays; evidence for slickensides; no other evidence for pedogenic alteration	Overbank deposition and modification by shrink-swell processes	Op	Figure 3.6c and 3.7b

*Architectural element definitions
DA: Downstream accretion – accretion of downstream bars
LA: Lateral accretion – accretion of lateral bars or point bars
SB: Sandy bedforms - Channel sands that aggrade with little to no horizontal migration during deposition (not within a migrating bar).
TSB: Thin sandy bedforms –delta-like deposits that form adjacent to the margins of channels – crevasse splays.
PO: Proximal overbank – sheet-like deposition of overbank sands, silts and fines
Op: Distal overbank (paleosol) – pedogenically modified overbank deposits.

height, with cross-set thicknesses of approximately 30-60 cm) and ripple laminated sandstones (Sr) are the most common sandstone facies within the channel (Table 3.1; Figures 3.6a, e, f). Each inclined large-scale low-angle cross-stratified set consists of a fining-upward package that undertakes a transition from relatively massive (Sm) to rippled sandstone (Sr) to rooted silty-mudrock (Fp; Table 3.1; Figures 3.6a, f). These low-angle cross-stratification surfaces dip towards the channel margin, southeast in the eastern sections (not illustrated in measured sections of this manuscript) and southwest in the western sections (Figures 3.3 and 3.6a). The fill succession has a laterally continuous red (10R) paleosol weathered into its upper boundary that extends across the channel to proximal and distal interfluve positions (Figures 3.3 and 3.6a, c, d). Paleocurrent measurements from ripple laminae within the axis of the channel indicate southwesterly flow with a predominant flow direction at 240˚ (Figures 3.3 and 3.6e). Several laterally continuous erosional surfaces occur within the channel-fill and partition the Newspaper Rock succession into unconformity-bounded fluvial sequences that suggest fluvial aggradation punctuated by periods of degradation (Figures 3.3 and 3.6a, d).

Sandstone facies are interpreted as lateral-accretion architectural elements (Table 3.1) based on their extent and presence within a channel. Lateral-accretion deposits can be traced laterally across a 500-m linear distance and exhibit the morphology of accretionary meander bend scroll bars in aerial photographs (Figure 3.6b). Rooted silty mudrocks that cap individual lateral-accretion sandstones are interpreted as proximal overbank architectural elements because they are rooted but do not contain paleosol horizonation (Figures 3.6a, f; Table 3.1; Miall, 1985).

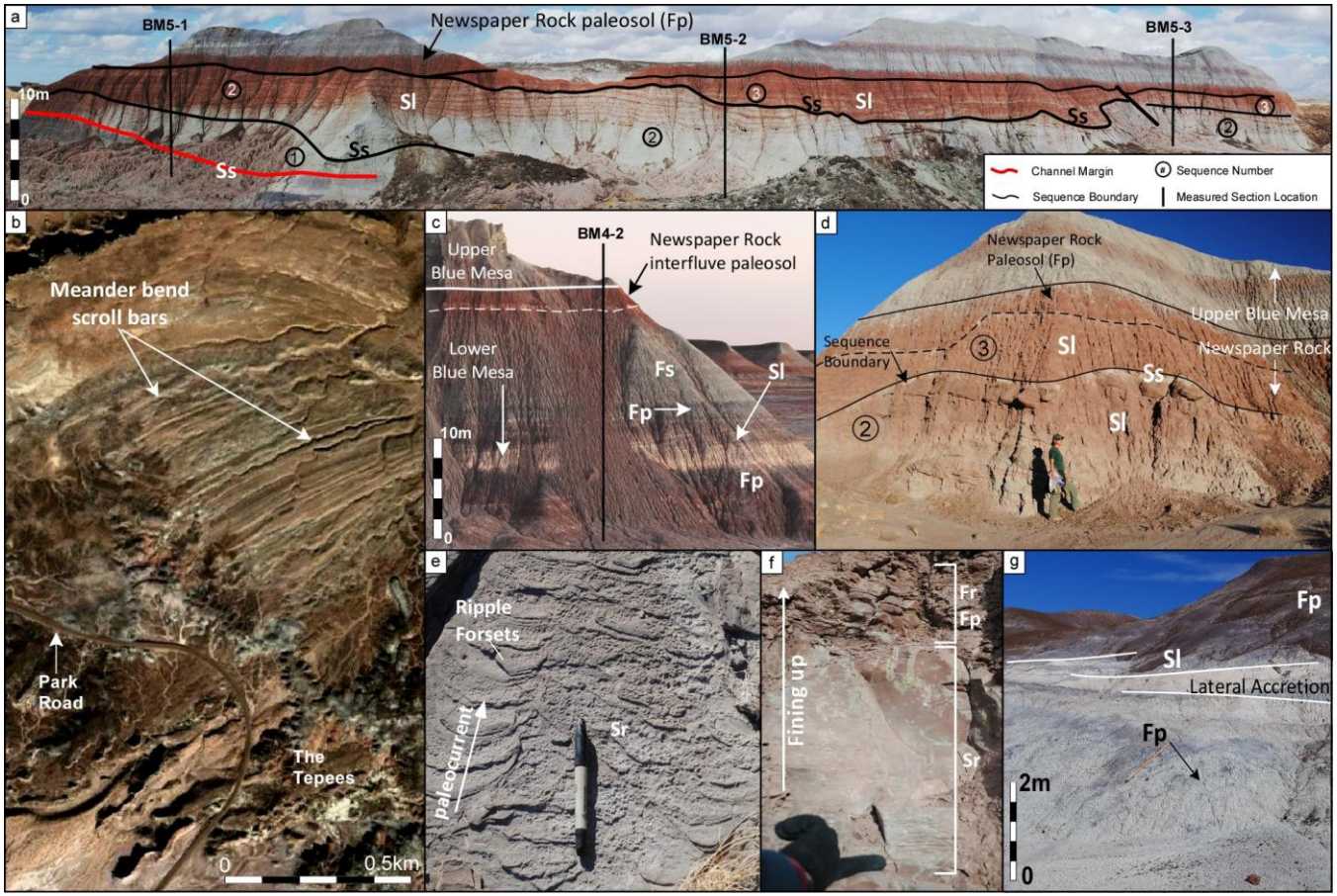

Figure 3.6. Photographs of a) Newspaper Rock channel fill. Red and green heterolithic strata are low-angle cross-stratified. Measured section locations, channel margin (red line), sequences (black lines and circled numbers) and the location of Newspaper Rock paleosol are highlighted; b) accretionary meander bend scroll bars within the Newspaper Rock interval and their lateral extent within the Tepees area; c) lower Blue Mesa Member strata with measured section BM4-2, Newspaper Rock paleosol (interfluve of Newspaper Rock Channel), and Fp, Fs, Sl facies (Table 3.1) indicated; d) the upper portion of the Newspaper Rock channel-fill showing Sl and Ss facies (Table 3.1), sequence boundaries and Newspaper Rock paleosol; e) plan-view of current ripple foresets within the Newspaper Rock channel; f) the upper portion of a low-angle foreset characterized by fining-upward grain size, ripple lamina, and drab root traces; g) upper Blue Mesa Member outcrop with Sl and Fp facies and lateral-accretion channel element (Table 3.1).

Upper Blue Mesa Member. One outcrop section of the Upper Blue Mesa Member (Section BMQ, Figures 3.1 and 3.4) was described to stratigraphically bridge the Newspaper Rock and Sonsela Member intervals. From the top of the Newspaper Rock interfluve paleosol to the base of the Sonsela Member, total stratal thickness is approximately 20 m and consists predominantly of fine-grained mudrocks (90%) and interbedded sandstones and pebble conglomerates (10%). Mudrocks are gray laminated (Fh), drab-green slickensided (Fs) or dark-blue (5PB) and purple (5R) pedogenically modified (by rooting, ped formation and shrink-swell processes; Fp) deposits (Table 3.1; Figures 3.4 and 3.6g). Thin (<0.6 m), lenticular (Sw), fining-upward current-rippled (Sr) and low-angle cross-stratified (Sl) sandstones within the upper Blue Mesa Member are separated by thick successions of mudrocks (Table 3.1; Figures 3.4 and 3.6g). Sandstones are grouped into thin sandy bedforms and lateral-accretion architectural elements. Thin sandy bedforms are commonly underlain and overlain by overbank deposits, and likely accumulated within crevasse-splays (Miall (1978; 1985; 1996); Table 3.1). Lateral accretion elements are channelized, correlate laterally with channel margins and overbank deposits and are interpreted to represent point-bar deposits (Miall (1978; 1985; 1996); Table 3.1). Mudrocks are interpreted as proximal and distal overbank architectural elements (Miall (1978; 1985; 1996); Table 3.1). The upper Blue Mesa Member and the drab-green mudrocks contain metopsaurid amphibians and phytosaurian archosaur fossils (Long and Padian, 1986)

Intervals of drab-green (10GY) mudrocks are observed within the Blue Mesa Member 7 m above the Newspaper Rock interfluve paleosol and 6 m below the base of the Sonsela Member (Figures 3.4 and 3.7b). This relatively thick (approximately 8 m)

succession of drab-green and gray mudrocks contains large, abundant curvilinear fracture surfaces that are interpreted as slickensides that formed as a result of shrink-swell processes due to wetting and drying of clays (Southard et al., 2011; Fs; Table 3.1; Figure 3.7b). Slickensides are interpreted as syndepositional as they do not cross-cut bedding planes. The light-greenish-gray interval indicates deposition in an iron-reducing environment (Vepraskas 1992; 2001). Drab-green predominates in the upper 1.5-2 m of the mudrock interval and transitions downwards to drab-gray (Figure 3.7b). The mudrock succession contains interbedded lenticular (Sw) and tabular sandstones that are massive (Sm) or contain ripples (Sr; Table 3.1; Figures 3.4 and 3.7b), which are interpreted as thin sandy bedforms elements (Miall (1978; 1985; 1996); Table 3.1). As they are underlain by lateral accretion and overbank deposits and overlain by overbank deposits, thin sandy bedforms are interpreted as channel-proximal crevasse-splay deposition (Miall (1978; 1985; 1996); Table 3.1). The drab-green mudrocks (Fs facies) contain in-situ petrified stumps (Figure 3.7c). Fish remains (Murry and Long, 1989; Heckert, 2004) and other semi-aquatic forms combined with an anoxic depositional environment are suggestive of ponds or oxbow lakes (Heckert, 2004).

Lower Sonsela Member. Eight outcrop sections were described across a continuous 0.5 km outcrop of the lower Sonsela Member in the Blue Mesa area of the Petrified Forest National Park (Figure 3.1). The lower Sonsela Member consists of interbedded sandstones (60%) and mudrocks (40%). Fine-grained deposits are either horizontally bedded (Sh, Fh) or pedogenically modified (Fp; Table 3.1; Figures 3.5 and 3.7a, e, f, g). Sandstones at the base of the succession are multistory, contain abundant reactivation and scour surfaces (Ss), and consist of Gt, St and Sl facies (Table 3.1;

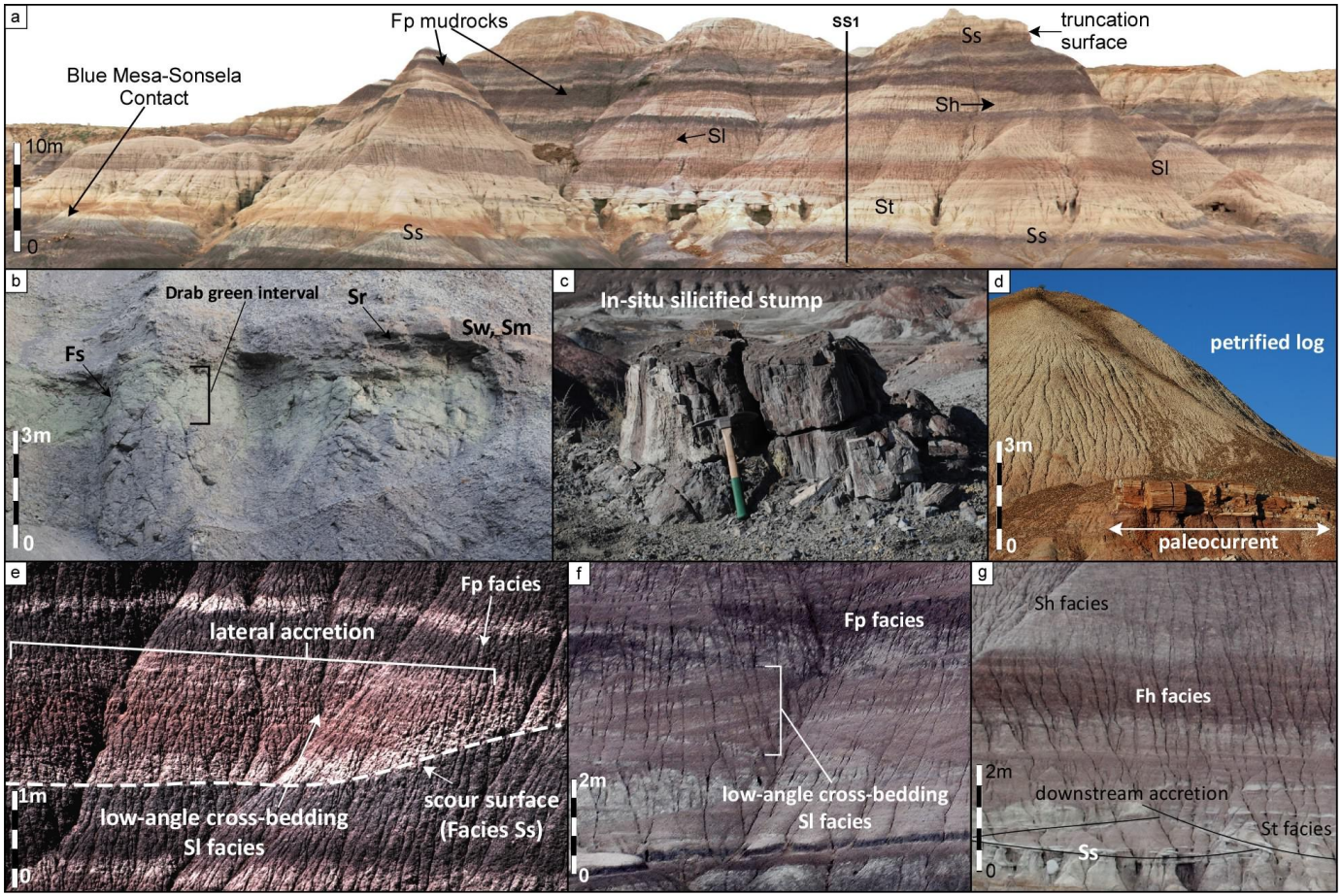

Figure 3.7. Photographs of a) lower Sonsela Member outcrop. Light colors are sandstones whereas darker colors are mudrocks. The Blue Mesa-Sonsela Member contact, distribution of fluvial facies (Table 3.1) and location of SS1 measured section are indicated; b) upper Blue Mesa Member drab green and gray mudrock interval with Fs (slickensides), Sr, Sw, and Sm facies indicated; c) in-situ silicified stump from drab green interval in the upper Blue Mesa Member; d) petrified log oriented downstream within channel facies of the lower Sonsela Member; e) scour surface and infill with lateral-accretion deposits within the lower Sonsela Member. Fp and Sl facies (Table 3.1) are indicated; f) low-angle cross-bedding (Sl facies) and pedogenically modified overbank deposits (Fp facies) within the lower Sonsela Member; g) downstream accretion architectural element and associated fluvial facies (Table 3.1) within the lower Sonsela Member.

Figures 3.5 and 3.7a). The succession fines upward and sandstones become single-story, thinner and predominantly composed of the Sh and Sl facies (Figures 3.5 and 3.7a). A truncation surface overlain by sandstones that contain Gt and St facies occurs at the top of the outcrop (Figures 3.5 and 3.7a). This facies succession is consistent across the entire 0.5 km outcrop (Figure 3.5). Paleocurrent data indicate an easterly to southeasterly flow direction (Figure 3.5; Rose diagrams 1 and 2). Sandstones are interpreted to have accumulated as channel-filling sandy bedform, downstream-, and lateral-accretion deposits and floodplain-draping crevasse-splays (Miall, 1978; 1985; 1996; Trendell et al., 2012). Mudrocks are interpreted as proximal and distal overbank deposits as they contain Fp, Fl, and Fs facies (Table 3.1; Miall, 1978, 1985, 1996; Trendell et al., 2012).

Paleosols

Three pedotypes (representative paleosols) were identified by lithostratigraphic location within the study interval (the Newspaper Rock interval, the Blue Mesa, and lower Sonsela Members).

Newspaper Rock Interval. The type paleosol for the Newspaper Rock interval is the red paleosol weathered into the channel deposits and its coeval interfluve overbank deposits (Figure 3.8). This paleosol is a composite of two welded soils that are non-calcareous with an A-Bss1-Bss2-C/B horizon sequence overlying a possibly truncated Bssb-Cb horizon sequence (Figure 3.8). These two paleosols have red (10R, 7.5R) matrix, angular blocky to wedge-shaped structure, few to common slickensides, and few to common iron-depleted calcified root traces (rhizoliths) that could have a diagenetic origin (Figure 3.8). The paleosols have characteristics similar to modern Vertisols, i.e.,

high clay content in the presence of slickensides (Soil Survey Staff, 1999). The decompacted solum thickness is 297 cm (2.97 m). The parent material of these soils was ripple-laminated mudrock. The CALMAG index of weathering suggests mean annual precipitation at the time of pedogenesis was approximately 1335 mm (Table 3.2).

Blue Mesa Member. The Blue Mesa pedotype is a non-calcareous Bss1-Bss2-Bss3-C horizon sequence weathered into the top of a fining-upward fluvial succession approximately 4 m below the Blue Mesa-Sonsela Member contact (Figures 3.4 and 3.8). Truncated at the top, the paleosol is dark blue (5PB 4/1) with angular blocky to wedge-shaped ped structure, few to common slickensides, and few to common iron-depleted rhizoliths (Figure 3.8). Both high clay content and slickensides suggest this paleosol is similar to modern Vertisols (Soil Survey Staff, 1999). The decompacted solum thickness is 160 cm (1.60 m). The parent material consisted of laminated overbank fines, and the CALMAG weathering index suggests mean annual precipitation of approximately 1316 mm (Table 2).

Lower Sonsela Member. The type paleosol for the lower Sonsela Member includes a non-calcareous, A-Bss1-Bss2-C/B horizon sequence characterized by 5R3/1 matrix colors, subangular blocky to wedge-shaped peds, few to many slickensides and zones of iron depletion that decrease from the upper horizon downward (Figure 3.8). Both high clay content and slickensides suggest this paleosol is similar to modern Vertisols (Soil Survey Staff, 1999). The decompacted thickness of the paleosol solum is 231 cm (2.31 m), and the parent material is horizontally or ripple laminated very fine

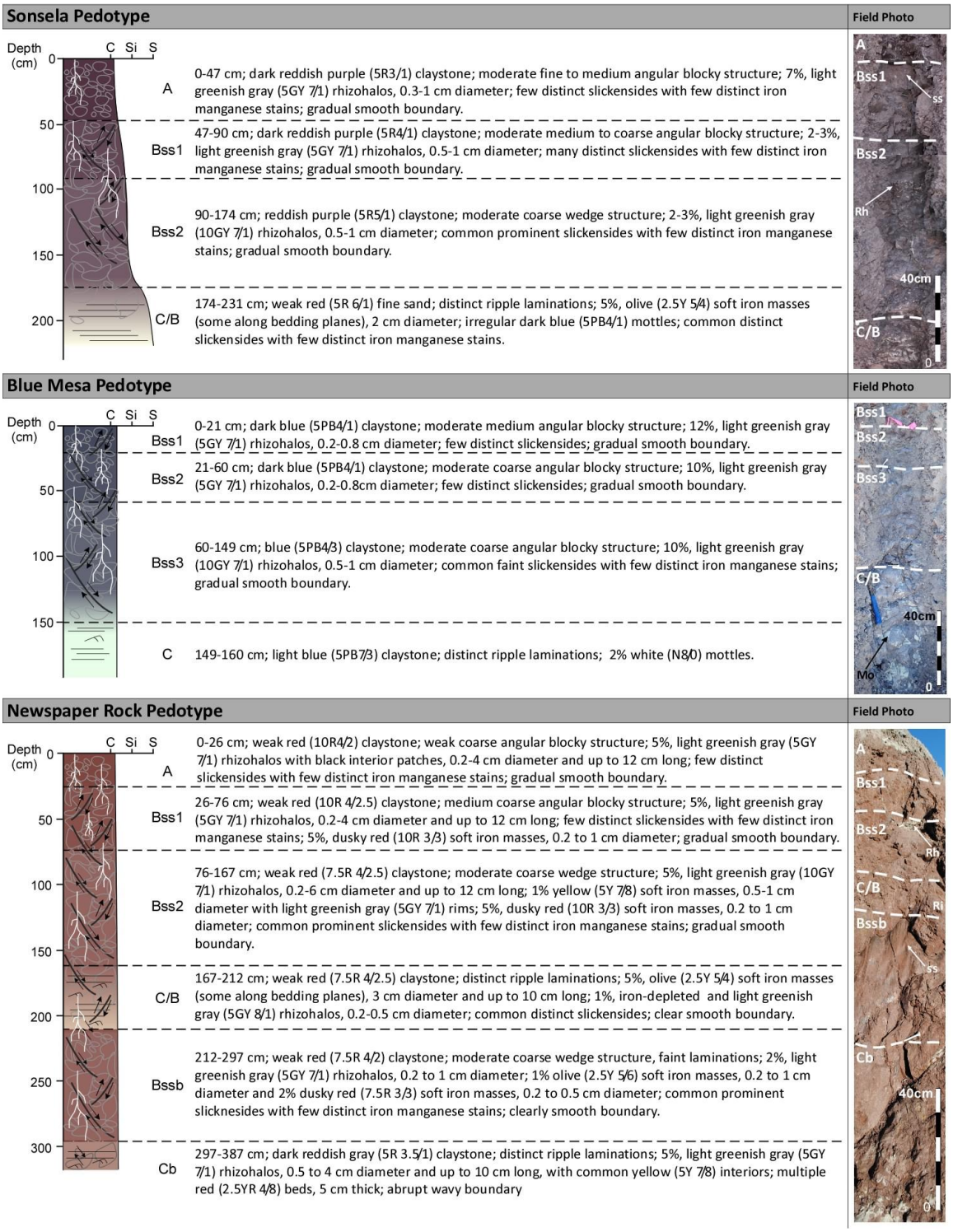

Figure 3.8. Graphical illustrations, thicknesses, horizon designations, field descriptions and field photograph of the Newspaper Rock, Blue Mesa and Sonsela pedotypes. Colors of graphical illustrations are representative of matrix colors within the paleosols. Field photos show matrix color, horizons, rhizohalos (Rh), slickensides (ss) and mottles (Mo).

Table 3.2. Bulk elemental data and calculated CALMAG and Mean Annual Precipitation (MAP; mm/yr) from B horizons of the study area paleosols. Paleosols which are pedotypes are highlighted within the 'Pedotype' column. MAP values are plotted by paleosol ID on Figure 3.12 (those with two values were described twice and are averaged in Figure 3.12).

Paleosol ID #	Pedotype	Al_2O_3 (%)	CaO (%)	MgO (%)	CALMAG	MAP (mm/yr)
1	N/A	18.08	0.67	1.64	76.9	1306
2	Newspaper Rock	14.45	0.39	1.29	78.2	1335
3	N/A	19.46	0.64	1.44	79.9	1375
3	N/A	17.82	0.57	1.41	79.3	1359
3	N/A	10.96	0.34	0.98	77.8	1327
4	N/A	14.28	0.46	1.11	79.5	1364
5	N/A	17.35	0.69	1.31	79.0	1353
6	N/A	16.02	0.39	1.41	78.7	1347
7	N/A	15.55	0.71	1.82	72.2	1200
8	Blue Mesa	17.35	0.69	1.49	77.3	1316
9	N/A	16.78	0.70	1.46	77.0	1308
10	N/A	16.36	0.74	1.82	73.0	1219
11	N/A	14.89	0.49	1.38	77.1	1310
11	N/A	15.74	0.41	1.43	78.2	1334
12	N/A	15.57	0.59	1.44	76.5	1298
13	N/A	14.91	0.55	1.41	76.4	1294
13	N/A	15.68	0.46	1.39	78.0	1331
14	N/A	16.23	0.57	1.34	78.3	1338
14	Sonsela	15.91	0.53	1.48	77.0	1307
15	N/A	16.08	0.60	1.49	76.5	1298
16	N/A	16.93	0.57	1.51	77.5	1319

sand and silty-mudrock. The CALMAG weathering index suggests mean annual precipitation of 1307 mm (Table 3.2).

Pedogenic Summary. Red coloration across the surface of Newspaper Rock low-angle cross-stratification may suggest that the Newspaper Rock matrix color is inherited from eroded upland soils. Unlike the Newspaper Rock, Blue Mesa and Sonsela paleosols display a down-profile increase in color value and their BC and C horizons do not contain mudrock rip-up clasts, which suggests that their matrix colors are not inherited from

upland soil sediments. Although red matrix is interpreted to represent formation within a well-drained environment with high microbial oxidation of organic matter (Retallack, 1988; Retallack, 2001; Kraus and Hasiotis, 2006), this color may not be reflective of Newspaper Rock paleosol drainage due to its potential upland inheritance. Blue and purple matrix (characteristic of Blue Mesa and Sonsela paleosols, respectively) are interpreted to be post-burial diagenetic color alteration, inasmuch as blue and purple are not common modern soil colors (Retallack, 1991; Soil Survey Staff, 1999; Kraus and Hasiotis, 2006). Given that paleosols were subjected to the same burial history, however, it follows that variation in paleosol matrix colors may suggest variability in initial soil drainage (PiPujol and Buurman, 1994). Purple matrix is interpreted to reflect moderate to poor drainage (Kraus and Hasiotis, 2006), whereas blue matrix is from Fe reduction and may indicate saturated, anoxic conditions (Vepraskas, 1992; 2001). Major pedogenic processes for the Newspaper Rock, upper Blue Mesa and lower Sonsela paleosols include rooting, ped formation and shrink-swell processes (as indicated by abundant slickensides). Slickensides indicate soils were subjected to seasonal moisture deficits (Blodgett, 1984; Nordt et al., 2004). Morphologic characteristics suggest paleosols are similar to modern Vertisols where slickensides and ped structure form within decades to centuries (Soil Survey Staff, 1999; Nordt et al., 2004).

Petrography

Forty-two thin-sections were point-count analyzed and Quartz-Feldspar-Lithic (QFL) modal percentages were used to determine sandstone composition (Figure 3.9). One thin section was prepared from the lower Blue Mesa Member, sixteen from the Newspaper Rock, four from the upper Blue Mesa Member, and twenty-one from the

Sonsela Member. Average Quartz-Feldspar-Lithic values for each lithostratigraphic interval are shown in Table 3.3. The lower Blue Mesa Member sample was collected from a lateral-accretion deposit and is classified as a feldspathic litharenite (McBride, 1963; Figure 3.9). Newspaper Rock specimens were predominantly collected from lateral-accretion deposits and are classified as sublitharenites and litharenites (*sensu* McBride, 1963). Upper Blue Mesa sandstone samples were collected from crevasse-splay and lateral-accretion sandstones and are classified as feldspathic litharenites and sublitharenites (*sensu* (McBride, 1963). Sandstone samples from the lower Sonsela Member are classified as litharenites, feldspathic litharenites, and lithic sub-arkoses (*sensu* McBride 1963).

Table 3.3. Average QFL values, number of thin sections, and the range of QFL values for each lithostratigraphic subdivision.

		Quartz		Feldspar		Lithic Grains	
Stratal subdivision	#	Average %	Range	Average %	Range	Average %	Range
lower Sonsela	21	42	76 - 25	16	25 - 5	42	67 - 17
upper Blue Mesa	4	52	56 - 44	17	23 - 13	31	40 - 24
Newspaper Rock	16	81	89 - 56	1	4 - 0	18	43 - 11
lower Blue Mesa	1	41	N/A	18	N/A	41	N/A

Sandstones have high proportions of quartz and lithic grains. Lithic fragments are composed of altered volcanogenic fragments, and metamorphic and plutonic fragments. Newspaper Rock sandstones consist predominantly of quartz (with minor lithic grains) and the Blue Mesa and Sonsela Members have increasing proportions of lithic fragments. Sandstone compositional maturity systematically decreases upwards through the succession (Figure 3.9). Despite changing abundance, lithic fragments have similar composition throughout the succession, which suggests similar provenance.

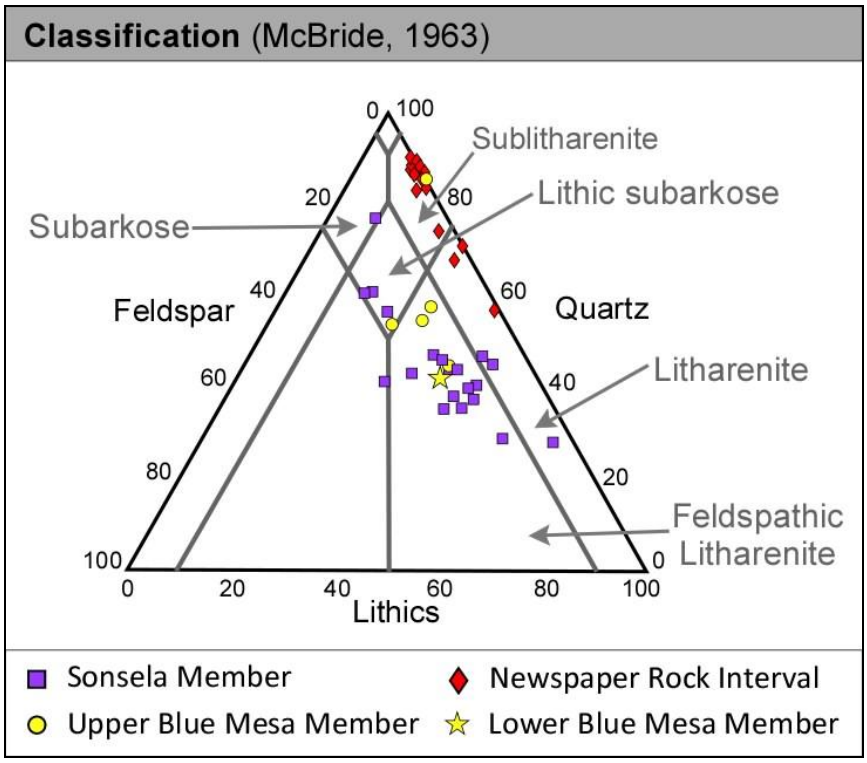

Figure 3.9. Sandstone compositional ternary diagrams for sandstone classification (McBride, 1963). Data are sorted by lithologic interval (Newspaper Rock, Blue Mesa and Sonsela Members). Data indicate that compositional maturity decreases up-section. The composition of the one lower Blue Mesa Member sample is represented by a yellow star.

Sandstone composition is consistent with studies by Cadigan (in Stewart et al., 1972) that report high proportions of volcanic detritus (25%) and quartz (35%) with considerably lower proportions of feldspar (11%). These data represent compositional averages for the entire 'Petrified Forest Member' (which included the current Blue Mesa, Sonsela and Petrified Forest Members; Martz and Parker, 2010). Sandstone compositions are also consistent with the Sonsela Member point-count data point in (Dickinson and Gehrels, 2008)). Unlike studies by Cadigan (1972) and Dickinson and Gehrels (2008), this study provides high-resolution vertical (every sandstone encountered within measured sections) and lateral (one to six sandstone point counts laterally per bed) sandstone composition data for the study interval at the "Blue Mesa" and "Tepees" areas

of PFNP. Petrographic data within this study is of the same resolution as sedimentological and stratigraphic observations and, therefore, can be used to compare provenance changes directly with changes in depositional style.

Sediment Accumulation Rates

Rates of sediment accumulation have been calculated using three absolute age estimates from detrital zircon grains. Age estimates within the study interval are from the green mudrocks in the upper Blue Mesa Member (223.036 ±0.27 Ma), the mid-lower Sonsela Member (219.317 ±0.27 Ma) and from laterally-equivalent Jasper Forest Beds of the Sonsela Member (218.017 ±0.28 Ma; Ramezani et al., 2011; Figures 3.1 and 3.10). Calculated rates of actual sediment accumulation vary throughout the succession from as little as 0.9 m/ 100 ka to 3.8 m/ 100 ka (Figure 3.10). The highest rates of sediment accumulation (3.8 m/ 100 ka) occur near the section base between the top of the Newspaper Rock to the green mudrock beds within the upper Blue Mesa Member (Figure 3.10). Above the green mudrock beds, rates of sediment accumulation decrease dramatically to 0.9 m/ 100 ka (Figure 3.10). Sediment accumulation rates increase slightly to 1.3 m/ 100 ka in the middle portion of the lower Sonsela Member (Figure 3.10). Only three zircon age dates provide relatively low-resolution sediment accumulation rates when compared with the high-resolution sedimentological and stratigraphic data presented. These data may not capture higher-frequency fluctuations in sediment accumulation and their interpretations are, therefore, tentatively applied.

Evolving Fluvial Deposition

Interpretations of fluvial style within each sub-division are based upon diagnostic characteristics (i.e. channel: overbank ratio, channel connectivity, characteristic elements, channel width: depth ratio, paleosol occurrence, and overall grain size) of suspended-, mixed- and bedload systems summarized by Miall (1996; and references therein; Figure 3.11).

Newspaper Rock Interval

The Newspaper Rock interval is interpreted here to have accumulated within a large (20m depth) channel. The succession of architectural elements within the Newspaper Rock interval is suggestive of suspended-load transport (Figure 3.11). Newspaper Rock channel deposits are interpreted as lateral accretion elements that were deposited within amalgamated bar forms and are separated by scour surfaces produced by chute and neck cutoff avulsions within the channel fill (Miall, 1996). Dip orientation of the lateral accretion surfaces suggest that point bars migrated towards the channel margin (cut-bank). Within the channel fill, scour surfaces likely reflect autocyclic variation in flood intensity. Thicker paleosols at the top of the BM5-2 and BM5-3 measured sections may represent abandoned channel fill deposits which were pedogenically modified.

Overbank mudrocks located on interfluve positions adjacent to the Newspaper Rock channel were pedogenically modified. Upon channel fill and abandonment, pedogenic processes then altered the top of the channel-fill deposits while continuing to modify interfluve sediments. This resulted in a welded paleosol (‘composite’ paleosol after Kraus (1999) in interfluve positions (Newspaper Rock pedotype of Figure 3.8). The

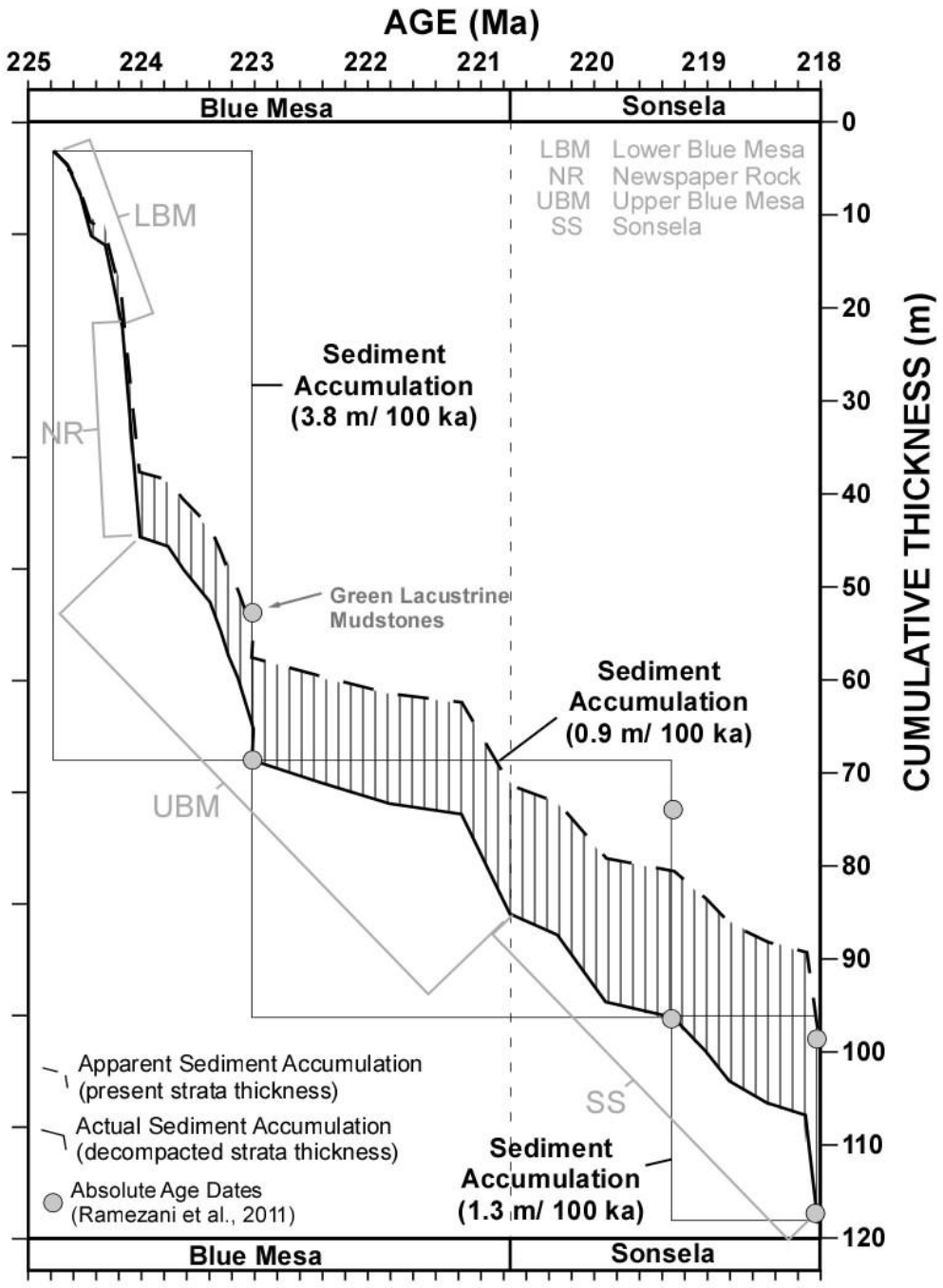

Figure 3.10. Sediment accumulation analysis of the study interval. Curves for both apparent sediment accumulation (present stratal thickness between paleosols) and actual sediment accumulation (decompacted stratal thickness between paleosols) are provided. Paleosol age assignments are derived from cumulative paleosol maturity interpolation between detrital zircon age dates (see the Methods section above). Plotted on the sediment accumulation chart are age-calibrated distribution of lithostratigraphic boundaries, absolute ages, and subsidence 'zones' (i.e., 3.4 cm/1000yrs, 0.8 cm/1000 yrs, and 1.2 cm/1000 yrs).

A.

Stratigraphic Interval		Bedload						Mixed-load						Suspended-load					
Features		**C:O -** high	**CC** - multi-story	**E*** - DA, SB	**W/D** - >40	**P** - rare	**GS** - coarsest	**C:O -** approx. equal	**CC** - multi- and single	**E*** - DA, LA, SB, PO	**W/D** - 10 - 40	**P** - present	**GS** - coarse to fine	**C:O -** low	**CC** - single story	**E*** - LA, Op, CS	**W/D** - <10	**P** - common	**GS** - finest
Sonsela	Jasper Forest Bed	X	X	X	X	X	X												
	Lot's wife Beds													X	X	X	X	X	X
	Camp Butte Bed	X			X				X	X		X	X						
Upper Blue Mesa														X	X	X	X	X	X
Newspaper Rock									X		X	X	X	X		X			
Lower Blue Mesa													X	X	X	X	X	X	

*Only major architectural elements are listed, although there are sometimes less common architectural elements within each fluvial style (see B)

B.

Features	Bedload	Mixed-load	Suspended-load
Channel:overbank ratio (C:O)	High channel to overbank; isolated interfluves	Channel and overbank elements	Low channel to overbank
Channel connectivity (CC)	Multi-story channel complexes	Some multi-story and single channels	Single channels isolated within overbank fines
Characteristic elements (E)**	DA, SB, (PO), (Op)	DA, LA, SB, PO, (Op)	LA, Op, TSB, (SB)
Channel width to depth ratio (W/D)	>40	10-40	<10
Paleosols (P)	Very rare, when preserved represent interfluve deposits	Rare, poorly to moderately developed	Common, moderately to well developed
Grain size (GS)	Coarse	Coarse to fine	Medium to fine

**Elements are listed in order of abundance from most to least common. Those elements in brackets are minor. See Table 1 for definition.

Figure 3.11. A) Table illustrates which features (channel: overbank ratio, channel connectivity, characteristic elements, channel width: depth ratio, paleosols, and grain size) are associated with bedload, mixed-load, or suspended load fluvial style to the various lithostratigraphic units. Blue Mesa Member - features are suggestive of deposition within a suspended-load system. Newspaper Rock interval - features of both suspended-load and mixed-load deposition. Sonsela Member - has characteristics that suggest fluctuation between bedload, mixed-load and suspended-load. B) Summary table of characteristic features in bedload, mixed-load and suspended-load fluvial systems (Schumm, 1963; 1985; Miall, 1985; 1996).

red coloration of sediment within the Newspaper Rock lateral-accretion deposits suggests that the red matrix of the Newspaper Rock paleosol may have been inherited from eroded upland soils. Considering the potential inheritance of color and that the CALMAG weathering index suggests mean annual precipitation of 1340 mm (similar to that of Blue

Mesa and Sonsela paleosols, which are blue and purple; Figure 3.12[1]), paleosol drainage may likely have been similar to the Blue Mesa Member.

Sandstones within the Newspaper Rock interval have a high proportion of stable quartz grains, and a low proportion of volatile feldspars and lithic fragments, suggesting different source regions than the Blue Mesa and Sonsela Members, lower rates of sedimentation, greater reworking and destruction of labile grains prior to deposition or a grain-size bias (Figure 3.12). Considering that lithic grain types remain relatively similar throughout the study succession (consistent presence of volcanic rock fragments), a change in source region is not likely to have caused the increased sandstone maturity. With increasing time and distance from the fluvial source region, there is a progressive increase in sediment maturity (Johnsson and Stallard, 1989; Johnsson and Meade, 1990; Johnsson et al., 1991). Sandstone composition may suggest that the Newspaper Rock interval represents either the most 'distal' portion of the study succession or may have the lowest rates of sedimentation from an immature source region.

Alternatively, sandstone composition may reflect a grain size bias. The smaller grain size of the Newspaper Rock sandstones (when compared with upper Blue Mesa and Sonsela sandstones) may have resulted in a lower proportion of volcanic lithic grains within the sandstones. Volcanic detritus is relatively weatherable when compared with other sand types, resulting in their preferential reduction in finer size fractions.

---

[1] This measured section includes both the total stratal thickness of the Newspaper Rock interval (as described in BM 5-2) and the total thickness of the lower Blue Mesa strata (as described in measured section BM4-2). The conceptual measured section represents a time-sequence of stratal characteristics (as determined by cross-cutting relationships) rather than true stratal thickness of the study succession. Thicknesses of individual strata are accurate to the measured sections. Lithostratigraphy (after Martz and Parker, 2010) is shown on the left. Sedimentary key for this measured section is the same as Figure 3.4.

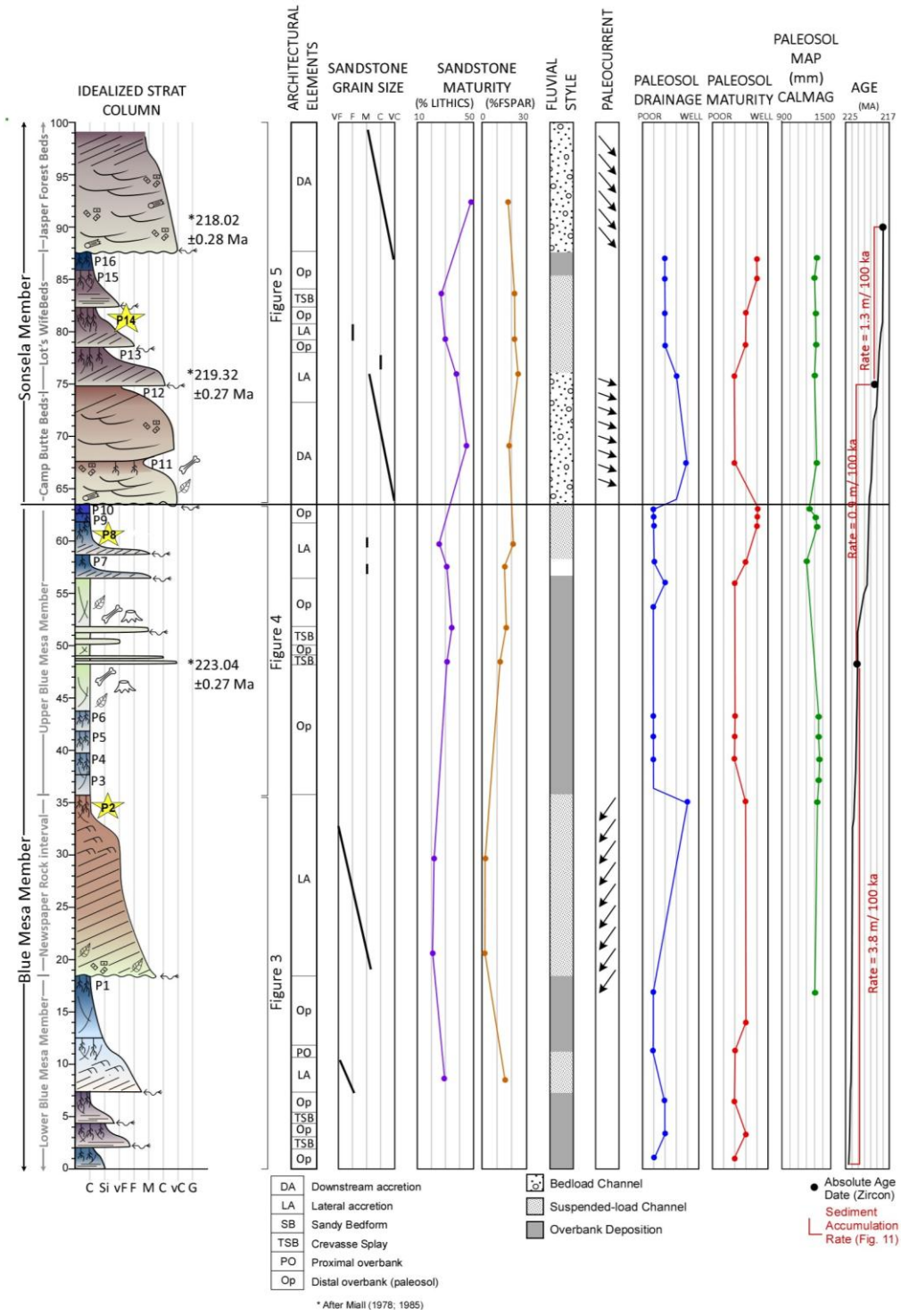

Figure 3.12. A conceptual composite measured section that documents the vertical succession of lithofacies and their attributes (colors reflect color of rock units). Adjacent to the measured section are columns summarizing figures of cross-sections, architectural elements, sandstone grain size, sandstone maturity (displayed as % of lithic grains and feldspars; calculated as averages when more than one sandstone sample was point-counted), interpreted fluvial style (based on succession of architectural elements), paleocurrent, paleosol maturity (based on paleosol morphological features) and drainage (based on paleosol color), calculated MAP, and subsidence rates.

Blue Mesa Member

Blue Mesa Member (lower and upper) channel deposits are relatively thin, isolated and separated by thick overbank successions (Figure 3.12). Channels were significantly smaller than that of the Newspaper Rock channel with thickness ranging from 1 to 3 meters depth and having lateral extent of only tens of meters. As with the Newspaper Rock interval, channel deposits are dominated by lateral-accretion architectural elements and depositional features are suggestive of suspended-load transport (Figures 3.11 and 3.12). Crevasse-splay deposits make up a higher proportion of the stratigraphic interval, suggesting splay processes played an important role in the Blue Mesa system. The size and architectural elements of upper and lower Blue Mesa channel deposits suggest that the fluvial system had lower competence and capacity than the Sonsela fluvial system (Figures 3.11 and 3.12). High crevasse-splay to channel deposition combined with high preservation of overbank deposits suggests that the fluvial system may have been poorly confined within a relatively large fluvial valley (Nichols and Fisher, 2007; Weissmann et al., 2011).

Drab-green intervals within the upper Blue Mesa Member are interpreted as ephemeral back-swamp or vernal floodplain ponds due to their color (suggesting iron-reduction) and fossil assemblage (e.g. fish fossils; Murry and Long, 1989; Heckert, 2004). Blue (10PB) and purple (5R) paleosol matrix colors suggest upper Blue Mesa floodplains were poorly drained (Vepraskas, 1992; 2001). Abundant slickensides in both drab-green deposits and paleosols indicate periodic drying of overbank environments. Despite an apparent decrease in overbank drainage (paleosols and lacustrine intervals) within the Blue Mesa Member (relative to the Newspaper Rock interval), mean annual

precipitation does not significantly increase (Table 3.2). Saturation of modern soils has been attributed to both epi-saturation (from above) and endo-saturation (from below; Vepraskas, 1992; 2001). Considering that saturation of overbanks does not appear to be due to an increase in water input from the surface, Blue Mesa paleosol saturation may be attributed to high groundwater table.

Rates of sediment accumulation were greatest at the time of deposition of this part of the study succession and may indicate high subsidence rates. High rates of subsidence could have resulted in a relative rise in base-level and water table. Increased proportions of crevasse-splay and overbank rocks may have been deposited and preserved due to increased aggradation and decreased self-cannibalization of the fluvial system in the high-accommodation setting.

Sandstone maturity decreases within the upper Blue Mesa Member (relative to the Newspaper Rock interval; Figures 3.10 and 3.12). A change in provenance may be responsible for the influx of immature detritus or, alternatively, sandstones of the Blue Mesa Member may have undergone less overall chemical and physical weathering due to increased sediment bypass in regions proximal to the source (Johnsson and Stallard, 1989; Johnsson and Meade, 1990; Johnsson et al., 1991). As argued above, a change in provenance seems unlikely as the entire succession contains similar lithic grains but in varying proportions.

Sonsela Member

The contact between the Blue Mesa and Sonsela Members is abrupt and overlain by medium-grained, multi-story sandstone elements with abundant scour and reactivation surfaces. Sandstones of the Sonsela Member are thicker, coarser-grained and more

abundant than sandstones of the Blue Mesa Member (Figure 3.12). Channel size at the base of the Sonsela Member (in the Lot's Wife Beds) range from 3 to 10 meters depth. Features of the Sonsela Member suggest that it accumulated within a fluvial system with a greater proportion of mixed- and bedload transport than the Newspaper Rock and Blue Mesa (Figure 3.11). The Sonsela sedimentary succession evolved from deposits suggestive of deposition from bedload transport at the base (Camp Butte Bed, Figure 3.11) to deposits suggestive of deposition from suspended-load transport (Lot's Wife Beds, Figure 3.11). These channels are smaller, and range from 1 to 3 meters in depth. This succession has been interpreted to represent the gradual migration of the fluvial channel away from the study area (Trendell et al., 2012). An erosional unconformity at the top of the succession is overlain by sediments with characteristics suggestive of deposition from bedload transport (i.e., the Jasper Forest Bed, Figure 3.11), which has been interpreted to be suggestive of avulsion or migration of the fluvial channel back to the study area (Trendell et al., 2012). Channels at the top of the Sonsela study succession range in depth from 4 to 10 meters, similar to those of the base of the Sonsela succession.

The lack of overbank deposits in the lower portion of the succession is attributed to cannibalization and reworking as a result of channel drift across the alluvial valley (*sensu* Cain and Mountney, 2009; Figure 3.12). Low rates of sediment accumulation (and therefore accommodation generation; Figure 3.10) result in channel elements that became vertically stacked in a multi-story complex. Each successive stacking of fluvial channel elements likely cannibalized the upper part of the older underlying elements, resulting in a high channel: overbank ratio. Channel sandstones at the base (Camp Butte's beds) and top (Jasper Forest bed/Rainbow Forest bed) of the Sonsela outcrop extend continuously

across the outcrop (0.5 km) and have been correlated across much of the Petrified Forest National Park (380 km^2; Martz and Parker, 2010). This suggests the fluvial channel was free to drift across a large, non-confined valley (Figures 3.5 and 3.7a). Paleocurrent indicators suggest flow was perpendicular to that observed within the Newspaper Rock interval (Figure 3.12), however, these in-channel flow indicators indicate channel rather than overall fluvial system flow direction.

Sonsela paleosols are predominantly purple in color with lesser red and blue (Figure 3.12). Purple matrix is interpreted to reflect moderate paleosol drainage (Kraus and Hasiotis, 2006). From the Blue Mesa to the Sonsela Member, paleosols have lesser proportions of blue paleosols indicating improved soil drainage. Despite this, estimates of mean annual precipitation are similar to those for the Newspaper Rock and Blue Mesa paleosols (Table 3.2; Figure 3.12). Better drainage may reflect an increase in evaporation (climate) or a lowering of the groundwater table (base-level change; Retallack, 2001).

The decrease in sandstone compositional maturity from the Newspaper Rock through the Sonsela Member may reflect decreased destruction of labile detritus related to increased sediment bypass in proximal portions of the fluvial system (Johnsson and Stallard, 1989; Johnsson et al., 1991), or may reflect increased erosion in the source area.

Chinle Depositional Model

Fluvial systems in continental basins contain both large fluvial fans and tributary systems (Sinha and Friend, 1994; DeCelles and Cavazza, 1999; Hartley et al., 2010; Weissmann et al., 2010; Weissmann et al., 2011). Depositional processes within large fluvial fans depart from those of tributary systems in that nodal avulsion and unconfined flow play a more dominant role in sediment distribution (Kelly and Olsen, 1993; Shukla

et al., 2001; Billi, 2007; Fisher et al., 2007; Nichols and Fisher, 2007). These less-stable fluvial systems that experience high rates of avulsion are commonly within flashy discharge regimes within semi-arid ((Friend, 1978; Kelly and Olsen, 1993; Billi, 2007; North et al., 2007) or monsoonal (Leier et al., 2005; Gibling et al., 2005) climates. This results in more than one simultaneously active channel and 'underfitting' resulting in decreased discharge within the original channel (Dury, 1964; Friend, 1978; Smith et al., 1989; Hirst, 1991; Fisher et al., 2007; Nichols and Fisher, 2007). Decreased discharge combined with high rates of avulsion result in changes in fluvial facies downstream that may be recognized in the rock record.

The literature catalogues the diagnostic sedimentological attributes that may allow the interpretation of ancient fluvial fans (a progressive downstream decrease in grain size, a decrease in channel depth and width, an increase in overbank preservation and crevasse-splay and/or sheetflood deposition on a basin scale, and a decrease in lateral and vertical connectivity of channel deposits (Hirst, 1991; DeCelles and Cavazza, 1999; Shukla et al., 2001; Horton and DeCelles, 2001; Nichols and Fisher, 2007; Cain and Mountney, 2009; 2011; Weissmann et al., 2011). Large fluvial fans contain four general regions: 1) Proximal fan, 2) Medial fan, 3) Distal fan, and 4) Axial or inter-fan river (Hirst, 1991; Shukla et al., 2001; Horton and DeCelles, 2001; Nichols and Fisher, 2007; Cain and Mountney, 2009; Cain and Mountney, 2011; Weissmann et al., 2011), whose attributes are summarized within Table 3.4.

Overall, large fluvial fans have the capacity for much higher overbank preservation than tributary fluvial systems (Hartley et al., 2010; Weissmann et al., 2010; Weissmann et al., 2011) because fluvial channels are non-confined and occupy a small

proportion of the total fan (fluvial valley) area. If vertical aggradation is not possible (accommodation decreases), non-confined active fluvial channels will increase rates of lateral migration and avulsion across the fan surface carving erosional bases and cannibalizing overbank deposits. Preservation potential of various deposits is, therefore, influenced by both location within the depositional system and accommodation setting.

To date, ancient fluvial deposits interpreted as large fluvial fans have been demonstrated to have accumulated as lobe-shaped sediment wedges on the basis of correlative basin-scale data (Graham, 1983; DeCelles and Cavazza, 1999; Horton and DeCelles, 2001; Nichols and Fisher, 2007; Cain and Mountney, 2009; Cain and Mountney, 2011). Exposure and preservation of Chinle Formation outcrops, however, are not amenable to determining laterally-continuous three-dimensional stratal relationships without rigorous age control. Geochronologic correlation of isolated Chinle outcrop successions has predominantly relied on palynological and vertebrate correlations with marine equivalents in Europe (Cornet, 1993; Lucas, 1998; Irmis and Mundil, 2008), paleomagnetics (Zeigler et al., 2008), and isolated zircon age dates (Riggs et al., 1996; Riggs et al., 2003; Irmis and Mundil, 2008; Dickinson and Gehrels, 2009; Heckert et al., 2009; Ramezani et al., 2011).

Blue Mesa and Sonsela Members

Although the preservation potential of large fluvial fans has been a contentious topic (Fielding et al., 2012), large fluvial fans represent a class of fluvial systems that largely accumulate within continental basins (Hartley et al., 2010; Weissmann et al., 2010; Weissmann et al., 2011) and it follows that ancient continental basins, such as the Chinle Basin, may be filled by large fluvial fans. The study interval at the Petrified Forest

Table 3.4. Summary of characteristic sedimentological attributes of large fluvial fan subareas (Hirst and Nichols, 1986; Hirst, 1991; DeCelles and Cavazza, 1999; Shukla et al., 2001; Horton and DeCelles, 2001; Fisher et al., 2007; Nichols and Fisher, 2007; Cain and Mountney, 2009; 2011; Weissmann et al., 2011).

Features	Proximal Fan	Medial Fan	Distal Fan
Gradient	highest in the system	medium	lowest in the system
Discharge	highest in the system	medium	lowest in the system
Competence and capacity	highest in the system	medium	lowest in the system
Grain size	coarsest in the system	medium	finest in the system
Sediment load	most likely bedload	depending on competence and capacity, may be mixed-, suspended-, or bedload	most likely to be suspended load
Architectural elements*	downstream accretion and gravel bars	crevasse splay, channel (including downstream and lateral accretion), and overbank	overbank, crevasse splay, and lateral accretion
Channel: overbank ratio	highest in the system	decreased relative to proximal fan, increased relative to distal fan	lowest in the system
Scour and reactivation surfaces	common	decreased abundance relative to proximal fan, increased relative to distal fan	rare
Channel connectivity	highest in the system	decreased relative to proximal fan, increased relative to distal fan	lowest in the system
Sandstone maturity	most immature in the system (dependant on source region)	increased relative to proximal fan, decreased relative to distal fan	most mature in the system (but is dependent upon the source region)
Overbank preservation	lowest in the system	increased relative to proximal fan, decreased relative to distal fan	highest in the system
Overbank drainage	topographically the highest portion of the depositional system with the coarsest sediments = greater drainage	decreased relative to proximal fan, increased relative to distal fan	low topography and fine grain sizes = decreased drainage, ponding of water ("Spring Line" of Weissmann et al., 2010; 2011)**

* Architectural elements listed in order of likely abundance. Architectural elements most likely to occur are included; however, those deposited and preserved are dependent upon the overall grain size, fluvial competence and capacity, and discharge of the fluvial system.

** Modern distributive fluvial systems are distinct from more proximal regions because the regional groundwater table commonly meets the fan surface (i.e., "Spring line" of Hartley et al., 2010; Weissmann et al., 2010; Weismann et al. 2011; see Figure 3.12 this text). As a result, water commonly ponds and overbanks become saturated (see Figure 3.13). This results in sediment accumulating within lacustrine environments and overbank paleosols forming under saturated conditions (Hartley et al., 2010; Weissmann et al., 2010; Weissmann et al., 2011).

National Park may be one such example of a progradational fan. The stratal succession from the Blue Mesa through Sonsela Member coarsens upwards, unlike fining-upward patterns typical of tributary fluvial system basin-fill (Wright and Marriott, 1993; Shanley and McCabe, 1994; Catuneanu, 2006). The succession suggests a history of progressively increasing channel depth and width, increasing lateral and vertical connectivity of channel-fill elements, decreasing abundance of crevasse-splay and/or sheetflood deposits, and decreasing preservation of overbank deposits (Figure 3.12). Similar observations within the Permian Organ Rock Formation (Cain and Mountney, 2009; Cain and Mountney, 2011), the Oligo-Miocene Ebro Basin (Hirst, 1991; Nichols and Fisher, 2007), the Tertiary in the central Andes (Horton and DeCelles, 2001) and the Campanian-Maastrichtian in Utah (DeCelles and Cavazza, 1999) have been attributed to large fluvial fan deposition.

Features within the lower and upper Blue Mesa Member are consistent with the distal portion of a large fluvial fan (Table 3.4; Figure 3.13). The Blue Mesa is dominated by overbank mudrock, has evidence for ponded water and overbank saturation, and has isolated channel sandstones with abundant crevasse-splay deposits (Figures 3.12 and 3.13; Table 3.4). The overlying Sonsela Member has coarser grain-sizes and a higher proportion of bedload channel deposits that are consistent with more proximal (medial) fan deposition (Figures 3.12, 3.13, and Table 3.4). Increasingly better drained paleosols (from the Blue Mesa to the Sonsela) may record progradation of the large fluvial fan wedge, i.e., the vertical stratal succession records progressively more upland positions through time. The "progradation of a large fluvial fan" model provides a mechanism that accounts for depositional element trends, paleosol drainage changes within stable MAP,

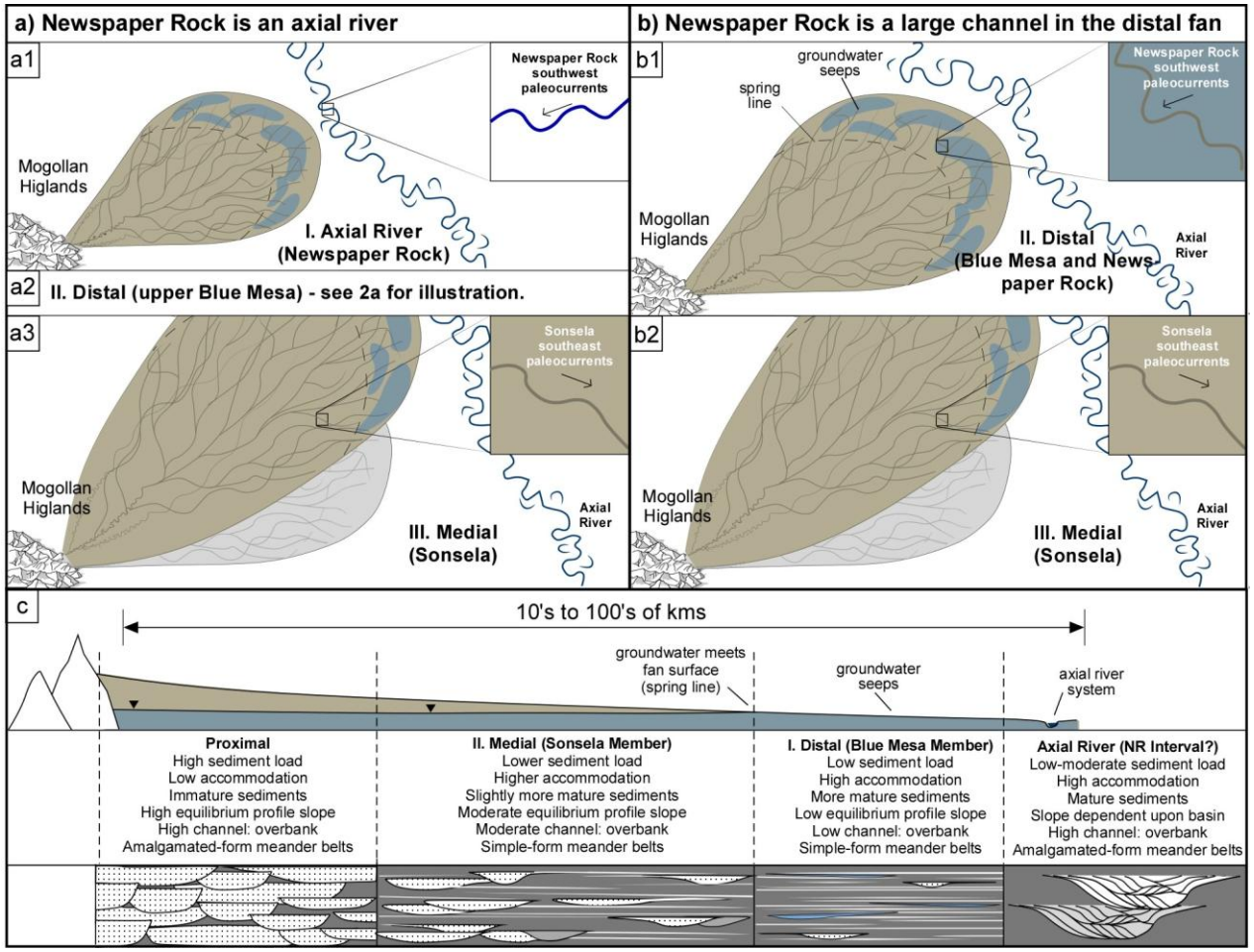

Figure 3.13. Conceptual illustrations showing the evolution of the Chinle system for interpretations of the Newspaper Rock interval: a) the Newspaper Rock was an axial river and the system evolves from a1) axial river to a3) medial fan; or b) the Newspaper Rock is a large channel within the distal fan and the system evolves from b1) distal fan to b2) medial fan. (c) A conceptual cross-section of a fluvial fan shows facies trends and drainage patterns within different fan regions. Large fluvial fan diagnostic attributes based on observations, descriptions and aerial photographs by Hirst, (1991), DeCelles and Cavazza (1999), Shukla et al. (2001); Horton and DeCelles (2001), Nichols and Fisher (2007), Cain and Mountney (2009), Cain and Mountney (2011), Weissmann et al. (2011).

and decreased sandstone maturity within a decreasing-subsidence regime, characteristics that are difficult to explain if the succession had been deposited within a classic tributary fluvial system.

Although the study succession displays characteristics similar to deposits of modern and ancient avulsion systems (characterized by coarsening-upwards heterolithic alluvial deposits containing ribbon sandstones encased in overbank deposits with poorly-developed, hydromorphic paleosols; (Kraus, 1996; Kraus and Wells, 1999), it is not likely that the study succession was deposited within a large splay complex off of a large tributary system. Although avulsion complexes may have long modern lifespans (>100 years; Kraus and Wells, 1999), it is difficult to fathom an avulsion complex that is present and potentially active for the 6 Ma time-span represented by the study succession. Considering the 6 Ma time-span, it also seems unlikely that there would be a complete lack of age-equivalent trunk channel-deposits preserved or exposed for the study succession if it had accumulated purely as avulsion deposits. Additionally, the apparent connectivity of the lower Chinle depositional system, as suggested by stratal thicknesses, paleocurrent, volcanic compositions, and conglomerate clast sizes up to 300 km south of the study area, is indicative of a large depositional system and inconsistent with a pure 'large splay complex' model.

Newspaper Rock Interval

The Newspaper Rock, which contains architectural elements of suspended-load transport similar to other Blue Mesa Channels, may represent either deposition within a tributary river system located adjacent to the fan (DeCelles and Cavazza, 1999; Hartley et

al., 2010; Weissmann et al., 2010; Weissmann et al., 2011);e.g., Figure 3.13a), or within a large channel within the distal fan (Figure 3.13b).

Compositional maturity of Newspaper Rock sandstones may suggest considerably more reworking than those in the lower Blue Mesa, upper Blue Mesa, and Sonsela Members (Figures 3.9 and 3.12), as would be expected within a channel that is distal to the fluvial source. Newspaper Rock paleoflow directions, perpendicular to those observed within the Sonsela Member, suggest axial flow along the edge of the fan system, however, these in-channel features are indicative of in-channel flow direction, and not necessarily the overall flow direction of the fluvial system. Given that the Newspaper Rock interval is both under- and overlain by distal fan deposits (lower and upper Blue Mesa), it is difficult to explain mechanisms that could account for the succession of facies observed if the Newspaper Rock is interpreted as an axial channel. This scenario would require pulses of progradation and retrogradation of the fan at high frequencies.

Considering that the Newspaper Rock interval is both under- and overlain by deposits suggestive of distal fan sedimentation, an alternative interpretation is that the Newspaper Rock channel is a large channel within the distal portions of the fan system. Studies of modern large fluvial fans document channels of varying sizes within the different sub-regions of a large fluvial fan (Weissmann et al., 2011).

Regional Context

Within the context of the proposed depositional model, the northwest trending trunk river of the Chinle Formation (Blakey and Gubitosa, 1983; Blakey and Gubitosa, 1984; Dubiel and Skipp, 1992; Dubiel, 1994; Riggs et al., 1996) may be an axial river

system within the Chinle Basin. Consistently north to northwest paleocurrents and increasing conglomerate clast sizes, stratal thicknesses, and volcanic content in the lower Chinle towards the south suggest that detritus originated from a major southerly source area (Stewart, 1969; Stewart et al., 1972; Blakey and Gubitosa, 1983; Stewart et al., 1986). In contrast, paleoflow directions within the study interval are dominantly southeast to southwest, which may be due to meander bends and a radial drainage pattern within the large fluvial fan system. Petrified Forest National Park is approximately 300 – 400 km from the hypothesized location of the Mogollan highlands to the southeast (Figure 3.2). Large fluvial fans of this size do exist in modern foreland and compressional continental basins (Hartley et al., 2010; Weissmann et al., 2010; Weissmann et al., 2011; Geddes, 1960; Mohindra et al., 1992; Sinha, 1996; Gibling et al., 2005; Sinha et al., 2005).

Forcing Mechanisms

High rates of sediment accumulation (3.8 m / 100 ka years) throughout deposition of the Blue Mesa may have accommodated aggradation of the distal fluvial system. Within the context of this model, transition from depositional elements within the Blue Mesa Member to the Sonsela Member could be attributed to: 1) transition of the basin from under- to overfilled; or 2) an increased sediment-load relative to subsidence that resulted in the progradation of a large fluvial fan wedge. If the basin transitioned from underfilled (accommodation gain) to overfilled (accommodation deficit), increased channel avulsion and migration would have resulted in cannibalization of overbank deposits and increased preservation of channel deposits as observed from the Blue Mesa to Sonsela. This mechanism alone, however, cannot explain increased grain sizes and

decreased sandstone maturity that is observed upsection. Progradation of a coarse clastic wedge, however, can explain these observations. The systematic decrease in sandstone compositional maturity from the Newspaper Rock through the Sonsela Member may be representative of increased erosion and sediment bypass and resultant deposition of coarse, immature sediments in increasingly more distal locations. Onset of reduced sediment accumulation rates (0.9 m/ 100 ka) may be reflective of decreased subsidence during deposition of the upper-most portion of the upper Blue Mesa Member. This may be the mechanism that resulted in a shift in the balance between availability of unfilled accommodation and the rate at which sediment is being supplied to fill that space.

Although the study succession was not likely deposited within a large splay or avulsion complex adjacent to a large trunk channel (as discussed above), it is likely that the Chinle system underwent avulsion at varying scales (ka to Ma) throughout deposition. Avulsion occurs on aggrading floodplains and occurs when flow is diverted away from the parent channel and seeks pathways of the highest gradient and greatest flow efficiency (Smith et al., 1989). Decelerating accommodation gain and progradation of the Chinle system would likely have promoted avulsion of the fan axis to higher gradient locations (Figure 3.13). Paleocurrent data indicate that the fan axis was initially located east of the study area (west-southwest paleocurrents within the Newspaper Rock) and was later located west of the study area (southeast paleocurrents within the Sonsela Member. Sediment build-up on the initial fan axis may have led to avulsion or redirection of the fan to a position west of its initial location, resulting in southeasterly paleocurrents in the Sonsela Member due to radial drainage of the fan system (Figure 3.13).

Study Area Limitations

Given the small extent and size of the study area relative to the Chinle Basin, observations for this succession cannot be conclusive in interpreting depositional systems and associated landforms that extend across hundreds of square kilometers. However, progradation of a large fluvial fan provides a mechanism that can account for depositional element trends, paleosol drainage changes within stable MAP, and decreased sandstone maturity within a decreasing-subsidence regime. Additionally, the lower Chinle strata have paleocurrent data with consistently north to northwest trends and increasing clast sizes, stratal thicknesses and volcanic content up to 300 km south of the study area. These features may suggest that the system was large and extended to the Mogollan highlands (Stewart, 1969; Stewart et al., 1972; Blakey and Gubitosa, 1983; Stewart et al., 1986). Increased basin-wide age control and stratigraphic correlations would aid in confirming a 'large fluvial fan' depositional model.

Implications of the Model

Previous studies of the Chinle and its equivalents within the southwestern USA have suggested aridification of western Pangea during the latest Late Triassic and Early Jurassic (Dubiel, 1987; Dubiel, 1994; Driese and Mora, 2002; Tanner, 2003; Prochnow, Nordt, et al., 2006; Tanner and Lucas, 2006; Cleveland et al., 2008; Dubiel and Hasiotis, 2011). Changing paleosol drainage indicated by changing paleosol matrix colors within the study succession at Petrified Forest National Park has been cited as evidence for early onset of this known long-term aridification (Tanner, 2003; Tanner and Lucas, 2006). Results from the present study, however, suggest that rather than the onset of Triassic-Jurassic aridification, the interval of time represented by the study interval more likely

records stable and high MAP. Improved drainage may have resulted, instead, from topographic position of the paleosols (i.e., evolution of the land surface to more upland positions on a large fluvial fan or a splay complex; Figure 3.13).

The Chinle Formation contains abundant vertebrate and paleobotanical fossils that have been crucial in understanding the distribution and evolution of Late Triassic ecosystems (Murry and Long, 1989; Ash and Creber, 1992; Therrien and Fastovsky, 2000; Ash and Creber, 2000; Parker and Irmis, 2005; Ash, 2005). The large fluvial fan depositional model is important to consider when interpreting faunal migration patterns, connectivity of ecosystems, and causes for extinction (fauna) or mass erosion (fossilized forests).

Summary

1. The study succession records a progressive up-section increase in grain size, increase in channel depth and width, increase in lateral and vertical connectivity of channel deposits, decrease in overbank preservation and crevasse-splay and/or sheetflood deposition, and increase in paleosol/ overbank drainage. Mean annual precipitation, however, (calculated using the CALMAG paleosol weathering proxy) remained relatively constant at ~1300 mm/yr throughout deposition of the succession.
2. Sandstones contain quartz, lithic fragments (volcanogenic, metamorphic, and igneous), and lesser proportions of feldspar grains. Sandstone composition displays an up-section decrease in mineralogical maturity through the Newspaper Rock-Blue Mesa-Sonsela succession.

3. The study interval at the Tepees and Blue Mesa areas of PFNP is interpreted to record deposition within a progradational large fluvial fan that underwent avulsion of varying scales throughout its history.
    a. The Blue Mesa Member has saturated conditions, high overbank: channel ratios, and high proportion of crevasse splay deposition consistent with accumulation within a high accommodation setting in low-lying topographic areas such as distal fan.
    b. Increasing channel depth and width, increasing lateral and vertical connectivity of channel-fill elements, and decreasing preservation of overbank deposits within the Sonsela Member are consistent with medial fan deposition and suggests that the Chinle fan underwent progradation.
    c. Decreasing sandstone maturity from the Newspaper Rock interval through the Blue Mesa and into the Sonsela reflects either increased sediment bypass in proximal regions or increased erosion and supply of immature sediments from the source region within a large fluvial fan.
    d. Given that MAP does not vary throughout the succession, increasingly better drained paleosols from the Blue Mesa to the Sonsela Member suggest progressively better-drained landscape positions due to progradation of a sediment wedge.
4. The Newspaper Rock channel is interpreted to represent either an ‘axial’ or ‘interfan’ channel or is a large channel within the distal fan area. Considering that the Newspaper Rock interval is both under- and overlain by deposits suggestive of distal fan sedimentation, it seems most likely that the Newspaper Rock is a large channel

within the distal fan area. Sequences within the Newspaper Rock channel-fill are interpreted autocyclic changes flood intensity.

5. Although the limited extent of the study area and succession cannot conclusively allow interpretation of large, basin-scale landforms without better age-control and well-correlated strata, the apparent size and extent of the lower Chinle system suggests that a ‘large fluvial fan’ may represent the lower Chinle depositional system.
6. Paleosol morphology and geochemistry, when combined with sedimentology, is a powerful tool that can aid in determining or refining depositional scenarios by providing a better-understanding of local climate.

CHAPTER FOUR

Determining Floodplain Plant Distributions and Populations using Paleopedology and Fossil Root Traces: Upper Triassic Sonsela Member of the Chinle Formation at Petrified Forest National Park, Arizona

This chapter has been submitted to the journal Palaios as: Trendell, A.M., Nordt, L.C., Atchley, S.C., LeBlanc, S.L. and Dworkin, S.I., Determining Floodplain Plant Distributions and Populations using Paleopedology and Fossil Root Traces: Upper Triassic Sonsela Member of the Chinle Formation at Petrified Forest National Park, Arizona: Palaios, *in review*.

Abstract

The Upper Triassic Sonsela Member of the Chinle Formation is an alluvial succession containing interbedded sandstones and pedogenically-modified mudstones. Despite preservation of silicified logs within channel sandstones, little is understood regarding the Sonsela plant ecosystem due to a lack of preservation of other plant taxa. Sonsela paleosols and rhizoliths are evaluated using macromorphology, micromorphology, and geochemistry to determine the spatial distribution of paleosol characteristics and plant sizes and densities across the study area. Three pedotypes identified within the Sonsela are classified as Inceptisols and Vertisols that exhibit fining of matrix textures (from clayey siltstone to claystone) and reduced drainage with distance from the paleo-channel. Overall, Sonsela paleosols are immature, suggesting that the Sonsela fluvial system experienced high rates of lateral migration and cannibalization of overbank sediments in a low-subsidence regime. Rhizohalos within the Sonsela Member are likely diagenetic and commonly include silicified roots (silica root petrifactions). Silicified roots provide information on root size and density that is not commonly afforded by other rhizolith types. Diagenetic rhizohalo diameters may be controlled by

paleosol matrix textures within the Sonsela Member. Rhizolith characteristics suggest that channel-proximal paleosols contained small-stature plants while distal floodplain paleosols may have hosted herbaceous understory, small-stature shrubby and arborescent plants. Paleosols within the Sonsela Member do not contain rhizoliths whose size or abundance are reflective of a dense coniferous forest. Floodplain plants were commonly small of stature and immature, unable to evolve into more mature communities due to high rates of cannibalization of floodplains during fluvial migration.

Introduction

The Sonsela Member at Petrified Forest National Park contains abundant (1-15 logs/ 100 m^2; Demko, 1995), spectacularly preserved silicified logs within fluvial channels (Daugherty, 1941; Ash, 1972; Demko, 1995; Ash and Creber, 2000; Creber and Ash, 2004). Their preservation within channels has been interpreted to suggest that coniferous forests inhabited the Sonsela floodplain ecosystem (Demko, 1995) and that paleosol characteristics may have been similar to modern forested soils (Retallack, 1997). However, conifers are only very rarely preserved *in-situ* within the lower Sonsela (W. Parker, personal communication, 2012), and channel logs rarely have roots and branches preserved, suggesting that logs may have been abraded during transportation for an undeterminable distance from an upstream source area (Demko, 1995). Some log orientations suggest that they were introduced (toppled) into the channel by cutbank erosion (Demko, 1995). Other than conifer logs, no other plant remains are preserved within the Sonsela Member (Demko et al., 1998) and as such, the Sonsela plant ecosystem is not well understood.

Because plant populations are both influenced by and alter soil characteristics (Brady and Weil, 2001), it follows that plant size, growth habits and lateral distributions may be inferred from paleosols. Rhizoliths are trace fossils or organosedimentary structures that preserve the activity of roots within paleosols (Klappa, 1980; Kraus and Hasiotis, 2006). Rhizoliths are the preserved features that reflect the zone of interaction between a plant root, the soil, and microorganisms ("rhizosphere" *sensu* Kraus and Hasiotis, 2006; Brady and Weil, 2001), making them useful for interpretation of paleosol moisture and drainage, depth to paleo-water table and paleosol primary productivity (Klappa, 1980; Pfefferkorn and Fuchs, 1991; Retallack, 2001; Kraus and Hasiotis, 2006; Hembree and Nadon, 2011; Nordt et al., 2011). Rhizoliths form from root-voids that (pedogenically or diagenetically) act as water-conduits resulting in the removal, translocation or precipitation of carbonate, clays, or iron (Fe) and manganese (Mn) constituents (Kraus and Hasiotis, 2006; Vepraskas, 1992; Vepraskas, 1996; Vepraskas, 2001; Retallack, 2001; Hembree and Nadon, 2011) and as a result, are preserved in various styles, sizes and morphologies. Plant sizes, heights, and densities may be inferred qualitatively from rhizolith characteristics (Pfefferkorn and Fuchs, 1991; LePage and Pfefferkorn, 2000; Hembree and Nadon, 2011); however, rhizolith dimensions are commonly an overestimation of the actual size of the living plant root (*cf.* Hembree and Nadon, 2011; Nordt et al., 2011). Using only rhizoliths, it is difficult to estimate actual plant size and below-ground plant biomass. Root petrifactions represent mineral replacement of root organic matter (Klappa, 1980) and, when present, provide information on root size, depth, and density that may only be qualitatively inferred from other rhizolith types (rhizohalos and rhizotubules). When rhizoliths are combined with

detailed paleosol morphological, geochemical, and micromorphological characteristics, and analyzed in conjunction with paleobotanical data, it may be possible to reconstruct plant formations and distributions inhabiting a paleo-landscape.

The goals of this paper are to examine Sonsela Member overbank deposits in order to: 1) determine the spatial distribution of paleosols and factors influencing their morphological, physical and chemical characteristics using detailed analysis of macromorphology, micromorphology and geochemistry; 2) analyze the morphologies and genesis (pedogenic vs. diagenetic) of rhizoliths and silica root petrifactions to determine what, if any, relationship may exist between rhizolith and root size; 3) understand what factors contribute to the limited preservation of *in-situ* tree stumps within the Sonsela Member at Petrified Forest National Park; and, 4) determine probable plant sizes, densities, heights and distributions by combining rhizolith and paleosol characteristics with the known paleobotanical record preserved within similar environments in strata underlying the study interval.

Geologic Setting

The Sonsela Member of the Chinle Formation is extensively exposed in the Petrified Forest National Park (PFNP; Figure 4.1). The Chinle Basin formed on the western margin of equatorial Pangea as a retro-arc basin and contained a north-west trending drainage system (Figure 4.1; Dickinson, 1981; Blakey and Gubitosa, 1983; Marzolf, 1993; Dickinson and Gehrels, 2008). Late Triassic Chinle sediments consist of paleosol-bearing alluvial strata (Stewart et al., 1972; Blakey and Gubitosa, 1983; Dubiel et al., 1991; Dubiel, 1994) that were deposited at approximately 5-15˚ paleo-latitude within a dynamic fluvial system (Van der Voo et al., 1976; Bazard and Butler, 1991;

Ramezani et al., 2011). The Sonsela Member accumulated as a mixed-load fluvial system (Demko, 1995; Woody, 2006; Trendell et al., 2012) during a period of low basinal subsidence rates (Ramezani et al., 2011). Previous paleopedological studies suggest that paleosols are similar to modern Calcic Alfisols (Tanner and Lucas, 2006), Alfisols (Retallack, 1997), and Vertisols of varying drainage (Trendell et al., 2012). Late Triassic climate in the southwestern United States was likely subtropical and strongly seasonal (Dubiel, 1987; Kutzbach and Gallimore, 1989; Dubiel et al., 1991; Dubiel and Skipp, 1992; Driese and Mora, 2002; Tanner, 2003; Prochnow et al., 2006; Tanner and Lucas, 2006; Cleveland et al., 2008).

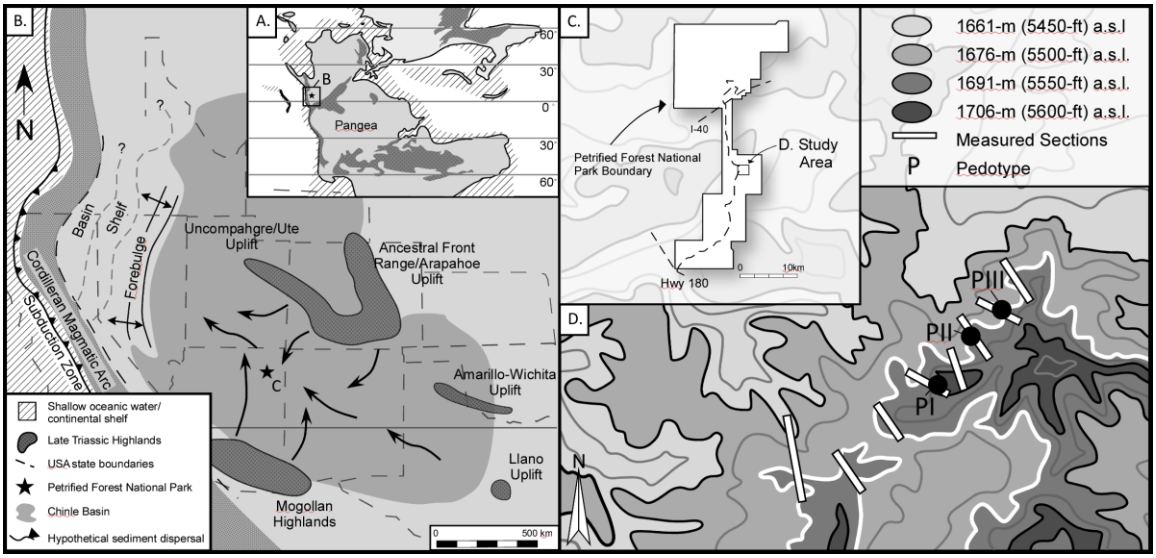

Figure 4.1. A. Global paleogeographic map during the Late Triassic (modified from Scotese, 2007); B. Paleogeographic map of the southwestern United States showing the location of the study area relative to the Chinle Basin and major Late Triassic structural features (Blakey and Gubitosa, 1983; Dubiel et al., 1991; Dubiel, 1994; figure modified from Riggs et al., 1996; Trendell et al., 2012). Solid arrows represent hypothetical sediment dispersal patterns in alluvial systems in the lower Chinle (Dickinson, 1981; Blakey and Gubitosa, 1983; Dubiel, 1987; Dubiel, 1989; Dubiel et al., 1991); C. Boundary of the Petrified Forest National Park showing the location of the study area; D. Topographic map of the study area (base of outcrop is outlined in white) showing the location of measured sections (see Trendell et al., 2012) and pedotype descriptions (this study; highlighted by black dots).

Sonsela Depositional System

Outcrops considered for this study include the Camp Butte Beds, Lots Wife Beds, and Jasper Forest Beds of the lower Sonsela Member exposed within the "Blue Mesa" geographical area of the Park (Figure 4.2; nomenclature follows Martz and Parker, 2010). The Sonsela study interval is 25-35 m thick and consists of interbedded alluvial sandstones and mudstones upon which paleosols are weathered (Figure 4.2; Trendell et al., 2012). Facies and facies associations of the study interval suggest deposition within bedload and suspended load channels, crevasse splays, and proximal and distal overbank environments within a mixed-load fluvial system (Trendell et al., 2012; Figure 4.2). The study succession contains meter-scale fining-upward fluvial cycles bound by unconformities (scours or paleosols) that stack into a longer-term thinning and fining-upward cycle (Trendell et al., 2012). This coincides with a change in fluvial style from bed- or mixed-load with multistory sand bodies and a limited volume of associated overbank mudrocks, to suspended-load style with meandering, single story sand bodies and higher proportions of overbank mudrocks (Trendell et al., 2012; Figure 4.2). Meter-scale cycles are interpreted to represent migration and avulsion of the fluvial channel, and the longer-term fining upward trend is interpreted to represent the gradual migration of the fluvial channel away from the study area (Trendell et al., 2012). Paleosols, therefore, represent an upsection increase in distance from the paleochannel. The fining upward trend is erosionally truncated at the top of the succession and overlain with coarse, bedload channel deposits of the Jasper Forest Bed (Trendell et al., 2012). Mudrock paleosols immediately below these sands represent the most distal overbank deposits preserved within the Sonsela.

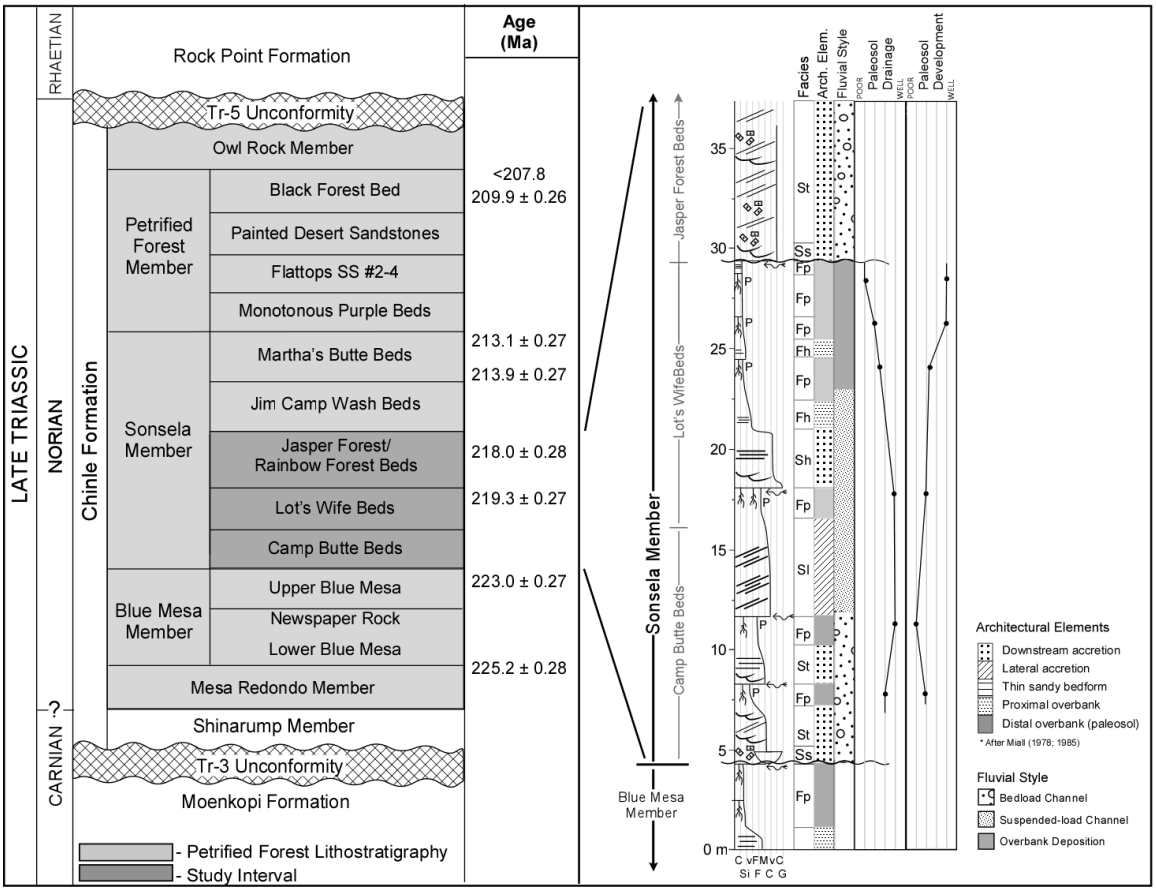

Figure 4.2. Chinle lithostratigraphic chart (left) highlighting Petrified Forest National Park strata and the study interval (nomenclature after Martz and Parker, 2010). Measured section (right) shows the 1-dimensional trends in stratal characteristics, facies, architectural element interpretations, fluvial style, and paleosol drainage and maturity of the study interval (modified from Trendell et al., 2012).

Late Triassic Flora at PFNP

The Sonsela Member at Petrified Forest National Park contains spectacularly preserved silicified conifer trunks as log jams within channel sandstones. These logs are from the conifer *Araucarioxylon arizonicum* (Knowlton, 1889; Ash and Creber, 1992; Demko, 1995; Ash and Creber, 2000), classified within the family Araucariaceae, although this extinct Late Triassic species is very different from modern species of the Araucariaceae (Ash and Creber, 2000). *A. arizonicum* logs average 1 m in diameter and 25 m in length (Daugherty, 1941; Ash and Creber, 1992; Demko, 1995; Ash and Creber,

2000) and likely underwent permineralization at very shallow burial depths (Sigleo, 1978; Demko, 1995; Dubiel et al., 1999; Trendell et al., 2012). Despite their abundance in channels, logs are rarely found *in-situ* within the lower Sonsela Member and other fossil plant assemblages (leaves and pollen) are not preserved (Demko, 1995; Demko et al., 1998). *In-situ* conifer stumps are found immediately below the Jasper Forest Bed (W. Parker, personal communication, 2012) within the most distal mudrocks preserved within the Sonsela Member (Trendell et al., 2012). In contrast to the Sonsela, several *in-situ* conifer stumps and abundant fossil leaves are preserved in channel-proximal positions within the Blue Mesa Member and Black Forest bed at PFNP (Demko et al., 1998). Compression and impression floras within the Blue Mesa Member (stratigraphically below the Sonsela Member; Figure 4.2) preserve a diverse assemblage of Late Triassic taxa, such as lycopods, horsetails, ferns, cycads, gingkoes, and cordaites suggesting humid, wet soil conditions (Daugherty, 1941; Ash, 1972; Demko, 1995; Dubiel et al., 1999; Ash, 2005). Assumed distributions of Blue Mesa taxa across the landscape are based on relative abundance of preserved specimens within fluvial depositional elements (i.e. channel margin, proximal or distal floodplain) and, more rarely, *in-situ* preservation (in the case of tree stumps and horsetails; Demko, 1995; Demko et al., 1998).

Methodology

Fifty-eight paleosol profiles were described in the study area following the standard guidelines of the Soil Survey Staff (1999), Retallack (1988; 2001), and Schoeneberger et al. (2003). Descriptions include field observations of horizon thickness, matrix color (described using the Munsell® Soil Color Book), structure, texture, horizon boundaries, root trace abundance and size, carbonate type, slickensides,

and iron concentrations and depletions. Micromorphologic description and terminology are based on Brewer (1976).

Three pedotypes are identified from the fifty-eight paleosol profiles described based on similarity of morphology, physical and chemical properties, micromorphological characteristics, and paleo-topographic position. Paleotopographic positions are interpreted from the fluvial facies and architectural elements upon which the paleosols are weathered. Each pedotype was excavated within a 1 m x 1 m trench on the outcrop face and photographed. Drab-colored root traces (rhizohalos; see detailed distinction of root trace types in Rhizoliths section below) in the B horizons are digitally traced in Canvas 11© to determine their total 2-D area. Rhizohalo densities of A horizons, when preserved, were estimated in the field. Rhizohalo density was determined by dividing their area by the total trench area. Average rhizohalo diameter, average silicified root (root petrifactions) diameter, and percentage of rhizohalos containing silicified roots were measured and estimated in the field. Not all rhizohalos contain silicified roots; however, all silicified roots were found within rhizohalos. Cathodoluminescence (CL) microscopy was used to determine silica provenance (detrital vs. diagenetic) following the methods of Boggs and Krinsley (2006).

Bulk samples of paleosol horizons were analyzed for elemental compositions by standard X-ray fluorescence procedures at ALS Chemex Laboratories. Oxide weight percentages are normalized to their molecular weight and are reported in Appendix A. Each pedotype contains ≥ 40% clay by visual estimation, and therefore, physical and chemical pedotransfer functions designed for use on paleo-Vertisols are used to estimate clay (%), fine clay (%), COLE (cm cm^{-1}), bulk density (g cm^{-3}), CEC ($cmol_c$ kg^{-1}),

$CaCO_3$ (%), pH (H_2O), base saturation (%), exchangeable sodium percentage (%), electrical conductivity (dS m^{-1}), dithionite-citrate extractable (Fe_d, %) and ammonium oxalate extractable (Fe_o, %) iron oxide content after Nordt and Driese (2010a). Paleosol molecular oxides from the uppermost B horizon of each paleosol are used to estimate mean annual precipitation (MAP) using the CALMAG weathering index (Nordt and Driese, 2010b). Physical and chemical characteristics are used in conjunction with morphological characteristics to determine the taxonomically-defined soil order (Soil Survey Staff, 1999).

X-ray diffraction was performed on bulk samples disaggregated and centrifugally size-fractionated to isolate the < 2 µm size fraction (fine clays). The < 2 µm fraction of each sample was separated into three sub-samples that were treated by exchange saturation with K and Mg, and with a separate Mg-saturated sampled solvated with a 1:4 glycerol: water solution. The K-saturated sample was heated at 550˚C for at least 3 hours prior to analysis. Sample suspensions were vacuum deposited on nylon membrane filters to produce oriented clay mounts. X-ray diffraction analysis of each treatment sample was performed at 25˚C on a Siemens D5000 Θ-2Θ X-ray diffractometer (XRD) with scans of CuKα-radiation between 2 to 30° 2Θ, and with scan steps of 0.05° 2Θ and dwell time of 1.2 seconds. Clay mineralogy of the samples is determined from x-ray peaks following methods outlined by Moore and Reynolds (1989).

Diagenesis

The study succession was buried by a minimum of 2.8-2.9 km of sediment (AAPG, 1988; Trendell et al., 2012). Paleosols are decompacted following the methods of Sheldon and Retallack (2001). Macro- and micromorphological properties appear to

reflect modern soil characteristics and likely represent conditions at the time of burial except porosity loss (>0.08 mm, Brewer, 1976) by compaction and potential iron depletions along root voids by post burial gley (see Retallack, 2001). Paleosol mudrocks, bounded by sandstones, likely experienced expulsion of pore water during burial compaction in response to overburden pressures (Neglia, 1979; Bjørlykke, 1999). Water loss, combined with paleosol mudrock impermeability (Bryant, 2002), provides greater potential for preservation of pre-burial chemical conditions, such as exchangeable cations within the clay fraction (Nordt et al., 2012). Solution properties such as pH, however, must be interpreted with greater caution (Nordt et al., 2012). X-ray diffraction suggests minor to no illitization indicating low burial temperatures (see Batten, 1996; Milliken, 2005) and, therefore, particle-size distributions and mineralogies similar to pre-burial conditions (Nordt et al., 2012).

Rhizoliths

Root traces are defined using terminology from Kraus and Hasiotis (2006) and Klappa (1980), in which rhizoliths are a general term to describe any organosedimentary structure that preserves the activity of roots of higher plants. Rhizoliths are common within paleosols of the Sonsela Member at PFNP, and can be subdivided into 3 types: rhizohaloes, rhizotubules, and root petrifactions. Rhizohalos are Fe and Mn depletion and accumulation zones that form around roots (Kraus and Hasiotis, 2006). Rhizotubules are cemented cylinders around root voids that can fill later with sediment (Klappa, 1980). Mineral impregnations or mineral replacements of organic matter are referred to as root petrifactions (Klappa, 1980). The three different root trace fossils and interpretation of their origin and paleobotanical significance are discussed below.

Rhizohalos

Sonsela Member paleosols contain elongate, vertically oriented, and bifurcating white (N 8/1) and light greenish gray (10Y 8/1) mottles that are interpreted as rhizohalos or iron (Fe) depletions. Rhizohalos are roughly circular or elongated in cross-section (Figure 4.3f) and have diameters ranging from large (10 cm) to small (<1 cm). The matrix textures of rhizohalos are the same as the hosting paleosol matrix textures (see pedotype descriptions for texture specifics). Rhizohalo abundances range from between 7% to 46% of the exposed paleosol surface area and commonly decrease in abundance down-profile unless paleosols are cumulative or welded. The absolute depth of rhizohalos is difficult to ascertain within Sonsela paleosols because the degree of welding or cumulative formation cannot be ascertained with certainty. Instead, depths are qualitatively compared between pedotypes. Some paleosols contain white rhizohalos with smaller-diameter dark bluish gray (5PB 4/1) cores (Figure 4.3b, i, j). Rhizohalos commonly have petrifactions (see below) within them and are sometimes found along slickenside planes.

Fe- and Mn- Rhizotubules

The Sonsela paleosols may contain black (N 2.5/1) to reddish black (2.5YR 2.5/1) cores that are elongate, vertically oriented cylinders that bifurcate (Figure 4.3c, e). These cylinders rarely have diameters greater than 2 mm. Micromorphologically, these cores appear to be accumulations of FeMn that are sometimes hollow with very-fine, fibrous FeMn tendrils extruding from their outer surface (Figure 4.4A) and sometimes bifurcating (Figure 4.4B). Some cylinders are infilled with fine-grained sediments of similar texture to the paleosol matrix and appear to have minor illuviated clay that coats

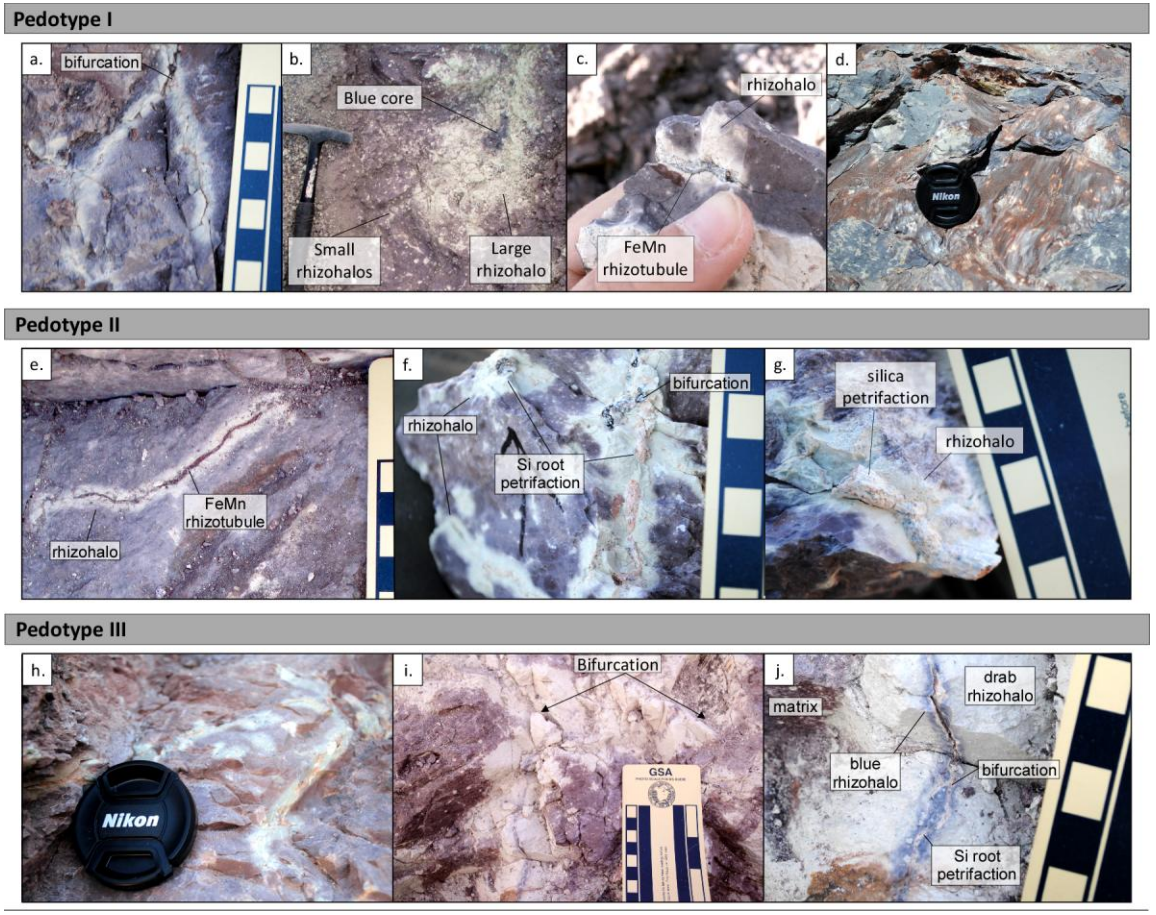

Figure 4.3. Field photographs of pedotype rhizoliths (for pedotype descriptions, see 'Sonsela Pedotypes' section): a) a bifurcating root trace; b) a 'large' rhizohalo with a blue internal rhizohalo surrounded by 'small' rhizohalos that show the bimodal diameters of Pedotype I paleosols; c) a black FeMn rhizotubule within a rhizohalo, d) slickensides coated in Fe and Mn; e) an Fe and Mn rhizotubule within a white rhizohalo; f) ped showing white rhizohalos around silica root petrifaction. Rhizohalo on the top of the ped illustrates spherical shape of rhizohalos in cross-section; g) a ~1cm diameter silica root petrifaction within a rhizohalos; h) rhizohalos with very fine silica root petrifactions within; i) thick bifurcating rhizohalos and blue internal rhizohalos; and, j) a large-diameter rhizohalo, a blue internal rhizohalo, and a silica root petrifaction.

their internal surface (Figure 4.4A). These features are similar to modern pore-linings in reduced soils (Vepraskas, 1992).

Silica Root Petrifactions

Sonsela paleosols commonly contain pale red (10R 7/4) to black (N 2.5/1) cores that are elongate, vertically oriented, and bifurcating within rhizohalos (Figure 4.3f, g, j). Pale red cores range in diameter from 1 mm to 1.5 cm, are smaller than their hosting rhizohalo, and have diameters that appear independent of rhizohalo diameter. Pale red cores, when thin-sectioned, are revealed to be composed of chalcedony/chert and may contain remnant organic matter at their centers (Figure 4.4D-H). Silica cores have similar chalcedony/ chert composition as Sonsela silicified wood (Figure 4.4C) and may represent the silicification of root organic matter. The percentage of rhizohaloes with these silica cores ranges from 8% to 40% (Table 4.1). Paleosols more proximal to paleochannels and with siltier textures have greater percentages of rhizohalos with silica cores. Silica cores are non-luminescent under cathodoluminescence, which is suggestive of a diagenetic origin (Boggs and Krinsley, 2006).

Rhizolith Interpretation

Rhizohalos can form pedogenically or diagenetically. Pedogenic rhizohalos represent the location of former root rhizosperes and root channels and form due to surface water gley, which redistributes ferrous iron into oxidized hypocoatings along the margins of pore walls (Vepraskas, 1992; PiPujol and Buurman, 1994; Vepraskas, 1996; PiPujol and Buurman, 1997; Vepraskas, 2001; Kraus and Hasiotis, 2006). Rhizohalos may also form diagenetically as postburial gley from microbial decomposition of residual

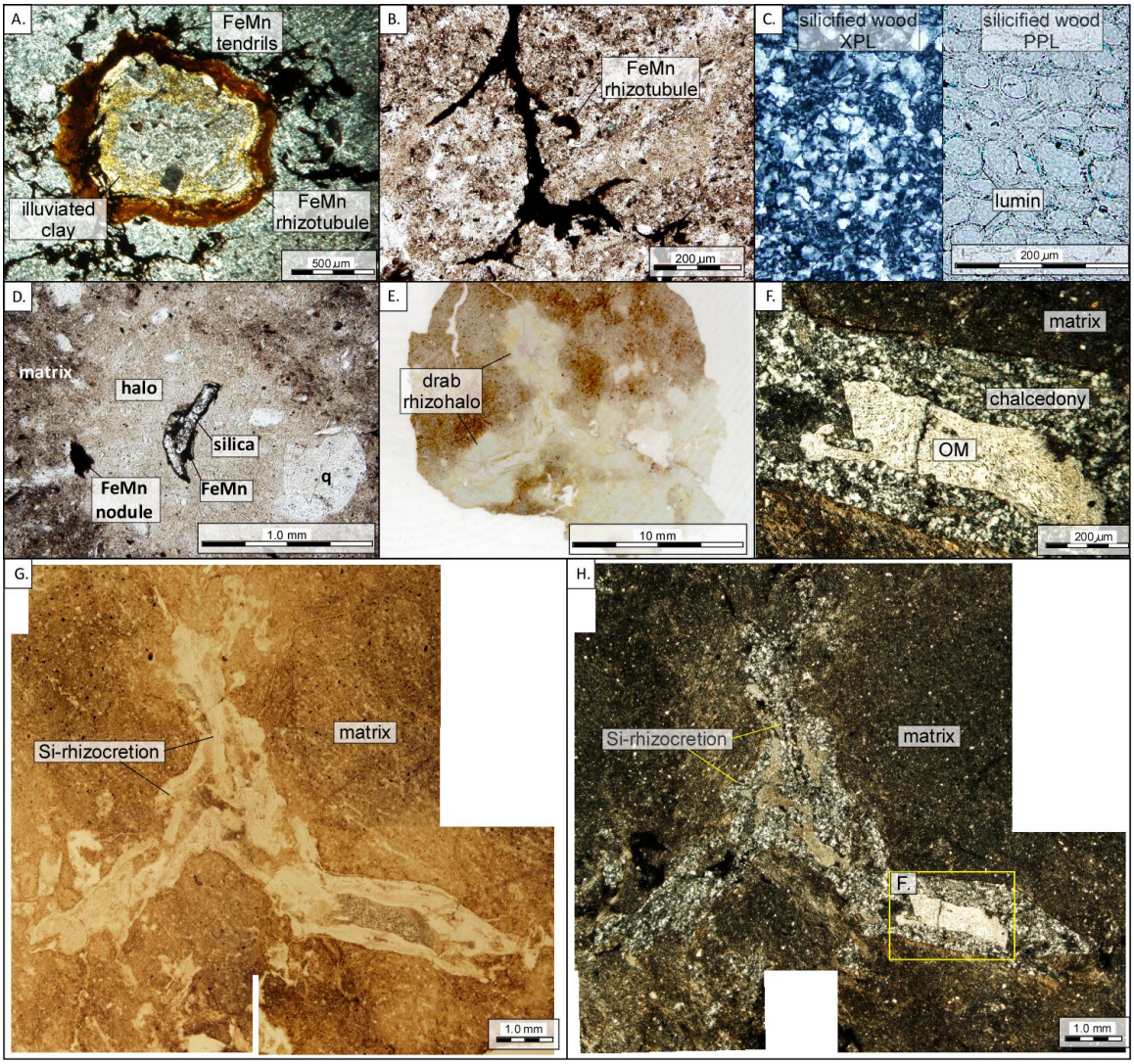

Figure 4.4. Photomicrographs of pedotype rhizoliths (for pedotype descriptions, see 'Sonsela Pedotypes' section): A) Cross-polarized light photomicrograph of an Fe and Mn rhizotubule cross section with illuviated clay in the center from the Pedotype I Bss1 horizon; B) FeMn rhizotubule that bifurcates within the Bw horizon of Pedotype III; C) Photomicrographs display the left and right sides of the same viewpoint in XPL (left) and PPL (right). Silicified logs from the Sonsela Member in cross polarized light are replaced by chalcedony crystals (left). Outlines of log cell structure can clearly be seen in PPL (right); D) silica with FeMn coating within a rhizohalo of the Bw horizon of Pedotype III; E) Flat bed scan of Pedotype II Bw horizon thin-section with a drab rhizohalo within which is a silica root petrifaction (see F, G, and H for photomicrographs); F) Cross-polarized light photomicrograph of a branch of the silica root petrifaction with potential internal organic matter (see G and H for lower magnification view); G) Photomosaic of plane-polarized light photomicrographs of silica root petrifaction (see E for rhizohalo) , and; H) Photomosaic of cross-polarized light photomicrographs of silica root petrifaction (see E for rhizohalo).

organic materials from the last crop of standing vegetation and do not have iron oxidized hypocoatings (see Retallack, 1991). Sonsela Member rhizohalos are predominantly solid white with no iron hypocoatings and are sometimes present around non-root voids

(slickensides). These features suggest that Sonsela rhizohalos formed as post-burial gley (Retallack, 2001; Kraus and Hasiotis, 2006). Sonsela rhizohalo textures are the same as paleosol matrix and, therefore, are not likely infilled voids of different sediment composition. Those rare rhizohalos with blue matrix cores may represent pedogenic redox concentrations of ferrous (reduced) iron.

Fe and Mn rhizotubules are rare, very small, and found within rhizohalos. Clays within Fe and Mn rhizotubules (Figure 4.3A) suggest infiltration of water through root voids. Although their surrounding rhizohalos appear diagenetic, rhizotubules are similar to modern Fe pore linings or iron hypocoatings that accumulated by redistribution of ferrous iron on soil walls around alive or dead roots (Vepraskas, 1992; Vepraskas, 2001). They represent mobilization and re-precipitation of Fe and Mn from ambient soil water and suggest seasonal hydromorphic pedogenic conditions (Vepraskas, 1992; Vepraskas, 1996; Vepraskas, 2001). After burial, matrix surrounding Fe pore linings may have experienced post-burial gleying that resulted in rhizohalos encasing Fe and Mn rhizotubules.

Silica root petrifactions may represent replacement of root organic matter by silica. Sonsela Member sandstones consist of abundant volcanic rock fragments, whose devitrification likely resulted in silica-rich pore-waters that contributed to silicification of logs within fluvial channels (Murata, 1940; Sigleo, 1979). Studies indicate that silicification occurred at a very shallow burial depth soon after deposition (Murata, 1940; Sigleo, 1979; Trendell et al., 2012). Considering the early and pervasive silicification of logs, it is possible that un-decomposed root organic matter remaining within soil macrovoids underwent silicification. Similar petrographic characteristics of silicified

Table 4.1. Morphological descriptions of the Sonsela pedotypes.

Horizon	Depth (cm)	Color	Texture	Structure*	Redoximorphic Features				Silicified Roots[#]		Slicks[§]	Boundary**
					Density	Diam. (cm)	Color	Type	Diam. (cm)	%		
Pedotype I												
A	47.4	5R 4/1, 5R 3/1	claystone	2f-msbk	7%	0.3-1	N8/1	rhizohalo	0.1-0.8	10%	ff	gs
Bss1	90.3	5R 4/1, 5R 3/1	silty claystone	2mabk	10%	0.5-1 (98%), 10-28 (2%)	10Y8/1	rhizohalo	0.1-0.8	15%	cd	gs
Bss2	173.7	5R 5/1, 5R 4/1	silty claystone	2cabk	10%	0.5-1 (97%), 10-20 (3%)	10Y8/1	rhizohalo	0.1-0.5	10%	cd	gs
C/B	231.3	N 8/1	fine sandstone??	bedded	5%	2-4	5R4/2	Non-elongate/ bifurcating mottles	N/A		Ff??	N/A
Pedotype II												
Bw	39.5	5R 4/1	silty claystone	1f-msbk	30%	0.5-3	10Y8/1	rhizohalo	0.1-1.5	35%	none	cs
BC	83.5	5R6/1, 5R5/1	silty very fine sandstone	2msbk	10%	0.5-4	10Y8/1	rhizohalo	0.1-1.5	40%	none	cs
C	111.7	N 8/1	medium sandstone	bedded	N/A	N/A	N/A	N/A	0.1-1.5	5%	none	N/A
Pedotype III												
Bw	56.4	7.5R 5/2	siltstone	2csbk	46%	<1-15	N8/1, 5PB 5/1	rhizohalo	0.1-0.4	20%	none	cs
BC	109.4	7.5R 6/2	clayey siltstone to very fine sandstone	bedded to 1msbk	15%	2-10	N8/1, 5PB 5/1	rhizohalo	0.1-0.4	30%	ff	cs
C	124.1	N 8/1	fine to medium sandstone	bedded	N/A	N/A	N/A	N/A	0.1-0.3	3%	none	N/A

*1—weak, 2—moderate, 3—strong grade; f—fine, m—medium, c—coarse size; sbk—subangular blocky, abk—angular blocky, we—wedge, m—massive, pl—platy type.
[#]diameter of silicified roots and percentage of rhizohalos with silicified roots in their core.
[§]f—few, c—common, m—many abundance; f—faint, d—distinct, p—prominent expression.
**a—abrupt, c—clear, g—gradual distinctness; s—smooth, w—wavy topography.

logs and silica root petrifactions (chalcedony silica textures) are consistent with this hypothesis. Those rhizohalos without silica root petrifactions may reflect root voids that did not contain organic matter at burial or may be an exposure bias, where the cross-section of the rhizohalo exposed is not the center of the rhizohalo. Unlike the thin-sections of logs that show wood cell structures, root cell structures are not observed in thin sections of silica root petrifactions. Woody cells are characterized by secondary xylem (Taylor et al., 2008) that creates structural rigidity within trees and, as a result, cells are less readily decomposed than other plant cells. Timing of silicification may have occurred prior to decomposition of the rigid wood cells, but after partial decay of non-woody root cells.

Sonsela Rhizolith Utility

Rhizolith dimensions are commonly an overestimation of the actual size of the living plant root, and therefore rhizolith interpretation (most commonly rhizohalos and $CaCO_3$ rhizocretions) has been limited to determining paleosol moisture and drainage, depth to the paleowater table, mean annual precipitation and primary productivity (Hembree and Nadon, 2011; Nordt et al., 2011). Unless rhizoliths can be demonstrated to represent the approximate original size of occupying roots prior to burial (i.e. Nordt et al., 2011), they are avoided for specific paleo-floral interpretations. It is difficult, therefore, to infer variations in plant formations along paleocatenas. Silicified roots within rhizohalos afford a unique opportunity to determine the size of plants inhabiting the paleolandscape, and what, if any relationship exists between root diameter and rhizohalo diameter. Small diameter and shallow silica rhizoliths with extensive root networks in paleosols may represent small herbaceous plants indicative of ground cover (LePage and

Pfefferkorn, 2000; Hembree and Nadon, 2011). Larger rhizoliths are more likely to represent larger plants that stand above the ground surface and are less likely to represent the roots of smaller, ground cover plants (Hembree and Nadon, 2011). The large rhizoliths could represent deeply penetrating roots of arborescent plant taxa such as the conifer *Araucarioxylon arizonicum* (Ash, 1972; Ash and Creber, 1992; Ash and Creber, 2000; Creber and Ash, 2004; Ash, 2005; Savidge and Ash, 2006; Hembree and Nadon, 2011).

Sonsela Pedotypes

Pedotype I

Description. Of fifty-eight Sonsela paleosol profiles described, twenty-nine were classified as Pedotype I. Pedotype I paleosols occur either as a single profile (thicknesses ranging from 200 cm to 280 cm) or as a stacked and welded series of two or three profiles (thicknesses ranging from 250 cm to 420 cm) that may be separated by thin C horizons. This pedotype has a noncalcareous A-Bss1-Bss2-C/B horizon sequence (Figure 4.5A; Table 4.1) with a decompacted solum thickness of 231 cm (Table 4.1). The A horizon is a subangular blocky, dark reddish gray (5R 4/1) claystone with white (N 8/1) rhizohalos and few, faint slickensides (Figure 4.3d; Table 4.1). The Bss1 and Bss2 horizons are dark reddish gray (5R 4/1) and reddish gray (5R 5/1) claystones with medium to coarse angular blocky to wedge shaped ped structure. The Bss1 and Bss2 horizons contain common distinct slickensides (Figure 4.3d) and light greenish gray (10Y 8/1) to white (N 8/1) rhizohalos (Figure 4.3a, b, c; Table 4.1). Underlying sediments of Pedotype I

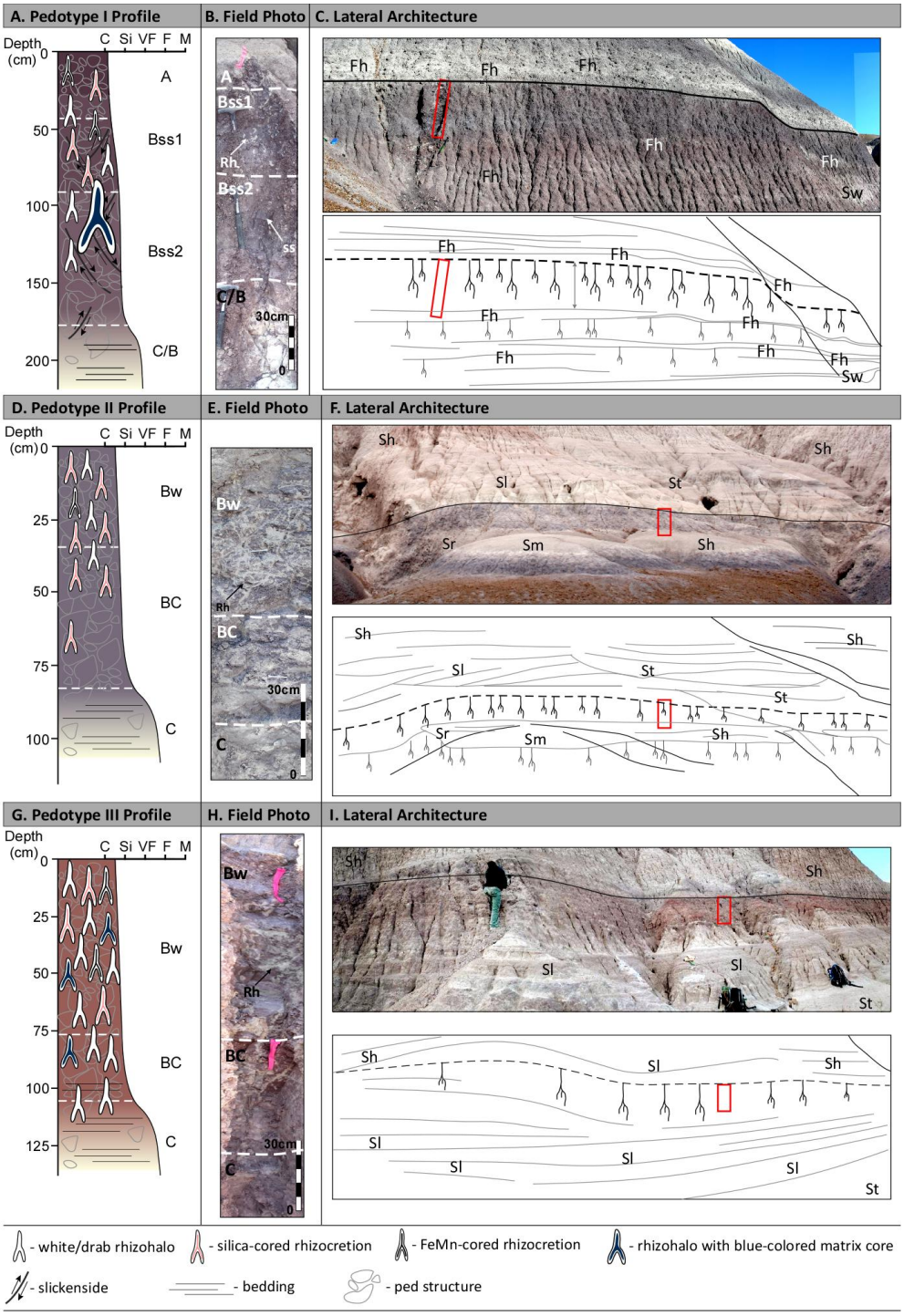

Figure 4.5. Pedotype summaries. Illustrated profiles that detail the types of rhizoliths, horizon thicknesses, and slickensides: A) Pedotype I, D) Pedotype II, and G) Pedotype III. Field photographs of the profiles for: B) Pedotype I, E) Pedotype II, and H) Pedotype III. Lateral photographs of position and interpreted lateral facies and architecture for each pedotype: C) Pedotype I is interpreted to form on distal overbank environments; F) Pedotype II is weathered into Sm and Sh facies interpreted as a crevasse splay; G) Pedotype III is weathered into Sl facies interpreted to be lateral accretion architectural elements. Gray lines represent sedimentary features, solid black lines represent the outcrop geography, and dashed black line represents the paleosol surface.

Table 4.2. Diagnostic attributes of fluvial facies and architectural elements (modified from Miall, 1978; 1985; 1996).

Facies	Lithology	Features	Interpretation	Architectural Element	Outcrop photos
St	Sandstone	Trough cross beds; poorly-sorted coarse to medium sand	Upper flow regime channel fill deposit, dunes	Downstream accretion; Lateral accretion	Figure 5F
Sl	Sandstone	Large-scale, low-angle cross beds; coarse to fine sand; fining upwards along beds	Point-bar deposit from fluvial migration	Lateral accretion	Figure 5F, I
Sh	Sandstone	Horizontally bedded	Crevasse splay or non-pedogenically altered overbank deposit	Lateral accretion; Proximal overbank	Figure 5F, I
Sr	Sandstone	Ripple laminated	Lower flow regime; often found in upper portions of Sl facies	Lateral accretion; Thin sandy bedforms	Figure 5F
Sw	Sandstone	Progradational wedge with pedogenic alteration along bedding planes; poorly sorted medium to very fine sands; border channels and are topographically higher than the adjacent floodplain facies	Crevasse splay	Thin sandy bedforms	Figure 5C, 5F
Sm	Sandstone	Contains no observable sedimentary structures; borders channels and are topographically higher than the adjacent floodplain facies	Crevasse splay	Thin sandy bedforms	Figure 5F
Fh	Mudrock	Laminated and horizontally bedded; very fine sands, silts, and clays; minor to abundant drab root halos that overprint sedimentary structure.	Overbank deposition	Proximal overbank; Thin sandy bedforms	Figure 5C

paleosols are commonly laminated mudstones to silty mudstones (Fh facies; Table 4.2; Figure 4.5C).

The micromorphology of Pedotype I is characterized by bimasepic and skelsepic plasmic microfabrics (Figure 4.6A). Skeletal grains are predominantly quartz with minor chert, mica, and feldspars. Pedotype I texture is visually estimated in thin section to be clay, with minor amounts of silt (Figure 4.6B). Rare and small FeMn nodules (Figure 4.5C) with diffuse and solid boundaries are observed within the paleosol matrix.

Biological features include FeMn rhizotubules (Figure 4.3e, 4.4a, b) and voids infilled by very fine sand to silty sediment (root voids or burrows). In outcrop, these horizons appear "purple" and, like the purple Willwood and Fort Union Paleosols described by Kraus and Hasiotis (2006), thin section microscopy reveals that the paleosol matrix contains widely dispersed red microspheres of Fe and Mn < 5 μm in diameter (Figure 4.6C). These microspheres are not present in rhizohalos.

Rhizoliths within this pedotype include solid white drab rhizohalos (Figure 4.3a), silica root petrifactions, white rhizohalos with blue internal rhizohalos (Figure 4.3b) and rare FeMn rhizotubules (Figure 4.3c). Rhizohalos have a bimodal size distribution with abundant 'small' drab rhizohalos (97% - 98% of rhizohalos; 0.3 mm to 1 cm in diameter) and rare 'large' rhizohalos with blue cores (2% - 3% of rhizohalos; 10-28 cm diameter; Table 4.1; Figure 4.3b). Small drab rhizohalos have a density of 7% in the A horizon, 10% in Bss horizons, and 5% in the C/B horizon (Table 4.1; Figure 4.7A). Silicified roots are found in 10-15% of small rhizohalos and have diameters that range from 0.1-0.8 cm in diameter (Table 4.1). Approximately 2% of small rhizohalos have blue internal rhizohalos, and some contain several 'rings' of blue and drab colors. Large rhizohalos (10-28 cm diameter) with dark blue internal mottling (5 cm to 12 cm diameter) are found in only 23% of Pedotype I profiles and make up only 2-3% of all rhizohalos in this pedotype (Figure 4.4b). These large rhizohalos commonly occur deeper in the paleosol profile (60-120 cm depth).

Clay mineralogy was analyzed from a Pedotype I profile at 51.5 cm depth in the Bss1 horizon and is composed primarily of smectite (Figure 4.8A). The peak at 12 Å in the bulk sample is interpreted to reflect a combination of smectite (15Å), biotite (10Å, 12

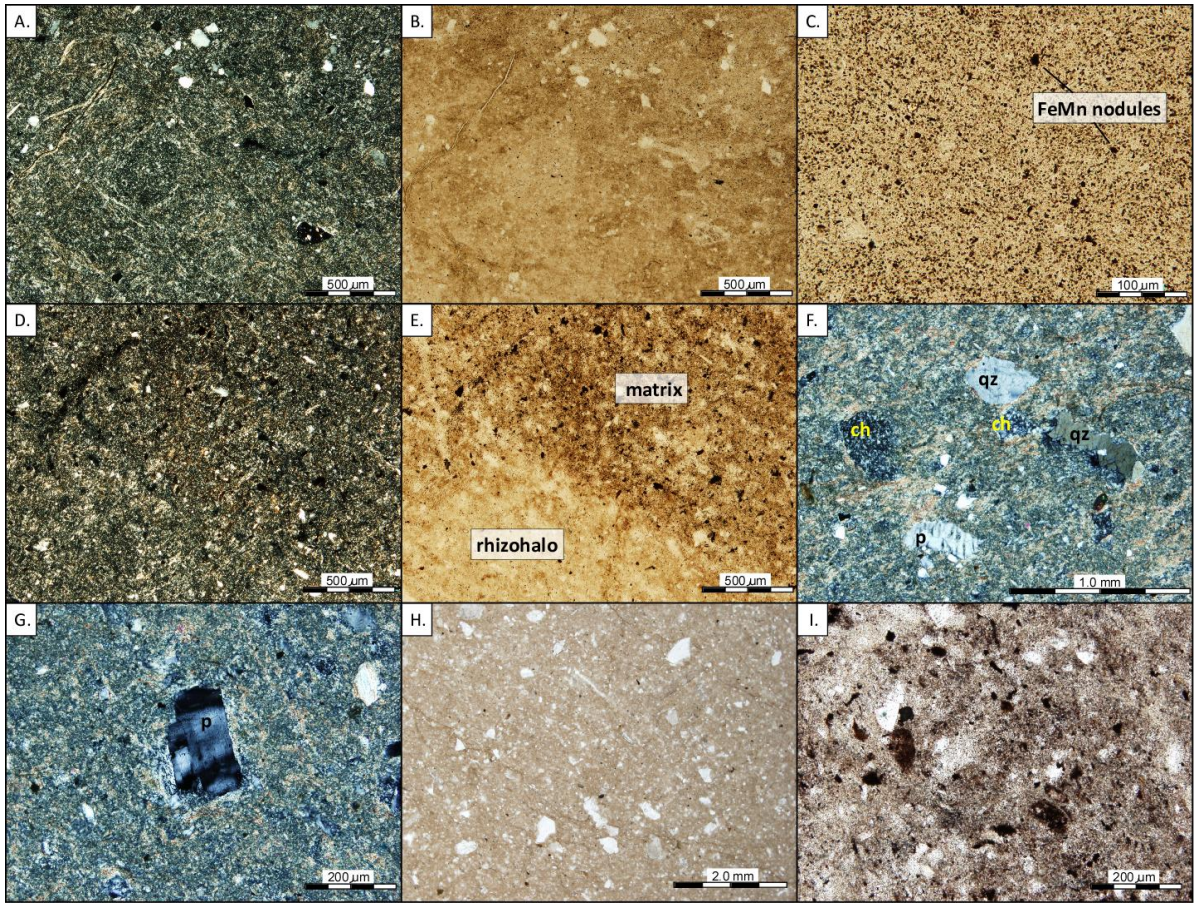

Figure 4.6. Photomicrographs of Pedotypes. XPL = cross-polarized light, PPL = plane-polarized light. A) bimasepic and skelsepic plasmic microfabric within Pedotype I matrix, XPL; B) texture of Pedotype I showing a dominance of clay with few very fine sand grains. Compare with Pedotype II (E) and Pedotype III (K), PPL; C) FeMn nodules and widely-dispersed microspheres within Pedotype I matrix, XPL; D) masepic plasmic fabric of Pedotype II matrix, XPL; E) high silt content characteristic of Pedotype II. Compare with Pedotype I (B) and Pedotype III (K), PPL; F) Pedotype II masepic and skelsepic plasmic fabric with chert (ch), plagioclase (p), and quartz (qz) skeletal grains, XPL; G) Pedotype III plagioclase skeletal grain, within masepic and skelsepic plasmic fabric, XPL; H) texture of Pedotype III showing very fine sand and silt skeletal grains. Compare with Pedotype I (B) and Pedotype II (E), PPL; L) irregular and abundant FeMn nodules within Pedotype III, PPL.

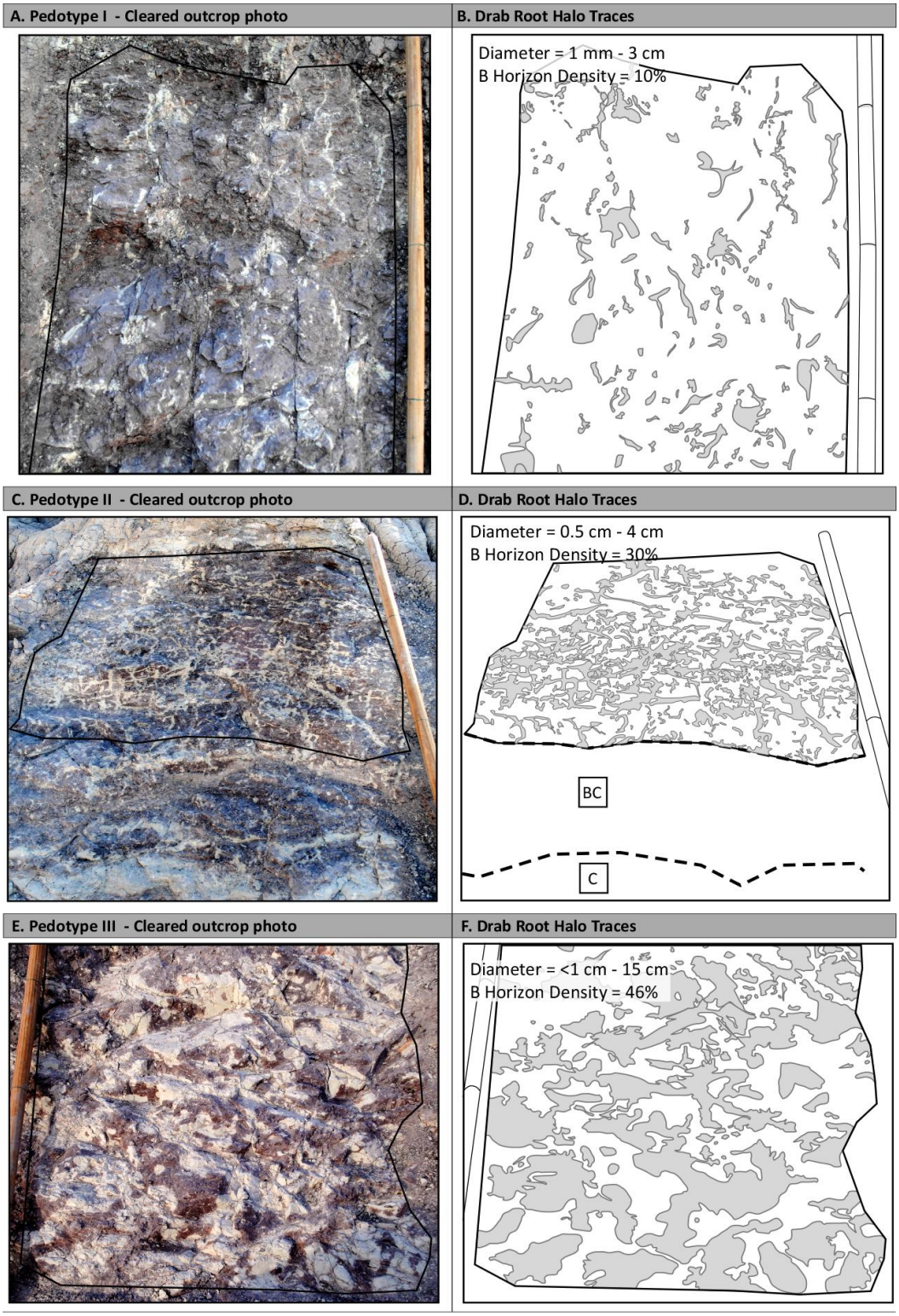

Figure 4.7. Rhizohalo summaries for Sonsela Pedotypes. Field photo of 1m x 1m exposures showing the distribution of rhizohalos for: A) Pedotype I, C) Pedotype II, and E) Pedotype III. Traced rhizohalos for illustration of rhizohalo diameter, density and shape for: B) Pedotype I, D) Pedotype II, and F) Pedotype III.

Å, 14 Å), zeolites (heulandite 9 Å), or mixed-layer micas (12 Å; Moore and Reynolds, 1997). Both zeolites and biotite were observed in thin-section within the lower Sonsela Member study interval sandstones (Trendell et al., 2012).

Pedotype I samples from the center of each horizon at 24 cm (A horizon), 69 cm (Bss1 horizon), 132 cm (Bss2 horizon) and 202 cm (C/B horizon) were analyzed for bulk geochemical composition. The CALMAG molecular weathering ratio is calculated for the bulk geochemistry of the uppermost B horizon, and has a value of 76.5 (Table 4.3). Chemical and physical characterization data derived from bulk molecular oxides are shown in Table 4.3. Pedotype I has a high fine clay/total clay ratio supporting the presence of smectite, which tends to form in the fine clay fraction (Brady and Weil, 2001). A uniform depth distribution is also consistent with observations of minimal clay translocation, or lessivage, as a major soil-forming process and the absence of an argillic (Bt) horizon (Table 4.3). This pedotype has a relatively high COLE value, which indicates high shrink-swell potential (Soil Survey Staff, 2011), and is consistent with the presence of slickensides. CEC is high, which is consistent with smectitic clay mineralogy and abundant clay content. This pedotype is neutral and nearly base saturated. ESP and EC values are below the thresholds for concerns regarding sodicity or salinity problems for plants (Brady and Weil, 2001). Fe_d values indicate a moderate accumulation of pedogenic iron, and moderate Fe_o values are suggestive of periodic anaerobiosis (Nordt and Driese, 2010a).

Interpretation. Purple matrix colors have been interpreted to result from post-burial diagenetic color alteration, inasmuch as purple matrix is not common in modern soil colors (Retallack, 1991; Soil Survey Staff, 1999; Kraus and Hasiotis, 2006). Sonsela

Table 4.3. Physical and chemical properties of Sonsela Pedotypes determined using bulk molecular oxides after Nordt and Driese (2010a).

Horizon	Depth	Physical Properties					Chemical Properties									CALMAG
	(cm)	Total Clay	Fine clay	Fine clay/ Total clay	COLE	Bd	CEC	CEC/clay	$CaCO_3$	pH	BS	ESP	EC	Fe_d	Fe_o	
		(%)	(%)		(cm cm^{-1})	(g cm^{-3})	($cmol_c$ kg^{-1})		(%)	(H_2O)	(%)	(%)	(dS m^{-1})	(%)	(%)	
Pedotype I																
A	47	68	35	0.51	0.14	1.08	43	0.64	0	7.0	90	7	1	1.1	0.02	76.5
Bss1	90	65	36	0.55	0.14	1.08	42	0.64	0	7.0	89	7	1	1.6	0.02	
Bss2	174	67	36	0.54	0.14	1.11	42	0.63	0	7.0	89	7	1	0.7	0.02	
C/B	231	68	35	0.51	0.14	1.11	44	0.64	0	7.0	90	6	1	0.4	0.02	
Pedotype II																
Bw	39	63	36	0.57	0.14	1.13	40	0.64	0	6.9	88	6	1	0.5	0.02	77.0
BC	83	64	36	0.56	0.13	1.14	39	0.61	0	6.9	87	6	1	0.5	0.02	
C	111	59	33	0.56	0.15	1.15	46	0.77	1	7.1	91	7	1	0.4	0.02	
Pedotype III																
Bw	76	68	36	0.53	0.14	1.09	41	0.60	0	6.9	88	6	1	0.7	0.02	78.0
BC	124	69	37	0.54	0.14	1.12	40	0.59	0	6.9	88	5	1	0.6	0.02	

pedotypes contain both purple and red matrix colors. Considering that they were subjected to the same burial history, variation in paleosol matrix colors may suggest that colors represent initial soil drainage (PiPujol and Buurman, 1994). Purple matrix colors are interpreted to reflect imperfectly drained conditions during pedogenesis (*cf.* Kraus and Hasiotis, 2006). Small Fe and Mn nodules and Fe and Mn rhizotubules are indicative of fluctuating hydrologic conditions (Vepraskas, 1992; Vepraskas, 1996; Vepraskas, 2001).

Major pedogenic processes for Pedotype I included rooting, ped formation, and shrinking and swelling of clays as suggested by abundant slickensides. Slickensides indicate soils were subjected to seasonal moisture deficits (Birkeland, 1999; Nordt et al., 2004). Shrink-swell processes, which cause lateral and vertical stress within paleosols, are also reflected in bimasepic plasmic microfabrics and high COLE values. Clay content and presence of slickensides taxonomically classifies Pedotype I as a Vertisol. Purple matrix color with low chroma values and the occurrence of FeMn rhizotubules and concretions suggests that Pedotype 1 may be aquic at the subgroup level (Soil Survey Staff, 1999).

Stacked profiles of Pedotype I paleosols are commonly composite (*sensu* Kraus, 1999). This reflects successive increments of sedimentation where rates of pedogenesis outpaced rates of sediment accumulation (i.e., successive episodes of soil development where profile thickness exceeds the thickness of periodic sediment additions). Pedotype I compound paleosols are often (50% of profiles) truncated, and suggest erosion between periods of sedimentation and landscape stability (Kraus, 1999). The facies of Pedotype I

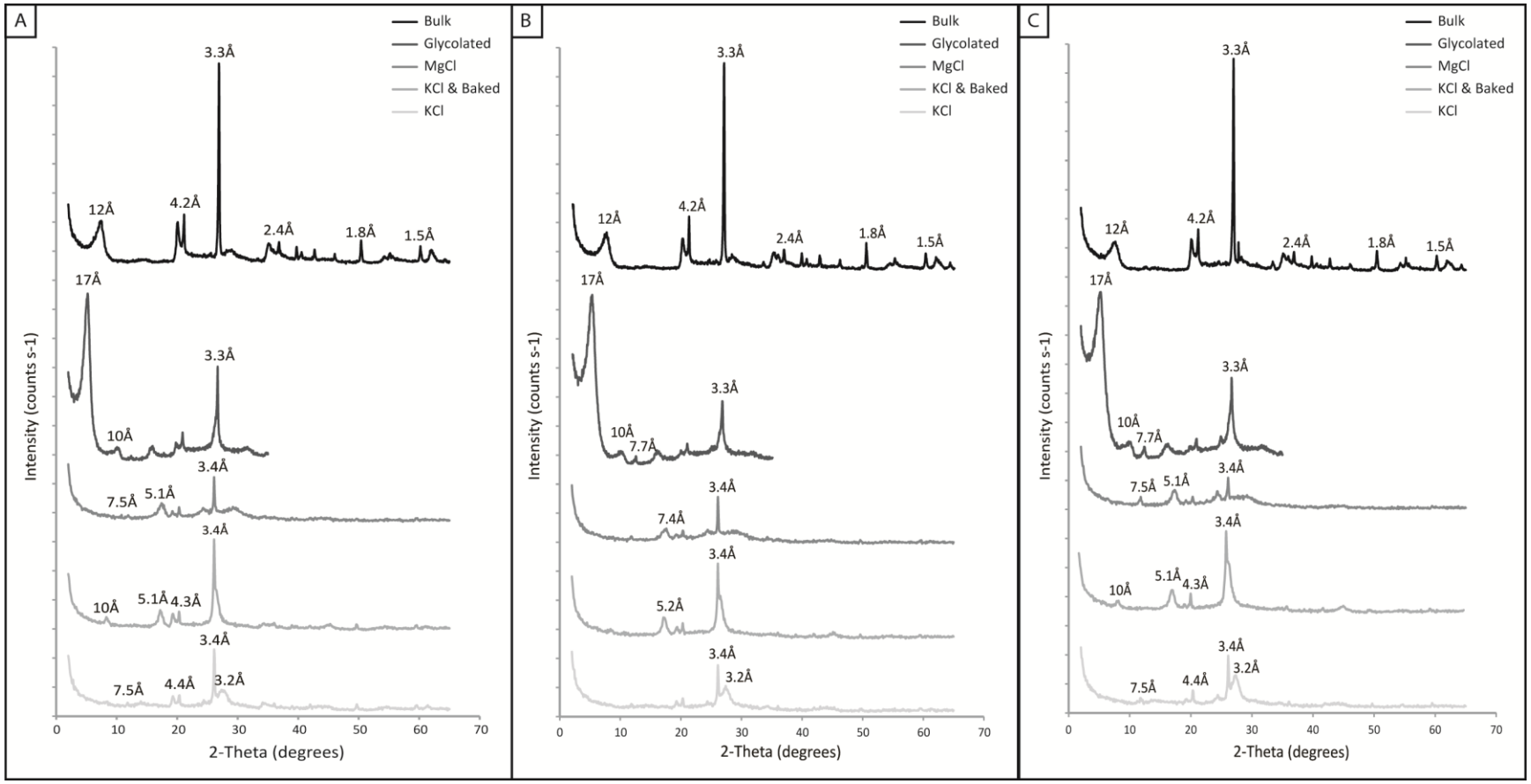

Figure 4.8. X-ray diffraction patterns of whole soil horizon samples (bulk) and the clay fraction with various pretreatments (glycolated, MgCl only, KCl and baked, and KCl only) of the: A) Bss1 horizon of Pedotype I; B) Bw1 horizon of Pedotype II; and C) Bw1 horizon of Pedotype III. For interpretations of x-ray peaks, see text.

parent materials (C horizons) are interpreted as thin overbank deposits and suggest that Pedotype I formed primarily in overbank paleotopographic positions (Figure 4.5C).

Although Pedotype I is likely the most well-developed pedotype with the Sonsela Member, it does not have the attributes of a mature paleosol. Clay mineralogy and morphology of Pedotype I are similar to modern Vertisols where slickensides and ped structure can form within only decades to centuries (Soil Survey Staff, 1999; Nordt et al., 2004). The predominance of smectitic clay mineralogy reflects paleosol immaturity, as it requires extended time, low pH, and high rainfall to transform smectite to kaolinite (Folkoff and Meentemeyer, 1987; Retallack, 2001). Additionally, production of kaolinite is encouraged by evergreen vegetation with a high affinity for nutrient uptake and a rapid organic matter decompositional environment (Marques et al., 2004). Considering that the CALMAG weathering ratio of 76.5 provides a high mean annual precipitation estimate of 1297 mm, the limiting factor for hydrolysis of smectite to kaolinite in these paleosols may be pedogenic duration or soil pH. Pedogenic features requiring long periods of landscape stability for formation, such as carbonate nodules or clay cutans (Retallack, 2001; Retallack, 2005), are absent within Pedotype I paleosols and suggest relative immaturity and either high floodplain aggradation rates or rapid lateral channel migration and overbank cannibalization. Pedotype I maturity variations are only reflected in terms of paleosol thickness, density and prominence of slickensides, and degree of paleosol welding.

Compared with other pedotypes, the small rhizohalos within Pedotype I are the least dense and have the smallest diameter (0.3 cm to 1 cm) and least silica root petrifaction cores (10% - 15%). Rhizohalos with bimodal size distributions are

suggestive of plants whose populations range between understory and arborescent. Smaller rhizohalo and silica root petrifactions likely represent root distributions of either small-stature herbaceous ground cover or shrubby plants (Pfefferkorn and Fuchs, 1991; LePage and Pfefferkorn, 2000) or high-density small-stature tree saplings. Deep, large rhizohalos may represent the roots or taproots of larger, taller-standing plants (*cf.* Hembree and Nadon, 2011). Silicified conifers preserved within Sonsela channels may be attributed to the large rhizoliths within Pedotype I; however, *A. arizonicum* trees had extensive root systems that were very large, usually consisting of a central tap root and four to six branching laterals that were of considerable size (Ash and Creber, 2000). The low occurrence and density of large rhizoliths is not consistent with a dense forest or woodland that is capable of producing the high volume of petrified logs observed within Sonsela channel sandstones.

Pedotype II

Description. Seventeen of fifty-eight Sonsela paleosol profiles were identified as Pedotype II, which most commonly occurs as a single profile having a thicknesses ranging between 50 cm to ~150 cm. Pedotype II profiles may be truncated and can contain cumulative horizons that display homogenous pedogenic characteristics. This pedotype consists of a noncalcareous and what appears to be truncated Bw-BC-C horizon sequence with a decompacted solum thickness of 83 cm (Figure 4.5D, Table 4.1). The Bw horizon is a subangular blocky, dark reddish gray (5R 4/1) silty claystone with light greenish gray (10Y 8/1) rhizohalos (Table 4.1). The BC horizon is a reddish gray (5R 5/1, 5R 6/1) silty claystone that is lightly bedded and overprinted with a medium

subangular blocky ped structure. Pedotype II has light greenish gray (10Y 8/1) rhizohalos that are less common in the BC horizon than in the Bw horizon (Table 4.1; Figure 4.7C, E). Some Pedotype II paleosol profiles may contain faint slickensides. The parent material (C horizon) of Pedotype II is massive (Sm facies), rippled (Sr facies), and horizontally laminated (Sh facies) lenticular fine-grained sandstone bodies (Table 4.1; Figure 4.5F).

Pedotype II micromorphology is characterized by sometimes pervasive masepic plasmic microfabrics with one preferred orientation (Fig 6D). Horizons contain small irregular FeMn nodules with solid and diffuse boundaries (Figure 4.6E). A thin-section from the Bw1 horizon contains an excellent example of a bifurcating, silicified root within a drab halo (Figure 4.4E-H). Skeletal grains are more diverse than Pedotype I and contain predominantly quartz, chert, plagioclase feldspar and minor volcanic rock fragments (Figure 4.6F). Pedotype II contains higher proportions of silt-sized grains, but likely still contains greater than 40% clay (Figure 4.6E). Clay mineralogy was analyzed from a Pedotype II profile at 57.5 cm depth in the Bw1 horizon and indicates predominantly smectitic clay mineralogy with minor kaolinite and illite (Figure 4.8B).

Rhizoliths within Pedotype II include solid drab rhizohalos (Figure 4.3e-g), silica root petrifactions (Figure 4.3f, g) and FeMn rhizotubules (Figure 4.3e). Drab rhizohalos range in diameter from 0.5 cm to 4 cm in diameter (Figure 4.7C) and have a density of 30% in the Bw horizon and 10% in the BC horizon (Table 4.1; Figure 4.7D). Rhizolith density decreases downward in all Pedotype II paleosols other than those that are cumulative. Rhizohalo architecture appears to follow ped structure (Figure 4.7C, D), suggesting that plants were exploiting and expanding macrovoids within the soil as they

followed the path of least resistance for root growth and, thus, aiding in ped formation. This pedotype is most likely to contain some, albeit rare FeMn rhizotubules (2% of rhizohalos; Figure 4.3e). Rhizohalos of this pedotype are dense and have slightly larger diameter than Pedotype I 'small rhizohalos' (0.5 cm -4 cm). In addition, rhizohalos within Pedotype II have the most abundant silica root petrifaction cores (35% – 40% of rhizohalos). These petrifactions are spectacularly preserved, bifurcating silicified roots with diameters that range from 0.1 cm to 1.5 cm in diameter (Figure 4.3f, g, 4E-H).

Bulk paleosol matrix samples were obtained from the middle of each horizon at 19.5 cm (Bw horizon), 61 cm (BC horizon), and 97.6 cm (C horizon) and were analyzed for bulk geochemical composition. The CALMAG molecular weathering ratio was calculated for the bulk geochemistry of the uppermost B horizon, and has a value of 77.0 (Table 4.3). The smectitic clay mineralogy in association with >40% clay content and occasional faint slickensides, suggest that physical and chemical transfer functions for paleo-Vertisols may be applied.

Chemical and physical characterization data derived from bulk molecular oxides are shown in Table 4.3. Pedotype II has a high total clay and moderate fine clay content. This pedotype has a relatively high COLE value, which indicates high shrink-swell potential (Soil Survey Staff, 2011). CEC is high, which is consistent with smectitic clay mineralogy and abundant clay content. This pedotype is neutral and has a slightly lower base saturation than Pedotype I. ESP and EC values are below the thresholds for negative plant impacts (Brady and Weil, 2001). The Fe_d values indicate a moderate accumulation of pedogenic iron, and moderate Fe_o values are suggestive of periodic anaerobiosis (Nordt and Driese, 2009; Nordt and Driese, 2010a).

Interpretation. Like Pedotype I, Pedotype II has 'purple' matrix colors that are interpreted to result from post-burial diagenetic color alteration (Retallack, 1991; Soil Survey Staff, 1999; Kraus and Hasiotis, 2006), suggesting imperfectly drained pedogenic conditions (Kraus and Hasiotis, 2006). FeMn nodules in thin-section, Fe and Mn rhizotubules, and Fe_o values suggest fluctuating hydrologic conditions with periods of anaerobiosis (Vepraskas, 1992). Pedotype II underwent rooting and ped formation pedogenic processes, but unlike Pedotype I, does not appear to have undergone extensive clay shrink-swell processes (very few and faint slickensides). Shrink-swell processes may have been inhibited due to higher silt in the soil matrix of this pedotype (Southard et al., 2011).

Pedotype II paleosols taxonomically classify as Inceptisols due to the presence of a Cambic (Bw) subsurface horizon (Soil Survey Staff, 1999). This paleosol may also be aquic at the subgroup level as suggested by its purple matrix colors. CALMAG weathering ratio of 77.0 provides a mean annual precipitation of 1310 mm for this pedotype (Nordt and Driese, 2010b). This CALMAG value suggests that the soil classifies within a Udic soil moisture regime (Nordt and Driese, 2010b).

Truncated paleosol profiles of Pedotype II reflect sedimentation and pedogenesis punctuated by periods of erosion (Kraus, 1999). Pedotype II paleosols are single profiles that are weakly developed, vertically stacked and separated by minimally weathered sediment ('composite' *sensu* Kraus, 1999). Paleosol profiles displaying thick B horizons are cumulative and reflect continuous and slow sedimentation during relatively stable rates of pedogenesis (Kraus, 1999). Single Pedotype II profiles have limited solum thicknesses and likely formed in higher sedimentation rates relative to pedogenesis.

Pedotype II contains no pedogenic features that require long periods of landscape stability for formation (Retallack, 2001; Retallack, 2005). A lack of vertic features within this pedotype suggests that grain size was too coarse for the formation of slickensides. Parent material facies of Pedotype II are interpreted as thin crevasse splay and proximal overbank deposits (Table 4.1) that suggest Pedotype II formed in a more channel-proximal landscape position than Pedotype I (Figure 4.5F).

Rhizohalos are larger in diameter than the 'small rhizohalos', but smaller than the 'large rhizohalos' of Pedotype I. They commonly contain well-preserved bifurcating silicified roots that are dense, shallow, and have slightly larger diameters than those in the 'small rhizohalos' of Pedotype I. Silica root petrifactions may represent root distributions of small-stature herbaceous or woody shrub plants or tree saplings and indicate dense ground cover with rare to no large arborescent plants (Pfefferkorn and Fuchs, 1991; LePage and Pfefferkorn, 2000; Hembree and Nadon, 2011).

Pedotype III

Description. Twelve of fifty-eight Sonsela paleosol profiles were grouped as Pedotype III. Pedotype III paleosols are commonly truncated and stacked profiles of thickness that ranges from 40 cm (single profile) to 170 cm (stacked). Individual paleosols within stacked profiles commonly occur as thin Bw-BC sequences interbedded with thin (< 10 cm) C/B and A/C horizons (Entisols). Pedotype III consists of a noncalcareous and possibly truncated Bw-BC-C horizon sequence (Figure 4.5G, H; Table 4.1). The Bw horizon appears to be cumulative and is a weak red (7.5R 5/2) siltstone with medium to coarse subangular blocky ped structure, and contains white (N 8/1)

rhizohalos with few dark bluish gray (5PB 4/1) internal halos (Figure 4.3i, j; Table 4.1). The BC horizon is a pale red (7.5R 5/1) faintly bedded clayey siltstone to very fine sandstone overprinted with medium subangular blocky ped structure (Table 4.1; Figure 4.5G, H). The C horizon is a bedded fine to medium sandstone. Some Pedotype III paleosol profiles may contain rare, faint slickensides. Pedotype III parent materials are commonly composed of fine- to medium-grained rippled (Sr facies), laminated (Sh facies) or large-scale low-angle cross stratified (Sl) sandstones (Table 4.2; Figure 4.5I).

Pedotype III is characterized in thin-section by masepic and skelsepic plasmic microfabrics (Figure 4.6G). Skeletal grain mineralogy is diverse and contains quartz, chert, plagioclase, devitrified volcanic rock fragments, and mica (Figure 4.6G). FeMn nodules range in diameter (from 25 μm to 200 μm), and are commonly irregular with both diffuse and solid boundaries (Figure 4.6I). Thin-sections contain silicified roots within drab root halos (Figure 4.4D), elongated FeMn accumulations that bifurcate (Figure 4. 4B), and FeMn coatings around silica (silicified root?) within drab halos (Figure 4.4D). Pedotype III contains sand-sized and silt-sized skeletal grains within a matrix of clay (greater than 40% clay; Figure 4.6H).

Pedotype III rhizoliths include solid drab rhizohalos, drab rhizohalos with small blue internal rhizohalos, silica root petrifactions, and FeMn rhizotubules. Rhizohalos range in diameter from < 1 to 15 cm, with an average of 10 cm (Figure 4.7E, F). Rhizohalo density is highest in the Bw horizon with 46% drab zones within the matrix. The high rhizohalo density is due to the large diameter of rhizohalos (up to 15 cm) rather than greater abundance (Table 4.1; Figure 4.7E, F). These large rhizohalos may overlap or merge if rhizohalo diameters exceed the distance between original roots, and as such,

the number of rhizohalos within the Bw horizon is difficult to quantify. If little overlap and merging has occurred, then rhizohalo density within Pedotype III appears to be slightly less than that of Pedotype II, but greater than Pedotype I. Few large white rhizohalos have small-diameter dark blue rhizohalos at their cores (Figure 4.3i, j). Silicified roots have very small diameters (0.1 cm to 0.4 cm) and are found within 20-30% of the drab halos (Figure 4.3j).

Bulk geochemical samples obtained from each horizon at 38 cm (Bw horizon) and 92.5 cm (BC horizon) were analyzed using the CALMAG weathering ratio. The CALMAG weathering ratio is 78.02 (Table 4.3). Physical and chemical transfer functions for paleo-Vertisols may be applied to Pedotype III due to its smectitic clay mineralogy, >40% clay, and rare faint slickensides. Chemical and physical characterization data derived from bulk molecular oxides indicate Pedotype III has a high total clay and moderate fine clay content (Table 4.3). This pedotype has a relatively high COLE value, which indicates high shrink-swell potential (Soil Survey Staff, 2011). High CEC is due to smectitic clay mineralogy and high clay content. This pedotype has a neutral pH and high base saturation (similar to Pedotypes I and II; Table 4.3). ESP and EC values are below thresholds for negative plant impacts (Brady and Weil, 2001). Fe_d values indicate a lower accumulation of pedogenic iron than Pedotype I, and Fe_o values are suggestive of periodic anaerobiosis (Nordt and Driese, 2010a).

Interpretation. Unlike Pedotype I and II, Pedotype III paleosols have red matrix colors interpreted to represent well-drained conditions during pedogenesis (Vepraskas, 1992; Retallack, 2001; Vepraskas, 2001; Kraus and Hasiotis, 2006). Pedogenic processes dominating Pedotype III are rooting and ped formation. Like Pedotype II, Pedotype III

did not undergo extensive clay shrink-swell processes as indicated by the rarity of slickensides. This is unusual given the smectitic clay mineralogy, although the coarse matrix texture may have inhibited shrink-swell processes (*sensu* Southard et al., 2011).

Pedotype III paleosols taxonomically classify as Inceptisols due to the presence of a Cambic (Bw) subsurface horizon (Soil Survey Staff, 1999). Paleosols are compound and cumulative, and compound Pedotype III paleosols commonly occur as composite truncated sets (*sensu* Kraus, 1999). Facies of Pedotype III parent materials are interpreted as lateral accretion and proximal crevasse splay deposits (Table 4.1). Pedotype III likely formed on channel margins and proximal crevasse splay positions in channel-proximal landscape positions. CALMAG weathering ratio of 78.0 provides a mean annual precipitation of approximately 1331 mm $year^{-1}$ and a Udic soil moisture regime (Nordt and Driese, 2010b). Pedotype III does not contain paleosol features suggestive of long-period pedogenesis (Retallack, 2001; Retallack, 2005). Limited solum thicknesses, common interbedding with B/C and A/C horizons and dominance of composite and cumulative paleosols suggest Pedotype III formed over the shortest time-frame and during the highest rates of sedimentation.

Rhizohalos of Pedotype III are dense due to their thick diameter, but appear to have lower abundance than Pedotype II. Silica root petrifactions occur in similar abundance to Pedotype II, but have smaller diameters. Small, dense and shallow rhizoliths may represent the root distributions of either small herbaceous plants (Pfefferkorn and Fuchs, 1991; LePage and Pfefferkorn, 2000) or small-stature tree saplings or woody shrubs. As silica root petrifactions reflect more reliably the plant root

size, plants inhabiting Pedotype III appear to be of smaller stature than those of Pedotype II.

Sonsela Paleocatena and Ecosystem

Paleosols and rhizoliths described within the lower Sonsela Member allow the interpretation of spatial variations in paleosol drainage, texture, soil processes and the inferred plant ecosystem. Paleosol properties and associated depositional facies may be used to reconstruct paleotopographic setting and relative rates of sedimentation and erosion (McCarthy et al., 1997; Kraus, 1999; Retallack, 2001; Hembree and Hasiotis, 2007; Hembree and Nadon, 2011). Paleosols of the Sonsela Member within the study area indicate a decrease in drainage and textural grain size, and bimodality of rhizoliths (small: 0.5 cm - 1 cm, 97 - 98% abundance, large: 10 cm – 28 cm, 2% - 3% abundance) with increasing distance from the paleochannel.

Paleocatena

Pedotype III is only observed atop lateral accretion and proximal crevasse splay deposits. The cumulative and compound (interbedded with Entisols) habit of Pedotype III suggests frequent flooding and sedimentation that was variably steady and punctuated (Kraus, 1999). Red matrix colors indicate well-drained conditions in spite of their location adjacent to paleochannels that were likely frequently flooded. Well-drained conditions are most likely due to coarse textures. High sedimentation rates, the abundance of crevasse-splay deposits and well-drained paleosols suggest that Sonsela channels had elevated channel levees relative to surrounding floodplains (*cf.* Wright, 1992; Arndorff, 1993; Kraus, 1999; Figure 4.9). The lack of abundant, well-developed

slickensides in Pedotype II is attributed to the high proportion of silt and sand within the soil matrix (Southard et al., 2011).

Pedotype II paleosols are commonly weathered into paleoenvironmental positions that are relatively more distal to equivalent channels (e.g., distal crevasse splay and proximal overbanks), and consequently, were subjected to slightly less frequent flooding and lower sedimentation rates than Pedotype III. The more clay-rich texture (compare Figure 4.6E with 4.6H) and lack of interbedding with Entisols suggest rates of sedimentation lower than Pedotype III, but higher than Pedotype I (*cf.* Guccione, 1993; Kraus, 1999; Figure 4.9). The purple color of Pedotype II suggests less well drained conditions. The less well drained conditions are attributed to paleosol formation in more channel-distal positions where the landscape elevation is lower, and therefore closer to the water table (*cf.* Kraus, 1999; Arndorff, 1993; Figure 4.9). Pedotype II does not contain features suggestive of shrink-swell processes due to its silty matrix textures (Southard et al., 2011).

Pedotype I paleosol profiles form in mid- to distal overbank paleoenvironments. Paleosols are finer grained (Figure 4.5B compared with Figure 4.5E and 4.5H) and more commonly occur as composite successions. These attributes suggest lower rates of sedimentation than Pedotypes II and III (*cf.* Guccione, 1993; Kraus, 1999). The color of Pedotype I indicates less well drained conditions; consistent with formation across lower topographic positions that are closer to the water table (Arndorff, 1993; Kraus, 1999; Figure 4.9). Sediments deposited within more channel-distal positions are finer, enabling formation of slickensides within the high COLE, smectitic Sonsela pedosystems (Southard et al., 2011).

The fining-upward nature of the Sonsela Member within the "Blue Mesa" area of PFNP has been interpreted to record the progressive migration of a fluvial channel(s) away from the study area (Trendell et al., 2012). The base of the succession is dominated by mixed- or bed-load fluvial channels and a high channel: overbank ratio (Trendell et al., 2012). Overbank paleosols at the base of the succession classify only as Pedotypes II and III. Channel: overbank ratio decreases upsection (Trendell et al., 2012), and paleosols transition into Pedotype I. Within the uppermost portion of succession, deposits consist predominantly of overbank mudrock and exclusively Pedotype I. At the base of the succession, Pedotype III can be traced laterally and is observed to transition into a Pedotype II paleosol with increasing distance from the paleochannel (100 - 200 m). Up-section, Pedotype II can be traced laterally and is observed to transition into a Pedotype I paleosol with increasing distance from the paleochannel (0.2 to 0.5 km). In the middle portion of the succession, a lateral transition from Pedotype III to Pedotype II to Pedotype I is observed.

Mean annual precipitation remained approximately 1300 mm per year throughout the succession, and suggests that variations in paleosol characteristics were influenced primarily by topographic position rather than climate (Figure 4.9). Paleosol and sediment characteristics indicate that Sonsela channels consisted of elevated leveed margins (Figure 4.9). Decreasing permeability (due to fining grain size) and a loss of elevation away from the active channel resulted in decreased paleosol drainage and an increase in shrink-swell processes (Southard et al., 2011).

Overall, Sonsela paleosols are immature and do not contain paleosol features suggestive of prolonged pedogenesis. The most mature paleosols (Pedotype I) likely

formed within decades to centuries (Soil Survey Staff, 1999; Nordt et al., 2004). The study interval, which represents approximately 8-9 Ma of geologic time (Ramezani et al., 2011; Figure 4.2), contains between 9 and 14 single, compound and composite paleosols that only represent a maximum pedogenic duration of thousands to tens of thousands of years. Considering that most of geologic time in alluvial successions is recorded as non-deposition or weathering (pedogenesis), the limited length of pedogenesis relative to age of the study succession suggests that the record of time is missing within unconformities (scours, truncation of channels and paleosols) throughout the succession. The Sonsela system likely underwent high rates of erosion throughout deposition. Low rates of subsidence within the Sonsela Member (Ramezani et al., 2011) may have resulted in high rates of lateral channel migration and the recycling of overbank fines. The abundance of crevasse splay deposits and presence of truncated paleosols in all pedotypes throughout the study succession are consistent with this possibility. Overbank recycling may have reduced the overall duration of pedogenesis within the study interval, and therefore, account for the relative immaturity of the paleosols observed

Ecosystem

Pedotypes were likely fertile in terms of plant-available nutrients derived from high CEC, relatively high base saturation, and high available water holding capacity related to low bulk densities (Table 4.3; Blackmer, 2000; Brady and Weil, 2001). Therefore, limiting factors for plant growth within this system may include paleosol drainage and high rates of flooding and sedimentation. Sonsela rhizoliths show systematic changes with distance from the paleochannel. Despite little to no preservation

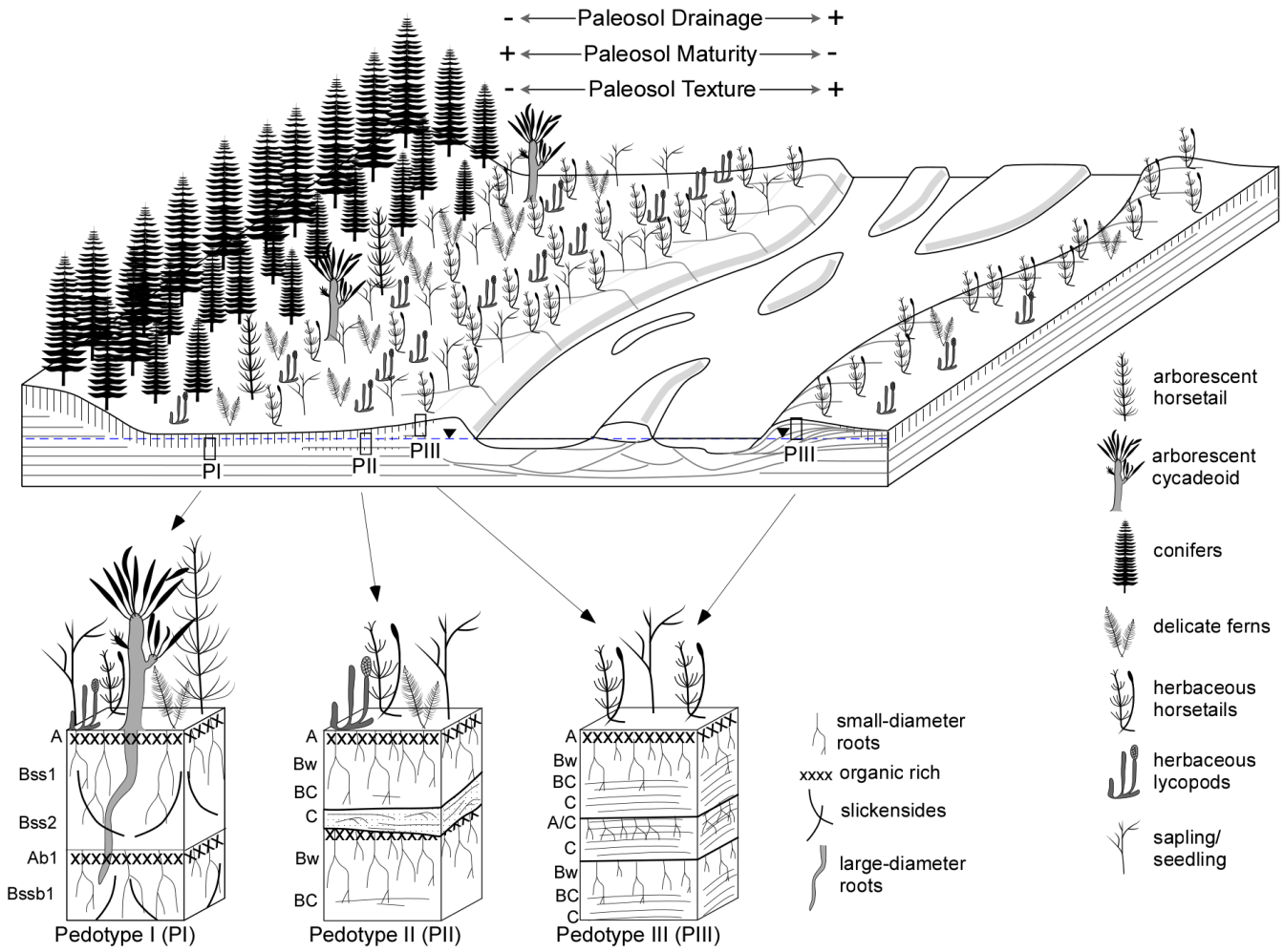

Figure 4.9. Conceptual model of the Sonsela fluvial system showing the relationship between channel, elevated channel levee, and floodplain landscape positions. The approximate location of mean high water table is interpreted from pedotype drainage. Interpreted plant distributions are shown for each paleoenvironment. Conifers are interpreted to grow within hypothetical upland locations that are not preserved within the study interval. Conceptual illustrations of Pedotypes I, II, and III show paleosol characteristics and the floodplain environment that they form in.

of plant material within the Sonsela, the distribution of plants may be inferred from rhizolith size, density, and architecture in combination with paleosol characteristics.

Channel proximal paleosols (Pedotype III) have silica petrifactions that represent small herbaceous and shrubby plants (Pfefferkorn and Fuchs, 1991; LePage and Pfefferkorn, 2000) or small-stature tree saplings. Considering the Blue Mesa Member paleobotanical record, channel-proximal positions within the Sonsela could have been inhabited by herbaceous lycopods, horsetails, ferns or saplings of arborescent plants (Daugherty, 1941; Ash, 1972; Demko, 1995; Ash, 2005; Ash, 2010). Lycopods, were unlikely to have grown on the well-drained, elevated, channel proximal positions in the Sonsela, as they predominantly grew in coal-forming swamps and preferred saturated soil conditions (DiMichele et al., 2001; Ash, 2010). Ferns of the Chinle Formation required shelter from more robust plant forms (Ash, 2001; Ash, 2010) and their delicate forms were not adapted to the high-frequency flooding and channel migration that characterized channel-margin positions within the Sonsela system. Horsetails are well-adapted to channel-proximal environments, as they survive partial burial and continue to grow (Demko, 1995; Demko and Gastaldo, 1992; Gastaldo, 1992). Channel-proximal positions within the Sonsela were most likely dominated by horsetails, which may have included the smaller-form *Neocalamites* genera (a member of the Calamitales family, belonging to the Sphenophytes; Figure 4.9). This is consistent with the findings of Demko (1995), who documented abundant fossils of *Neocalamites* preserved within 'crevasse splay' facies of the Blue Mesa Member. Small roots in channel proximal positions may also represent seedlings of arborescent plants, which commonly colonize

modern ‘active’ channels and proximal-channel floodplains during periods of low discharge (Gregory et al., 1991).

Pedotype II paleosols formed proximal to the channel, but more distal than Pedotype III, within conditions that were imperfectly drained and subjected to flooding events with slightly less frequency than characterized Pedotype III. Silica petrifactions reflect herbaceous or shrubby plants or saplings of arborescent plants of larger size than observed in Pedotype III. This is consistent with modern floodplains, whose plant communities display older and more established plant populations with distance from the active channel (Gregory et al., 1991). Imperfectly drained conditions in this topographic position would satisfy lycopod growth conditions (DiMichele and Phillips, 1985; DiMichele et al., 2001; Ash, 2010). Delicate ferns were likely still rare due to the destructive effects of flooding (Figure 4.9).

Pedotype I paleosols contain bimodal rhizolith size distributions that suggest both herbaceous understory and arborescent plants. This is consistent with the ‘wetland facies’ of Demko (1995) who documents elements of both herbaceous and arborescent overbank vegetation in Blue Mesa strata that underlie the study interval. Rhizolith sizes suggest that floodplains were unlikely to have supported a dense forest or woodland, which is consistent with the rarity of preserved in-situ stumps within the Sonsela (W. Parker, personal communication, 2012). Bimodal rhizohalos are interpreted to instead reflect dense understory plants and saplings with rare arborescent plants within a ‘savannah-like’ or open-woodland biome that is a transition between the channel-proximal disturbed ecosystem and an upland dense coniferous woodland or forest. The rare larger rhizoliths may be attributed to arborescent plants such as horsetails

(*Equisetites* and *Neocalamites*), cycads, cycadeoids, ginkgoes (*Ginkgoites watsonii*), cordaites or conifers (Ash, 1969; Ash, 1972; Ash, 2005; Savidge, 2006; Ash, 2010). Horsetails (*Equisetites* and *Neocalamites*) and cycadeoids (*Zamites powellii*) are of the most commonly found arborescent floral fossils within the Chinle, and, therefore, arborescent plants within distal floodplains may have had the highest proportions of these plants (Demko, 1995; Ash, 2010). In the presence of sheltering arborescent plants, delicate ferns may have grown in greater abundance (Ash, 2001; Figure 4.9). Modern ferns require water for reproduction, therefore distal floodplain positions may have provided ideal reproductive conditions (Evert and Eichhorn, 2004; Taylor et al., 2008). Those rare conifers preserved *in-situ* (W. Parker, personal communication, 2012) are found only inhabiting the most distal floodplains, likely along the fringe of unpreserved uplands. The abundant silicified logs preserved in channels are interpreted to have been sourced from upland landscape positions that are not preserved within the study area (Figure 4.9). High rates of lateral migration, avulsion and cannibalization within the Sonsela system eroded overbanks and their plant communities, forcing plants to re-colonize the new overbank deposits. The low abundance of large rhizohalos is likely due to short establishment periods that prevented preservation of older-growth trees due to high disturbance frequencies.

Lateral meandering and cutting of the Sonsela channel into older riparian or upland landscapes resulted in erosion of established plant communities allowing development of younger stands of plants along the inner margin of meanders. This is consistent with previous interpretations that silicified conifer logs were sourced by transportation from upland positions and introduced (toppled) into the channel via

cutbank erosion (Demko, 1995). The Sonsela Member within the "Blue Mesa" area of PFNP accumulated within a dynamic, and hence, sedimentologically unstable fluvial valley system where only immature ecosystems were preserved.

The Sonsela ecosystem differs from other members of the Chinle Formation. In the Blue Mesa and Black Forest Members, large silicified stumps are commonly found in-situ on proximal floodplain environments (Demko, 1995). Higher rates of subsidence within the Blue Mesa and Petrified Forest Members (Ramezani et al., 2011) may have resulted in decreased meander and avulsion rates and increased overbank stability relative to the Sonsela. This, in turn, may have allowed the establishment of more mature plants. Additionally, Blue Mesa channel-proximal deposits are commonly poorly drained and host lycopods (Demko, 1995) that indicate a lack of elevated channel levee environments.

Silica Root Petrifaction and Rhizohalo Trends

Silica root petrifactions increase in abundance with proximity to the paleo-channel (from Pedotype I to Pedotype III), and may be the result of both excess silica availability and/or stratal permeability. The excess silica that induced log petrification was likely sourced from the devitrification of volcanic detritus within Sonsela sandstones (Sigleo, 1979; Trendell et al., 2012; *cf*. Murata, 1940). Channel-proximal topographic positions (Pedotype III and Pedotype II, crevasse splay and proximal overbank) had a higher proportion of volcanic detritus than channel-distal positions. This may be due to the relative weatherability of volcanic detritus relative to other sand types, resulting in their preferential reduction in finer size fractions (which are deposited within more channel-distal landscapes). This resulted in more concentrated silica within groundwater

in channel proximal paleosols. Also, coarser textures in channel-proximal positions were more permeable and allowed for greater infiltration of silica-rich groundwater.

Interestingly, rhizohalo diameters decrease with distance from the paleo-channel and do not correlate with actual root size interpreted from silica root petrifactions. Although modern rhizohalo (Fe depletions) diameters may possibly be controlled by length of depletion time (Vepraskas, 1992), Sonsela paleosol characteristics suggest that Pedotype III (containing the largest rhizohalos) was subjected to more saturated and reduced conditions for shorter periods than Pedotypes II and I (which have smaller rhizohalos). Diagenetic rhizohalo diameters, instead, appear to correlate with paleosol matrix textures. Diagenetic iron reduction occurs within the zone that reduced waters can infiltrate into the soil matrix after post-burial flooding (Retallack, 2001). We propose that Sonsela paleosols with coarser, more permeable sediments have larger infiltration zones that can be affected by reducing conditions during diagenesis. In the Sonsela Member at PFNP, the size of diagenetic rhizohalos appears to be determined by paleosol texture rather than root size or length and frequency of saturated conditions.

Summary and Conclusions

The Late Triassic Sonsela Member at Petrified Forest National Park contains three distinct pedotypes that are differentiated by their degree of pedogenic development and welding, paleotopographic position, preserved macro- and micro-morphological characteristics, chemical and physical properties, and rhizolith morphologies. Each pedotype corresponds to a different sub-environment across the Sonsela alluvial floodplain that includes proximal-channel (point bar), crevasse splay and proximal overbank, and distal overbank. Lateral changes in paleosol characteristics are observed

with distance from the paleochannel. Pedotype I is interpreted as a Vertisol that formed in an aquic moisture regime across distal floodplain positions. Pedotype II is interpreted as an Inceptisol that formed in seasonally poorly-drained medial to distal crevasse splays and proximal overbank environments. Pedotype III is interpreted as a well-drained Inceptisol that formed across point bars and elevated channel levees. Mean annual precipitation estimates within the Sonsela Member vary little and suggest that variations in paleosol characteristics are controlled predominantly by landscape position and associated variability in the flooding frequency, paleosol texture, and rates of sedimentation. Pedotypes show increased welding and decreased rates of sedimentation away from the paleochannel. Sonsela pedotypes contain smectitic clay mineralogies, and the degree of shrink-swell processes are influenced by paleosol textures. Channel-proximal paleosols display coarser textures and do not exhibit extensive shrink-swell features.

Paleosol stacking and welding allows for interpretation of sedimentation rates and flooding within Sonsela subenvironments. Overall, Sonsela Member paleosols are immature and have characteristics that suggest high rates of sedimentation punctuated by stability and erosion. Abundant crevasse splays, and variability in paleosol drainage and maturity suggest the Sonsela fluvial system was characterized by rapid lateral channel migration and overbank recycling during a period of low subsidence rates.

Rhizolith morphology, size and depth within paleosols indicate changes in overall root architecture that may be used to infer plant type across the Sonsela landscape. Rhizolith characteristics suggest that Pedotype I hosted both herbaceous understory plants and arborescent plant populations, whereas plants inhabiting Pedotypes II and III

were predominantly herbaceous, shrubby or were saplings and seedlings of arborescent plants. Pedotype I hosted the oldest plant populations that included delicate ferns, herbaceous lycopods and horsetails, arborescent cycadeoids, arborescent horsetails, and rare conifers (and possibly others). Pedotype II was closer to the active channel and hosted less established plant populations including saplings and herbaceous horsetails and lycopods with rare ferns. Pedotype III paleosol plants were characterized by the youngest and least established vegetation stands due to increased flood frequency. Plant types associated with Pedotype III may have included herbaceous horsetails and saplings of arborescent plants. Rhizoliths suggest that conifer forests or woodlands did not inhabit preserved Sonsela floodplains, but rather, were restricted to upland positions that are not represented within the study interval. Overall, the Sonsela ecosystem consists of a relatively immature plant community due to high rates of lateral channel migration and overbank recycling.

Sonsela rhizoliths include rhizohalos, silica root petrifactions, and Fe and Mn rhizotubules. Sonsela rhizohalos are diagenetic due to their homogenous color, presence along non-root voids (such as slickenside planes), and lack of analogous modern features related to plant growth (such as Fe and Mn rims along rhizohalos or iron depletions). Silica cores within rhizohalos are interpreted as silicified roots and represent the living size of the plant root. Rhizohalo diameters decrease with distance from the paleo-channel and do not correlate with actual root size (interpreted from silica root petrifactions). Rhizohalo diameter, instead, appears to correlate with paleosol matrix textures. Silica root petrifactions are in greater abundance in channel-proximal positions, owing to

coarser textures and associated higher permeability, and availability of soluble silica in groundwaters.

The presence of silicified roots within rhizohalos afford a unique opportunity to determine the size of plants that inhabited the paleolandscape, and what, if any relationship exists between root diameter and rhizohalo diameter. The size of diagenetic rhizohalos within the lower Sonsela are influenced by matrix textures and permeability of the paleosol matrix. More coarse, permeable sediments can be more readily infiltrated and subsequently reduced along root voids during post-burial flooding. This results in larger rhizohalos surrounding root voids in coarser paleosols. This finding suggests caution when interpreting below-ground biomass and root size from rhizohalos.

This study improved the current understanding of the Sonsela ecosystem in the "Blue Mesa" outcrops at Petrified Forest National Park. Previously thought to be dominated by conifer forests or woodlands, the preserved overbank deposits did not host a dense coniferous forest or woodland, but more likely hosted early successional plant communities consisting of arborescent plant saplings and herbaceous and smaller arborescent plants. Silicified logs within the Sonsela were sourced from upland positions that are not preserved within the study area, or were introduced to the channel via cut-bank erosion of more established floodplain riparian communities. *In-situ* conifers in distal overbank sediments likely inhabited a 'fringe' area adjacent to upland positions. The immaturity of the Sonsela ecosystem, as reflected from rhizohalos, is caused by low rates of subsidence and high rates of lateral accretion and avulsion within the fluvial system.

CHAPTER FIVE

Conclusions

The Upper Triassic Sonsela Member at Petrified Forest National Park accumulated as a bedload to suspended-load fluvial system, and includes interbedded overbank mudrock and channel sandstones. The succession fines upward and has an increasing proportion of overbank: channel deposits, and increasing sandstone and paleosol maturity. Little variation in paleosol drainage and illuviation characteristics within the Sonsela Member suggests that the succession accumulated within relatively stable climate. Changes in fluvial style and lithologic proportions are attributed to both autocyclic and tectonic (or orogenic) pulses that resulted in base level changes and subsequent changes in fluvial style. The overall immaturity of Sonsela paleosols indicates either a high rate of floodplain aggradation or a high rate of avulsion and overbank cannibalization.

Devitrification of volcanogenic sediments within Sonsela sandstones resulted in the silicification of wood as well as the precipitation of interparticle authigenic clays. Limited compaction of petrified logs (range from 0-26%, average 9%) provides evidence to suggest replacement cementation at very shallow burial depths. Sonsela sandstones have little to no porosity due to precipitation of diagenetic products within pore space. Interparticle clays are indicative of primary porosity, which decreases up-section in association with decreasing grain size and increasing overbank deposition. This study documents the complete destruction of primary porosity in immature sandstones prior to burial and has clear implications to the risk associated with the exploration of mineralogically immature sandstones.

At a larger scale, the study succession from the Blue Mesa to the Sonsela Member, records a progressive up-section increase in grain size, increase in channel depth and width, increase in lateral and vertical connectivity of channel deposits, decrease in overbank preservation and crevasse-splay and/or sheetflood deposition, and increase in paleosol/ overbank drainage. Mean annual precipitation, however, (calculated using the CALMAG paleosol weathering proxy) remained relatively constant and sandstone composition displays an up-section decrease in mineralogical maturity. Progradation of a large fluvial fan provides a mechanism that can account for depositional element trends, paleosol drainage changes within stable MAP, and decreased sandstone maturity within a decreasing-subsidence regime. Apparent size of the Chinle system, as determined by paleocurrent data, clast size trends, stratal thicknesses and volcanic content, suggests a large system similar to modern large fluvial fans in compressional basins.

The Newspaper Rock channel is interpreted to represent either an 'axial' or 'interfan' channel or a large channel within the distal fan area. The Blue Mesa Member has characteristics consistent with accumulation within a high accommodation setting in low-lying topographic areas such as distal fan. Increasing channel depth and width, increasing lateral and vertical connectivity of channel-fill elements, and decreasing preservation of overbank deposits within the Sonsela Member are consistent with medial fan deposition and suggests that the Chinle fan underwent progradation. Increasingly better drained paleosols from the Blue Mesa to the Sonsela Member are interpreted to suggest progressively better-drained landscape positions due to progradation of a sediment wedge.

Within the large fluvial fan system, low rates of subsidence during deposition of the Sonsela Member likely increased rates of lateral channel migration and cannibalization of overbank deposits, resulting in relatively immature paleosols. The Late Triassic Sonsela Member at Petrified Forest National Park contains three distinct pedotypes that correspond to different sub-environments across the Sonsela alluvial floodplain. Pedotypes include an aquic Vertisol that formed in distal floodplain positions, a poorly-drained Inceptisol that formed in medial to distal crevasse splays and proximal overbank environments and a well-drained Inceptisol that formed across point bars and elevated channel levees. Laterally decreasing paleosol drainage and grain size are observed with distance from the paleochannel. Stable mean annual precipitation estimates suggest that variations in paleosol characteristics are controlled predominantly by landscape position and associated variability in flooding frequency, paleosol texture, and rates of sedimentation.

The Sonsela ecosystem, as determined from rhizoliths, consists of a relatively immature plant community caused by low rates of subsidence and high rates of lateral accretion and avulsion within the fluvial system. Rhizolith characteristics suggest that paleosols proximal to the paleochannel hosted the youngest and least established vegetation stands due to increased flood frequency and migration of fluvial channels while distal paleosols hosted the oldest plant populations that were understory, herbaceous and shrubby and arborescent. Rhizoliths suggest that conifer forests or woodlands did not inhabit preserved Sonsela floodplains, but rather, were restricted to upland positions that are not represented within the study interval.

Sonsela rhizoliths are likely diagenetic and influenced by matrix textures and permeability of the paleosol matrix, suggesting caution when interpreting below-ground biomass and root size from rhizohalos. Silica cores within rhizohalos are interpreted as silicified roots and likely represent the living size of the plant root. Silica root petrifactions are in greater abundance in channel-proximal positions, owing to coarser textures and associated higher permeability, and availability of soluble silica in groundwaters.

This research emphasizes the importance of integrating paleosols into fluvial sedimentological studies. Paleosols provide data regarding paleoclimate, palaeohydrology, fluvial system stability, and paleovegetation at a meter to decametre scale within successions that are unlikely to contain other high-resolution climatic data (such as paleontologic data). Paleosol morphology and geochemistry, when combined with sedimentology, are powerful tools that can aid in determining or refining depositional scenarios by providing a better-understanding of local climate.

APPENDICES

APPENDIX A

Copyright Permissions

Chapter Two Copyright Permission

This chapter published as: Trendell, A.M., Atchley, S.C., and Nordt, L.C., 2012, Depositional and diagenetic controls on reservoir attributes within a fluvial outcrop analog: Upper Triassic Sonsela Member of the Chinle Formation, Petrified Forest National Park, Arizona: AAPG Bulletin, v. 96, no. 4, p. 679–707.

_____

From: Mary Kay Grosvald
Sent: Wednesday, May 09, 2012 1:55 PM
To: Trendell, Aislyn
Subject: Ph.D. Dissertation & AAPG copyright

Aislyn, for this purpose, and only for this purpose, you may reproduce in total a copy of your article (as listed below) published in AAPG Bulletin April issue within your Ph.D. dissertation.

Where you are the author of an AAPG article we consider it fair use to reproduce portions, or select images within other articles published in non-AAPG journals. It isn't necessary to ask for permission to reproduce your own images; however, we request you give proper attribution. Please refer to section (c) under "Conditions of Grant of Permission" on the attachment.

Best of luck with your dissertation.

Sincerely,
Mary Kay Grosvald
Mary Kay Grosvald
AAPG Permissions Editor

Chapter Three Copyright Permission

This chapter published as: Trendell, A.M., Atchley, S. C., and Nordt, L.C., in press, Facies analysis of a probable large fluvial fan depositional system: the Upper Triassic Chinle Formation AT Petrified Forest National Park, Arizona: Journal of Sedimentary Research, *in press*.

The Journal of Sedimentary Research is published by the Society of Sedimentary Geology (SEPM). As is stated within the SEPM Publications Permissions website, "Authors may... include the whole article in a PhD or other thesis provided that it will not be published, and that the original source is fully acknowledged in a standard format."

http://www.sepm.org/pages.aspx?pageid=297

Chapter Four Copyright Permission

This chapter has been submitted as: Trendell, A.M., Nordt, L.C., Atchley, S.C., LeBlanc, S.L. and Dworkin, S.I., Determining Floodplain Plant Distributions and Populations using Paleopedology and Fossil Root Traces: Upper Triassic Sonsela Member of the Chinle Formation at Petrified Forest National Park, Arizona: Palaios, *in review*.

Palaios is published by the Society of Sedimentary Geology (SEPM). As is stated within the SEPM Publications Permissions website, "Authors may... include the whole article in a PhD or other thesis provided that it will not be published, and that the original source is fully acknowledged in a standard format."

http://www.sepm.org/pages.aspx?pageid=297

REFERENCES

AAPG, 1988, Correlation of stratigraphic units of North America (COSUNA) project: Central and southern Rockies region: AAPG, Tulsa, Oklahoma.

Aigner, T., Asprion, U., Hornung, J., Junghans, W. -D, and Kostrewa, R., 1996, integrated outcrop analogue studies for Triassic alluvial reservoirs: Examples from southern Germany: Journal of Petroleum Geology, v. 19, no. 4, p. 393–406, doi: 10.1111/j.1747-5457.1996.tb00446.x.

Akahane, H., 2004, Rapid wood silicification in hot spring water: an explanation of silicification of wood during the Earth's history: Sedimentary Geology, v. 169, p. 219–228, doi: 10.1016/j.sedgeo.2004.06.003.

Allen, J.R.L., 1978, Studies in fluviatile sedimentation: an exploratory quantitative model for the architecture of avulsion-controlled alluvial suites: Sedimentary Geology, v. 21, no. 2, p. 129–147, doi: 10.1016/0037-0738(78)90002-7.

Arndorff, L., 1993, Lateral relations of deltaic palaeosols from the Lower Jurassic Rønne formation on the island of Bornholm, Denmark: Palaeogeography, Palaeoclimatology, Palaeoecology, v. 100, no. 3, p. 235–250, doi: 10.1016/0031-0182(93)90056-O.

Ash, S.R., 1969, Ferns from the Chinle Formation (Upper Triassic) in the Fort Wingate area, New Mexico: U.S. Geological Survey Profession Paper, v. 613D, p. D1–D40.

Ash, S.R., 1972, Plant megafossils of the Chinle Formation: Museum of Northern Arizona Bulletin, v. 47, p. 23–43.

Ash, S.R., 2001, The fossil ferns of Petrified Forest National Park, Arizona, and their paleoclimatological implications, *in* Santucci, V.L. and McClelland, L. eds., Proceedings of the 6th Fossil Resource Conference. Geological Resources Division Technical Report NPS/NRGRD/GRDTR-01/01, National Park Service, Grand Junction, Colorado, p. 3–11.

Ash, S.R., 2005, Synopsis of the Upper Triassic flora of Petrified Forest National Park and vicinity, *in* Nesbitt, S.J., Parker, W.G., and Irmis, R.B. eds., Guidebook to the Triassic Formations of the Colorado Plateau in northern Arizona: Geology, Paleontology, and History, Mesa Southwest Museum Bulletin, p. 59–70.

Ash, S.R., 2010, Stop one: summary of the Upper Triassic flora of the Newspaper Rock bed and its paleoclimatic implications, *in* Paleosols and Soil Surface System Analogs, SEPM-NSF Research Conference and Workshop, SEPM-NSF, Petrified Forest National Park, Arizona, p. 136.

Ash, S.R., and Creber, G.T., 1992, Palaeoclimatic interpretation of the wood structures of the trees in the Chinle Formation (Upper Triassic), Petrified Forest National Park, Arizona, USA: Palaeogeography, Palaeoclimatology, Palaeoecology, v. 96, no. 3–4, p. 299–317, doi: 10.1016/0031-0182(92)90107-G.

Ash, S.R., and Creber, G.T., 2000, The Late Triassic Araucarioxylon Arizonicum trees of the Petrified Forest National Park, Arizona, USA: Palaeontology, v. 43, no. 1, p. 15–28, doi: 10.1111/1475-4983.00116.

Atchley, S.C., Nordt, L.C., and Dworkin, S.I., 2004, Eustatic control on alluvial sequence stratigraphy: A possible example from the Cretaceous-Tertiary transition of the Tornillo Basin, Big Bend National Park, West Texas, U.S.A.: Journal of Sedimentary Research, v. 74, no. 3, p. 391–404, doi: 10.1306/102203740391.

Barth, A.P., Tosdal, R.M., Wooden, J.L., and Howard, K.A., 1997, Triassic plutonism in southern California: Southward younging of arc initiation along a truncated continental margin: Tectonics, v. 16, no. 2, p. 290–304, doi: 10.1029/96TC03596.

Batten, D.J., 1996, Palynofacies and petroleum potential, *in* Jansonius, J. and McGregor, D.C. eds., Palynology: Principles and Applications, American Association of Stratigraphic Palynologists Foundation, Salt Lake City, Utah, p. 1065–1084.

Bazard, D.R., and Butler, R.F., 1991, Paleomagnetism of the Chinle and Kayenta Formations, New Mexico and Arizona: Journal of Geophysical Research, v. 96, no. B6, p. 9847–9871, doi: 199110.1029/91JB00336.

Beard, D.C., and Weyl, P.K., 1973, Influence of texture on porosity and permeability of unconsolidated sand: AAPG Bulletin, v. 57, no. 2, p. 349–369.

Beer, J., 2005, Sequence stratigraphy of fluvial and lacustrine deposits in the lower part of the Chinle Formation, south central Utah, United States: paleoclimatic and tectonic implications [M.S. Thesis]: University of Minnesota, 180 p.

Beerbower, J.R., 1964, Cyclothems and cyclic depositional mechanisms in alluvial plain sedimentation, *in* Merriam, D.F. ed., Symposium on cyclic sedimentation: State Geological Survey of Kansas Bulletin, p. 31–42.

Billi, P., 2007, Morphology and sediment dynamics of ephemeral stream terminal distributary systems in the Kobo Basin (northern Welo, Ethiopia): Geomorphology, v. 85, no. 1–2, p. 98–113, doi: 10.1016/j.geomorph.2006.03.012.

Bilodeau, W.L., 1986, The Mesozoic Mogollon Highlands, Arizona: An Early Cretaceous rift shoulder: Journal of Geology, v. 94, p. 724–735.

Birkeland, P., 1999, Soils and Geomorphology: Oxford University Press, USA.

Bjørlykke, K., 1999, Principal aspects of compaction and fluid flow in mudstones: Geological Society, London, Special Publications, v. 158, no. 1, p. 73–78, doi: 10.1144/GSL.SP.1999.158.01.06.

Blackmer, A.M., 2000, Bioavailability of major essential nutrients, *in* Sumner, M.E. ed., Handbook of Soil Science, 2nd Edition, CRC Press, Boca Raton, Florida, p. D–3–D18.

Blakey, R.C., 1974, Stratigraphic and depositional analysis of the Moenkopi Formation, southeastern Utah: Utah Geological and Mineral Survey Bulletin, v. 104, p. 81 p.

Blakey, R.C., 2008, Pennsylvanian-Jurassic sedimentary basins of the Colorado Plateau and southern Rocky Mountains, *in* Miall, A.D. ed., The Sedimentary Basins of the United States and Canada, Sedimentary Basins of the World, Elsevier, Amsterdam, Boston, p. 245–296.

Blakey, R.C., and Gubitosa, R., 1983, Late Triassic paleogeography and depositional history of the Chinle Formation, *in* Reynolds, M.W. and Dolly, E.D. eds., Mesozoic Paleogeography of West-Central United States, Rocky Mountain Section Society for Sedimentary Geology (SEPM), Denver, p. 57–76.

Blakey, R.C., and Gubitosa, R., 1984, Controls of sandstone body geometry and architecture in the Chinle Formation (Upper Triassic), Colorado Plateau: Sedimentary Geology, v. 38, p. 51–86.

Blodgett, R.H., 1984, Nonmarine depositional environments and paleosol development in the Upper Triassic Dolores Formation, southwestern Colorado, *in* Brew, D.C. ed., Field Trip Guidebook, 37th Annual Meeting, Rocky Mountain, Geological Society of America, p. 46–92.

Blodgett, R.H., Crabaugh, J.P., and McBride, E.F., 1993, The color of red beds: A geologic perspective, *in* Bigham, J.M. and Ciolkosz, E.J. eds., Soil color, Soil Science Society of America, Madison, Wisconsin, p. 127–159.

Bloom, A.L., 1964, Peat accumulation and compaction in a Connecticut coastal marsh: Journal of Sedimentary Research, v. 34, no. 3, p. 599–603, doi: 10.1306/74D710F5-2B21-11D7-8648000102C1865D.

Blum, M.D., and Törnqvist, T.E., 2000, Fluvial responses to climate and sea-level change: a review and look forward: Sedimentology, v. 47, p. 2–48, doi: 10.1046/j.1365-3091.2000.00008.x.

Boggs, S.J., and Krinsley, D., 2006, Application of Cathodoluminescence Imaging to the Study of Sedimentary Rocks: Cambridge University Press, Cambridge.

Bown, T.M., and Kraus, M.J., 1987, Integration of channel and floodplain suites; I, Developmental sequence and lateral relations of alluvial Paleosols: Journal of Sedimentary Research, v. 57, no. 4, p. 587–601, doi: 10.1306/212F8BB1-2B24-11D7-8648000102C1865D.

Brady, N.C., and Weil, R.R., 2001, The Nature and Properties of Soils, 13th Edition: Prentice Hall.

Brewer, R., 1976, Fabric and Mineral Analysis of Soils: Robert E. Krieger Publishing Company, New York, New York.

Bridge, J.S., 1984, Large-scale facies sequences in alluvial overbank environments: Journal of Sedimentary Research, v. 54, no. 2, p. 583–588, doi: 10.1306/212F8477-2B24-11D7-8648000102C1865D.

Bridge, J.S., Jalfin, G.A., and Georgieff, S.M., 2000, Geometry, lithofacies, and spatial distribution of Cretaceous fluvial sandstone bodies, San Jorge Basin, Argentina: Outcrop analog for the hydrocarbon-bearing Chubut Group: Journal of Sedimentary Research, v. 70, no. 2, p. 341 –359, doi: 10.1306/2DC40915-0E47-11D7-8643000102C1865D.

Bryant, W.R., 2002, Permeability of clays, silty-clays and clayey-silts: Transactions-Gulf Coast Association of Geological Societies, p. 1069–1078.

Bull, W.B., 1991, Geomorphic responses to climate change: Oxford University Press, New York.

Cain, S.A., and Mountney, N.P., 2009, Spatial and temporal evolution of a terminal fluvial fan system: the Permian Organ Rock Formation, South-east Utah, USA: Sedimentology, v. 56, no. 6, p. 1774–1800, doi: 10.1111/j.1365-3091.2009.01057.x.

Cain, S.A., and Mountney, N.P., 2011, Downstream changes and associated fluvial-eolian interactions in an ancient terminal fluvial system: the Permian Organ Rock Formation, SE Utah, U.S.A., *in* Davidson, S., Leleu, S., and North, C.P. eds., From River To Rock Record: The preservation of fluvial sediments and their subsequent interpretation, SEPM Special Publication 97, p. 165–187.

Catuneanu, O., 2006, Principles of Sequence Stratigraphy: Elsevier Science.

Cleveland, D.M., Atchley, S.C., and Nordt, L.C., 2007, Continental sequence stratigraphy of the Upper Triassic (Norian–Rhaetian) Chinle strata, Northern New Mexico, U.S.A.: Allocyclic and autocyclic origins of paleosol-bearing alluvial successions: Journal of Sedimentary Research, v. 77, no. 11, p. 909 –924, doi: 10.2110/jsr.2007.082.

Cleveland, D.M., Nordt, L.C., and Atchley, S.C., 2008, Paleosols, trace fossils, and precipitation estimates of the uppermost Triassic strata in northern New Mexico: Palaeogeography, Palaeoclimatology, Palaeoecology, v. 257, p. 421–444, doi: 10.1016/j.palaeo.2007.09.023.

Cornet, B., 1993, Applications and limitations of palynology in age, climatic and paleoenvironmental analysis of Triassic sequences in North America, *in* Lucas, S.G. and Morales, M. eds., The Nonmarine Triassic: New Mexico Museum of Natural History and Science Bulletin, p. 75–93.

Creber, G.T., and Ash, S.R., 2004, The Late Triassic Schilderia Adamanica and Woodworthia Arizonica trees of the Petrified Forest National Park, Arizona, USA: Palaeontology, v. 47, no. 1, p. 21–38, doi: 10.1111/j.0031-0239.2004.00345.x.

Dalrymple, M., 2001, Fluvial reservoir architecture in the Statfjord Formation (northern North Sea) augmented by outcrop analogue statistics: Petroleum Geoscience, v. 7, no. 2, p. 115–122, doi: 10.1144/petgeo.7.2.115.

Daugherty, L.H., 1941, The Upper Triassic flora of Arizona: Carnegie Institute of Washington Publication, v. 526, p. 1–108.

Deacon, M.W., 1990, Depositional analysis of the Sonsela Sandstone Bed, Chinle Formation, northeast Arizona and northwest New Mexico [Unpublished, M.S. Thesis]: Northern Arizona University, 127 p.

DeCelles, P.G., and Cavazza, W., 1999, A comparison of fluvial megafans in the Cordilleran (Upper Cretaceous) and modern Himalayan Foreland Basin systems: Geological Society of America Bulletin, v. 111, no. 9, p. 1315–1334, doi: 10.1130/0016-7606(1999)111<1315:ACOFMI>2.3.CO;2.

DeCelles, P.G., and Giles, K.A., 1996, Foreland basin systems: Basin Research, v. 8, no. 2, p. 105–123, doi: 10.1046/j.1365-2117.1996.01491.x.

Demko, T.M., 1995, Taphonomy of fossil plants in Petrified Forest National Park, Arizona: Southwest Paleontological Society and Mesa Southwest Museum, Mesa, AZ.

Demko, T.M., Dubiel, R.F., and Parrish, J., 1998, Plant taphonomy in incised valleys: implications for interpreting paleoclimate from fossil plants: Geology, v. 26, no. 12, p. 1119–1122.

Demko, T.M., and Gastaldo, R.A., 1992, Wetland environments of the Mary Lee Coal Zone Potsville Formation, Alabama: stacked clastic swamps and peat mires: Journal of Coal Geology, v. 20, p. 23–47.

Dickinson, W.R., 1981, Plate tectonic evolution of the southern Cordillera: Arizona Geological Society Digest, v. 14, p. 113–115.

Dickinson, W.R., 1989, Tectonic settings of Arizona through geologic time: Arizona Geological Society Digest, v. 17, p. 1–16.

Dickinson, W.R., 2004, Evolution of the North American Cordillera: Annual Review of Earth and Planetary Sciences, v. 32, p. 13–45, doi: 10.1146/annurev.earth.32.101802.120257.

Dickinson, W.R., and Gehrels, G.E., 2008, U-Pb ages of detrital zircons in relation to paleogeography: Triassic paleodrainage networks and sediment dispersal across southwest Laurentia: Journal of Sedimentary Research, v. 78, no. 12, p. 745 –764, doi: 10.2110/jsr.2008.088.

Dickinson, W.R., and Gehrels, G.E., 2009, Insights into North American paleogeography and paleotectonics from U–Pb ages of detrital zircons in Mesozoic strata of the Colorado Plateau, USA: International Journal of Earth Sciences, v. 99, no. 6, p. 1247–1265, doi: 10.1007/s00531-009-0462-0.

Dickinson, W.R., and Suczek, C.A., 1979, Plate tectonics and sandstone compositions: AAPG Bulletin, v. 63, no. 12, p. 2164–2182.

DiMichele, W.A., Pfefferkorn, H.W., and Gastaldo, R.A., 2001, Response of Late Carboniferous and Early Permian plant communities to climate change: Annual Review of Earth and Planetary Sciences, v. 29, no. 1, p. 461–487.

DiMichele, W.A., and Phillips, T.L., 1985, Arborescent lycopod reproduction and paleoecology in a coal-swamp environment of late Middle Pennsylvanian age (Herrin Coal, Illinois, USA): Review of Palaeobotany and Palynology, v. 44, no. 1-2, p. 1–26.

Donselaar, M.E., and Overeem, I., 2008, Connectivity of fluvial point-bar deposits: An example from the Miocene Huesca fluvial fan, Ebro Basin, Spain: AAPG Bulletin, v. 92, no. 9, p. 1109–1129, doi: 10.1306/04180807079.

Driese, S.G., and Mora, C.I., 2002, Paleopedology and stable-isotope geochemistry of Late Triassic (Carnian-Norian) paleosols, Durham Sub-basin, North Carolina, U.S.A.: implications for paleoclimate and paleoatmospheric pCO2, *in* Renault, R.W. and Ashley, G.M. eds., Sedimentation in Continental Rifts, SEPM Special Publication, SEPM, p. 207–218.

Dubiel, R.F., 1989, Sedimentology and revised nomenclature for the upper part of the Upper Triassic Chinle Formation and the lower Jurassic Wingate Sandstone, northwestern New Mexico and northeastern Arizona, *in* Anderson, O.J., Lucas, S.G., Love, D.W., and Cather, S.M. eds., New Mexico Geological Society, 40th Field Conference Guidebook, Southeastern Colorado Plateau, p. 213–223.

Dubiel, R.F., 1987, Sedimentology of the Upper Triassic Chinle Formation, Southeastern Utah: paleoclimatic implications: Journal of the Arizona-Nevada Academy of Science, v. 22, no. 1, p. 35–45.

Dubiel, R.F., 1994, Triassic deposystems, paleogeography, and paleoclimate of the Western Interior, *in* Caputo, M.V., Peterson, J.A., and Franczyk, K.L. eds., Mesozoic System of the Rocky Mountain Region, The Rocky Mountain Section (Society for Sedimentary Geology).

Dubiel, R.F., and Hasiotis, S.T., 2011, Deposystems, paleosols, and climatic variability in a continental system: the Upper Triassic Chinle Formation, Colorado Plateau, U.S.A., *in* From River To Rock Record: The preservation of fluvial sediments and their subsequent interpretation, SEPM Special Publication No. 97, SEPM, p. 393–421.

Dubiel, R.F., Hasiotis, S.T., and Demko, T.M., 1999, Incised valley fills in the lower part of the Chinle Formation, Petrified Forest National Park, Arizona: complete measured sections and regional stratigraphic implications of Upper Triassic rocks, *in* Santucci, V.L. and McClelland, L. eds., National Park Service Paleontological Research Volume 4, National Park Service Technical Report NPS/NRGRD/GRDTR -99/03, p. 78–84.

Dubiel, R.F., Parrish, J.T., Parrish, J.M., and Good, S.C., 1991, The Pangaean megamonsoon; evidence from the Upper Triassic Chinle Formation, Colorado Plateau: Palaios, v. 6, no. 4, p. 347–370.

Dubiel, R.F., and Skipp, G., 1992, Continental depositional environments and tropical paleosols in the Upper Triassic Chinle Formation, Eagle Basin, Western Colorado, *in* Flores, R.M. ed., SEPM 1992 Theme Meeting, Field Guidebook, p. 21–37.

Dury, G.H., 1964, Principles of underfit streams: US Government Printing Office.

Evert, R.F., and Eichhorn, S.E., 2004, Biology of Plants: W. H. Freeman.

Fielding, C.R., Ashworth, P.J., Best, J.L., Prokocki, E.W., and Smith, G.H.S., 2012, Tributary, distributary and other fluvial patterns: What really represents the norm in the continental rock record?: Sedimentary Geology, v. 261–262, no. 0, p. 15–32, doi: 10.1016/j.sedgeo.2012.03.004.

Fisher, J.A., Nichols, G.J., and Waltham, D.A., 2007, Unconfined flow deposits in distal sectors of fluvial distributary systems: Examples from the Miocene Luna and Huesca Systems, northern Spain: Sedimentary Geology, v. 195, no. 1–2, p. 55–73, doi: 10.1016/j.sedgeo.2006.07.005.

Folkoff, M.E., and Meentemeyer, V., 1987, Climatic control of the geography of clay minerals genesis: Annals of the Association of American Geographers, v. 77, no. 4, p. 635–650.

Friend, P.F., 1978, Distinctive features of some ancient river systems, *in* Miall, A.D. ed., Fluvial Sedimentology, Canadian Society of Petroleum Geologists, Memoir 5, p. 531–542.

Gastaldo, R.A., 1992, Regenerative growth in fossil horsetails following burial by alluvium: Historical Biology, v. 6, no. 3, p. 203–219, doi: 10.1080/10292389209380429.

Geddes, A., 1960, The alluvial morphology of the Indo-Gangetic Plain: Its mapping and geographical significance: Transactions and Papers (Institute of British Geographers), no. 28, p. 253–276, doi: 10.2307/621126.

Gehrels, G.E., Dickinson, W.R., and Riggs, N.R., 1993, Detrital zircon provenance link of the Chinle Formation and the Auld Lang Syne Group in Nevada: Geological Society of America, Abstracts with Programs, v. 25, p. 41.

Gibling, M.R., Tandon, S.K., Sinha, R., and Jain, M., 2005, Discontinuity-bounded alluvial sequences of the Southern Gangetic Plains, India: Aggradation and degradation in response to monsoonal strength: Journal of Sedimentary Research, v. 75, no. 3, p. 369–385, doi: 10.2110/jsr.2005.029.

Good, S.C., 1993, Molluscan paleobiology of the Upper Triassic Chinle Formation, Arizona and Utah [Ph.D. Dissertation]: University of Colorado, 276 p.

Good, S.C., and Dubiel, R.F., 1992, Architecture of fluvial sandstones of the Upper Triassic Chinle Formation, southeastern Utah: SEPM 1992 Theme Meeting, Mesozoic of the Western Interior, v. Abstracts with Program, p. 27.

Graham, J.R., 1983, Analysis of the Upper Devonian Munster Basin, an example of a fluvial distributary system, *in* Collinson, J.D. and Lewin, J. eds., Modern and Ancient Fluvial Systems, Blackwell Scientific Publications, Oxford, England, p. 473–483.

Gregory, S.V., Swanson, F.J., McKee, W.A., and Cummins, K.W., 1991, An ecosystem perspective of riparian zones: BioScience, v. 41, no. 8, p. 540–551.

Gubitosa, R., 1981, Depositional systems of the Moss Back Member: Chinle Formation, (Upper Triassic), Canyonlands, Utah: Northern Arizona University, 196 p.

Guccione, M.J., 1993, Grain-size distribution of overbank sediment and its use to locate channel positions, *in* M.rzo and Puigdefábregas, C. eds., Alluvial Sedimentation, Blackwell Publishing Ltd., p. 185–194.

Hampton, B.A., and Horton, B.K., 2007, Sheetflow fluvial processes in a rapidly subsiding basin, Altiplano plateau, Bolivia: Sedimentology, v. 54, no. 5, p. 1121–1148, doi: 10.1111/j.1365-3091.2007.00875.x.

Haq, B.H., Hardenbol, J., and Vail, P.R., 1988, Mesozoic and Cenozoic chronostratigraphy and cycles of sea level change, *in* Wilgus, C.K., Hastings, B.J., Posamentier, H.W., Van Wagoner, J.C., Ross, C.A., and Kendall, C.G.S.C. eds., Sea-level changes: An integrated approach, SEPM Special Publication, p. 71–108.

Hartley, A.J., Weissmann, G.S., Nichols, G.J., and Warwick, G.L., 2010, Large Distributive fluvial systems: Characteristics, distribution, and controls on development: Journal of Sedimentary Research, v. 80, no. 2, p. 167 –183, doi: 10.2110/jsr.2010.016.

Heckert, A.B., 2004, Late Triassic microvertebrates from the lower Chinle Group (Otischalkian-Adamanian: Carnian) southwestern U.S.A.: New Mexico Museum of Natural History and Science Bulletin, v. 27, p. 1–170.

Heckert, A.B., Lucas, S.G., Dickinson, W.R., and Mortensen, J.K., 2009, New ID-TIMS U-PB ages for Chinle Group strata (Upper Triassic) in New Mexico and Arizona, correlation to the Newark Supergroup, and implications for the "long Norian:" Geological Society of America: Abstracts with Programs, v. 41, no. 7, p. 123.

Hembree, D.I., and Hasiotis, S.T., 2007, Paleosols and ichnofossils of the White River Formation of Colorado: insight into soil ecosystems of the North American midcontinent during the Eocene-Oligocene transition: PALAIOS, v. 22, no. 2, p. 123–142, doi: 10.2110/palo.2005.p05-119r.

Hembree, D.I., and Nadon, G.C., 2011, A paleopedologic and ichnologic perspective of the terrestrial Pennsylvanian landscape in the distal Appalachian Basin, U.S.A.: Palaeogeography, Palaeoclimatology, Palaeoecology, v. 312, no. 1–2, p. 138–166, doi: 10.1016/j.palaeo.2011.10.004.

Hirst, J.P.., 1991, Variations in alluvial architecture across the Oligo-Miocene Huesca fluvial system, Ebro Basin, Spain, *in* Miall, A.D. and Tyler, N. eds., The Three Dimensional Facies Architecture of Terrigenous Clastic Sediments and Its Implications for Hydrocarbon Discovery and Recovery, SEPM Concepts in Sedimentology and Paleontology, p. 153–164.

Hirst, J.P.., and Nichols, G.J., 1986, Thrust tectonic controls on Miocene alluvial distribution patterns, southern Pyrenees, *in* Allen, P.A. and Homewood, P. eds., Foreland Basins, IAS Special Publication 8, p. 247–258.

Holbrook, J., and Schumm, S.A., 1999, Geomorphic and sedimentary response of rivers to tectonic deformation: a brief review and critique of a tool for recognizing subtle epeirogenic deformation in modern and ancient settings: Tectonophysics, v. 305, no. 1–3, p. 287–306, doi: 10.1016/S0040-1951(99)00011-6.

Horton, B.K., and DeCelles, P.G., 2001, Modern and ancient fluvial megafans in the foreland basin system of the central Andes, southern Bolivia: implications for drainage network evolution in fold-thrust belts: Basin Research, v. 13, no. 1, p. 43–63, doi: 10.1046/j.1365-2117.2001.00137.x.

Houghton, H.F., 1980, Refined techniques for staining plagioclase and alkali feldspars in thin section: Journal of Sedimentary Research, v. 50, no. 2, p. 629–631.

Irmis, R.B., and Mundil, R., 2008, New age constraints from the Chinle Formation revise global comparisons of Late Triassic vertebrate assemblages: Journal of Vertebrate Paleontology, v. 23, no. supplement to n. 3, p. 95A.

Johnsson, M.J., and Meade, R.H., 1990, Chemical weathering of fluvial sediments during alluvial storage; the Macuapanim Island point bar, Solimoes River, Brazil: Journal of Sedimentary Research, v. 60, no. 6, p. 827–842, doi: 10.1306/212F9296-2B24-11D7-8648000102C1865D.

Johnsson, M.J., and Stallard, R.F., 1989, Physiographic controls on the composition of sediments derived from volcanic and sedimentary terrains on Barro Colorado Island, Panama: Journal of Sedimentary Research, v. 59, no. 5, p. 768–781, doi: 10.1306/212F906B-2B24-11D7-8648000102C1865D.

Johnsson, M.J., Stallard, R.F., and Lundberg, N., 1991, Controls on the composition of fluvial sands from a tropical weathering environment: Sands of the Orinoco River drainage basin, Venezuela and Colombia: Geological Society of America Bulletin, v. 103, no. 12, p. 1622 –1647, doi: 10.1130/0016-7606(1991)103<1622:COTCOF>2.3.CO;2.

Kelly, S.B., and Olsen, H., 1993, Terminal fans—a review with reference to Devonian examples: Sedimentary Geology, v. 85, no. 1–4, p. 339–374, doi: 10.1016/0037-0738(93)90092-J.

Kent, D.V., and Muttoni, G., 2003, Mobility of Pangea: Implications for Late Paleozoic and early Mesozoic paleoclimate, *in* Letourneau, P.M. and Olsen, P.E. eds., The Great Rift Valleys of Pangea in Eastern North America; Volume 1: Tectonics, Structure, and Volcanism, Columbia University Press, New York, p. 11–20.

Klappa, C.F., 1980, Rhizoliths in terrestrial carbonates: classification, recognition, genesis and significance: Sedimentology, v. 27, no. 6, p. 613–629, doi: 10.1111/j.1365-3091.1980.tb01651.x.

Knowlton, F.H., 1889, New species of fossil wood (Araucarioxylon Arizonicum) from Arizona and New Mexico: National Museum Proceedings, v. 11, p. 1–4.

Kraus, M.J., 1987, Integration of channel and floodplain suites; II, Vertical relations of alluvial Paleosols: Journal of Sedimentary Research, v. 57, no. 4, p. 602–612, doi: 10.1306/212F8BB6-2B24-11D7-8648000102C1865D.

Kraus, M.J., 1996, Avulsion deposits in Lower Eocene Alluvial rocks, Bighorn Basin, Wyoming: Journal of Sedimentary Research, v. 66, no. 2, p. 354–363, doi: 10.1306/D4268347-2B26-11D7-8648000102C1865D.

Kraus, M.J., 1999, Paleosols in clastic sedimentary rocks: their geologic applications: Earth-Science Reviews, v. 47, no. 1–2, p. 41–70, doi: 10.1016/S0012-8252(99)00026-4.

Kraus, M.J., 2002, Basin-scale changes in floodplain paleosols: Implications for interpreting alluvial architecture: Journal of Sedimentary Research, v. 72, no. 4, p. 500–509, doi: 10.1306/121701720500.

Kraus, M., and Aslan, A., 1999, Palaeosol sequences in floodplain environments: a hierarchical approach: Special Publication – International Association of Sedimentologists, v. 27, p. 303–322.

Kraus, M.J., and Hasiotis, S.T., 2006, Significance of different modes of rhizolith preservation to interpreting paleoenvironmental and paleohydrologic settings: examples from Paleogene paleosols, Bighorn Basin, Wyoming, U.S.A.: Journal of Sedimentary Research, v. 76, no. 4, p. 633–646, doi: 10.2110/jsr.2006.052.

Kraus, M.J., and Middleton, L.T., 1987, Dissected paleotopography and base-level changes in a Triassic fluvial sequence: Geology, v. 15, no. 1, p. 18–21, doi: 10.1130/0091-7613(1987)15<18:DPABCI>2.0.CO;2.

Kraus, M.J., and Wells, T.M., 1999, Recognizing avulsion deposits in the ancient stratigraphical record, *in* Smith, N.D. and Rogers, J. eds., Fluvial Sedimentology VI, Special Publication of the International Association of Sedimentologists, Blackwell Publishing Ltd., p. 251–268.

Kutzbach, J.E., and Gallimore, R.G., 1989, Pangaean climates: megamonsoons of the megacontinent: Journal of Geophysical Research, v. 94, no. D3, p. PP. 3341–3357, doi: 198910.1029/JD094iD03p03341.

Larue, D.K., and Friedmann, F., 2005, The controversy concerning stratigraphic architecture of channelized reservoirs and recovery by waterflooding: Petroleum Geoscience, v. 11, no. 2, p. 131–146, doi: 10.1144/1354-079304-626.

Lawton, T.F., 1994, Tectonic setting of Mesozoic sedimentary basins, *in* Caputo, M.V., Peterson, J.A., and Franczyk, K.L. eds., Mesozoic Systems of the Rocky Mountain Region, Rocky Mountain Section Society for Sedimentary Geology (SEPM), Denver, Colorado, p. 1–25.

Leier, A.L., DeCelles, P.G., and Pelletier, J.D., 2005, Mountains, monsoons, and megafans: Geology, v. 33, no. 4, p. 289–292, doi: 10.1130/G21228.1.

LePage, B.A., and Pfefferkorn, H.W., 2000, Did ground cover change over geologic time?, *in* Gastaldo, R.A. and DiMichele, W.A. eds., Phanerozoic Terrestrial Ecosystems, Paleontological Society Papers, p. 171–182.

Long, R.A., and Padian, K., 1986, Vertebrate biostratigraphy of the Late Triassic Chinle Formation, Petrified Forest National Park, Arizona: preliminary results, *in* Padian, K. ed., The beginning of the Age of Dinosaurs: Faunal change across the Triassic-Jurassic boundary, Cambridge University Press, Cambridge, p. 161–169.

Lucas, S.G., 1998, Global Triassic tetrapod biostratigraphy and biochronology: Palaeogeography, Palaeoclimatology, Palaeoecology, v. 143, no. 4, p. 347–384, doi: 10.1016/S0031-0182(98)00117-5.

Marques, J.J., Schulze, D.G., Curi, N., and Mertzman, S.A., 2004, Major element geochemistry and geomorphic relationships in Brazilian Cerrado soils: Geoderma, v. 119, no. 3–4, p. 179–195, doi: 10.1016/S0016-7061(03)00260-X.

Martz, J.W., and Parker, W.G., 2010, Revised lithostratigraphy of the Sonsela Member (Chinle Formation, Upper Triassic) in the southern part of Petrified Forest National Park, Arizona: PLoS ONE, v. 5, no. 2, p. e9329, doi: 10.1371/journal.pone.0009329.

Marzolf, J.E., 1993, Sequence-stratigraphic relationships across the palinspastically reconstructed Cordilleran Triassic cratonal margin: New Mexico Museum of Natural History and Science Bulletin, v. 3, p. 331–343.

McBride, E.F., 1963, A classification of common sandstones: Journal of Sedimentary Research, v. 33, no. 3, p. 664 –669, doi: 10.1306/74D70EE8-2B21-11D7-8648000102C1865D.

McCarthy, P.J., Martini, I.P., and Leckie, D.A., 1997, Anatomy and evolution of a Lower Cretaceous alluvial plain: sedimentology and palaeosols in the upper Blairmore Group, south-western Alberta, Canada: Sedimentology, v. 44, no. 2, p. 197–220, doi: 10.1111/j.1365-3091.1997.tb01521.x.

Miall, A.D., 1978, Lithofacies types and vertical profile models of braided river deposits: a summary, *in* Miall, A.D. ed., Fluvial Sedimentology, Canadian Society of Petroleum Geologists, Memoir 5, p. 598–604.

Miall, A.D., 1985, Architectural-element analysis: a new method of facies analysis applied to fluvial deposits: Earth-Science Reviews, v. 22, p. 261–308, doi: 10.1016/0012-8252(85)90001-7.

Miall, A.D., 1996, The Geology of Fluvial Deposits: Sedimentary Facies, Basin Analysis, and Petroleum Geology: Springer.

Miall, A.D., 2006, Reconstructing the architecture and sequence stratigraphy of the preserved fluvial record as a tool for reservoir development: A reality check: AAPG Bulletin, v. 90, no. 7, p. 989–1002, doi: 10.1306/02220605065.

Millar, R.G., 2000, Influence of bank vegetation on alluvial channel patterns: Water Resources Research, v. 36, no. 4, p. 1109–1118, doi: 10.1029/1999WR900346.

Milliken, K.L., 2005, Late diagenesis and mass transfer in sandstone-shale sequences, *in* Mackenzie, F.T. ed., Sediments, Diagenesis, and Sedimentary Rocks, Elsevier-Pergamon, Amsterdam, p. 159–190.

Mohindra, R., Parkash, B., and Prasad, J., 1992, Historical geomorphology and pedology of the Gandak Megafan, Middle Gangetic Plains, India: Earth Surface Processes and Landforms, v. 17, no. 7, p. 643–662, doi: 10.1002/esp.3290170702.

Moore, D.M., and Reynolds, R.C.J., 1997, X-ray diffraction and the identification and analysis of clay minerals: Oxford University Press, USA.

Munsell® Soil Color Book 2009 Revised Edition.

Murata, K.J., 1940, Volcanic ash as a source of silica for the silicification of wood: American Journal of Science, v. 238, no. 8, p. 586–596, doi: 10.2475/ajs.238.8.586.

Murry, P.A., and Long, R.A., 1989, Geology and paleontology of the Chinle Formation, Petrified Forest National Park and vicinity, Arizona and a discussion of vertebrate fossils of the southwestern Upper Triassic, *in* Lucas, S.G. and Hunt, A.P. eds., Dawn of the age of dinosaurs in the American Southwest, New Mexico Museum of Natural History, Albuquerque, New Mexico, p. 29–64.

Nagtegaal, P.J.C., 1978, Sandstone-framework instability as a function of burial diagenesis: Journal of the Geological Society, v. 135, no. 1, p. 101–105, doi: 10.1144/gsjgs.135.1.0101.

Neglia, S., 1979, Migration of fluids in sedimentary basins: AAPG Bulletin, v. 63, no. 4, p. 573–597.

Nichols, G., and Fisher, J., 2007, Processes, facies and architecture of fluvial distributary system deposits: Sedimentary Geology, v. 195, p. 75–90, doi: 10.1016/j.sedgeo.2006.07.004.

Nordt, L.C., Atchley, S.C., and Dworkin, S., 2003, Terrestrial evidence for two greenhouse events in the latest Cretaceous: GSA Today, v. 13, no. 12, p. 4–9.

Nordt, L.C., and Driese, S.G., 2009, Hydropedological model of Vertisol formation along the Gulf Coast Prairie land resource area of Texas: Hydrol. Earth Syst. Sci., v. 13, no. 11, p. 2039–2053, doi: 10.5194/hess-13-2039-2009.

Nordt, L.C., and Driese, S.G., 2010a, A modern soil characterization approach to reconstructing physical and chemical properties of paleo-Vertisols: American Journal of Science, v. 310, no. 1, p. 37–64, doi: 10.2475/01.2010.02.

Nordt, L.C., and Driese, S.D., 2010b, New weathering index improves paleorainfall estimates from Vertisols: Geology, v. 38, no. 5, p. 407 –410, doi: 10.1130/G30689.1.

Nordt, L.C., Dworkin, S.I., and Atchley, S.C., 2011, Ecosystem response to soil biogeochemical behavior during the Late Cretaceous and early Paleocene within the western interior of North America: Geological Society of America Bulletin, v. 123, no. 9-10, p. 1745.

Nordt, L.C., Hallmark, C.T., Driese, S.G., Dworkin, S.I., and Atchley, S.C., 2012, Biogeochemical characterization of a lithified paleosol: implications for the interpretation of ancient critical zones: Geochimica et Cosmochimica Acta,.

Nordt, L.C., Wilding, L.P., Lynn, W.C., and Crawford, C.C., 2004, Vertisol genesis in a humid climate of the coastal plain of Texas, U.S.A.: Geoderma, v. 122, no. 1, p. 83–102, doi: 10.1016/j.geoderma.2004.01.020.

North, C.P., Nanson, G.C., and Fagan, S.D., 2007, Recognition of the sedimentary architecture of dryland anabranching (anastomosing) rivers: Journal of Sedimentary Research, v. 77, no. 11, p. 925–938, doi: 10.2110/jsr.2007.089.

Olsen, P.E., and Kent, D.V., 1996, Milankovitch climate forcing in the tropics of Pangaea during the Late Triassic: Palaeogeography, Palaeoclimatology, Palaeoecology, v. 122, p. 1–26, doi: 10.1016/0031-0182(95)00171-9.

Olsen, P.E., and Kent, D.V., 1999, Long-period Milankovitch cycles from the Late Triassic and Early Jurassic of eastern North America and their implications for the calibration of the Early Mesozoic time–scale and the long–term behavior of the planets: Philosophical Transactions of the Royal Society of London. Series A: Mathematical, Physical and Engineering Sciences, v. 357, no. 1757, p. 1761 – 1786, doi: 10.1098/rsta.1999.0400.

Pape, H., and Clauser, C., 2000, Variation of permeability with porosity in sandstone diagenesis interpreted with a fractal pore space model: Pure and Applied Geophysics, v. 157, no. 4, p. 603–619, doi: 10.1007/PL00001110.

Pape, H., Clauser, C., and Iffland, J., 1999, Permeability prediction based on fractal pore-space geometry: Geophysics, v. 64, no. 5, p. 1447–1460, doi: 10.1190/1.1444649.

Paredes, J.M., Foix, N., Colombo Piñol, F., Nillni, A., Allard, J.O., and Marquillas, R.A., 2007, Volcanic and climatic controls on fluvial style in a high-energy system: The Lower Cretaceous Matasiete Formation, Golfo San Jorge basin, Argentina: Sedimentary Geology, v. 202, no. 1–2, p. 96–123, doi: 10.1016/j.sedgeo.2007.05.007.

Parker, W.G., 2006, The stratigraphic distribution of major fossil localities in Petrified Forest National Park, Arizona: Museum of Northern Arizona Bulletin, v. 62, p. 46–61.

Parker, W.G., and Irmis, R.B., 2005, Advances in Late Triassic vertebrate paleontology based on new material from Petrified Forest National Park, Arizona: New Mexico Museum of Natural History and Science Bulletin, v. 29, p. 45–58.

Pfefferkorn, H.W., and Fuchs, K., 1991, A field classification of fossil plant substrate interactions: Neues Jahrbuch für Geologie und Paläontologie, Abhandlungen, v. 183, p. 17–36.

PiPujol, M.D., and Buurman, P., 1994, The distinction between ground-water gley and surface-water gley phenomena in Tertiary paleosols of the Ebro basin, NE Spain: Palaeogeography, Palaeoclimatology, Palaeoecology, v. 110, p. 103–113, doi: 10.1016/0031-0182(94)90112-0.

PiPujol, M.D., and Buurman, P., 1997, Dynamics of iron and calcium carbonate redistribution and palaeohydrology in middle Eocene alluvial paleosols of the southeast Ebro Basin margin (Catalonia, northeast Spain): Palaeogeography, Palaeoclimatology, Palaeoecology, v. 134, no. 1–4, p. 87–107, doi: 10.1016/S0031-0182(97)00076-X.

Pranter, M.J., Ellison, A.I., Cole, R.D., and Patterson, P.E., 2007, Analysis and modeling of intermediate-scale reservoir heterogeneity based on a fluvial point-bar outcrop analog, Williams Fork Formation, Piceance Basin, Colorado: AAPG Bulletin, v. 91, p. 1025–1051.

Prochnow, S.J., Atchley, S.C., Boucher, T.E., Nordt, L.C., and Hudec, M.R., 2006a, The influence of salt withdrawal subsidence on palaeosol maturity and cyclic fluvial deposition in the Upper Triassic Chinle Formation: Castle Valley, Utah: Sedimentology, v. 53, no. 6, p. 1319–1345, doi: 10.1111/j.1365-3091.2006.00821.x.

Prochnow, S.J., Nordt, L.C., Atchley, S.C., and Hudec, M.R., 2006b, Multi-proxy paleosol evidence for middle and late Triassic climate trends in eastern Utah: Palaeogeography, Palaeoclimatology, Palaeoecology, v. 232, p. 53–72, doi: 10.1016/j.palaeo.2005.08.011.

Ramezani, J., Hoke, G.D., Fastovsky, D.E., Bowring, S.A., Therrien, F., Dworkin, S.I., Atchley, S.C., and Nordt, L.C., 2011, High-precision U-Pb zircon geochronology of the Late Triassic Chinle Formation, Petrified Forest National Park (Arizona, USA): Temporal constraints on the early evolution of dinosaurs: Geological Society of America Bulletin, v. 123, no. 11-12, p. 2142–2159, doi: 10.1130/B30433.1.

Retallack, G.J., 1988, Field recognition of paleosols, *in* Reinhardt, J. and Sigleo, W.R. eds., Paleosols and Weathering Through Geologic Time: Techniques and Applications: Geological Society of America Special Paper, Geological Society of America, p. 181–200.

Retallack, G.J., 1991, Untangling the effects of burial alteration and ancient soil formation: Annual Review of Earth and Planetary Sciences, v. 19, p. 183–206, doi: 10.1146/annurev.ea.19.050191.001151.

Retallack, G.J., 1997, Dinos and dirt: Dinofest International Proceedings, p. 345–359.

Retallack, G.J., 2001, Soils of the Past: Wiley-Blackwell.

Retallack, G.J., 2005, Pedogenic carbonate proxies for amount and seasonality of precipitation in paleosols: Geology, v. 33, no. 4, p. 333, doi: 10.1130/G21263.1.

Riggs, N.R., Ash, S.R., Barth, A.P., Gehrels, G.E., and Wooden, J.L., 2003, Isotopic age of the Black Forest Bed, Petrified Forest Member, Chinle Formation, Arizona: An example of dating a continental sandstone: Geological Society of America Bulletin, v. 115, no. 11, p. 1315–1323, doi: 10.1130/B25254.1.

Riggs, N.R., Barth, A.P., Gonzalelz-Leon, C., Walker, J.D., and Wooden, J.L., 2009, Provenance of Upper Triassic strata in southwestern North America as suggested by isotopic analysis and chemistry of zircon crystals (abs.): Geological Society of America, Abstracts with Programs, v. 41, no. 7, p. 540.

Riggs, N.R., Lehman, T.M., Gehrels, G.E., and Dickinson, W.R., 1996, Detrital zircon link between headwaters and terminus of the Upper Triassic Chinle-Dockum paleoriver system: Science, v. 273, no. 5271, p. 97 –100, doi: 10.1126/science.273.5271.97.

Riggs, N.R., Mattinson, J.M., and Busby, C.J., 1993, Correlation of Jurassic eolian strata between the magmatic arc and the Colorado Plateau: New U-Pb geochronologic data from southern Arizona: Geological Society of America Bulletin, v. 105, no. 9, p. 1231–1246, doi: 10.1130/0016-7606(1993)105<1231:COJESB>2.3.CO;2.

Savidge, R.A., 2006, Xylotomic evidence for two new conifers and a ginkgo within the Late Triassic Chinle Formation of Petrified Forest National Park, Arizona, USA: Museum of Northern Arizona B, v. 62, p. 147–149.

Savidge, R.A., and Ash, S.R., 2006, Arboramosa semicircumtrachea, an unusual Late Triassic tree in Petrified Forest National Park, Arizona, USA: Museum of Northern Arizona Bulletin, v. 62, p. 65–81.

Schoeneberger, P.J., 2003, Field Book for Describing and Sampling Soils, Version 2.0 (D. A. Wysocki, E. C. Benham, & W. D. Broderson, Eds.): Natural Resources Conversation Service, National Soil Survey Center, Lincoln.

Schumm, S.A., 1963, A tentative classification of alluvial river channels: US Geological Survey.

Schumm, S.A., 1985, Patterns of alluvial rivers: Annual Review of Earth and Planetary Sciences, v. 13, p. 5–27.

Schumm, S.A., 1993, River response to baselevel change: Implications for sequence stratigraphy: The Journal of Geology, v. 101, no. 2, p. 279–294.

Scotese, C.R., 2007, Computer Animations: PALEOMAP Project: Arlington, Texas.

Shanley, K.W., and McCabe, P.J., 1994, Perspectives on the sequence stratigraphy of continental strata: AAPG Bulletin, v. 78, no. 4, p. 544–568.

Sheldon, N.D., and Retallack, G.J., 2001, Equation for compaction of paleosols due to burial: Geology, v. 29, no. 3, p. 247 –250, doi: 10.1130/0091-7613(2001)029<0247:EFCOPD>2.0.CO;2.

Shukla, U.K., Singh, I.B., Sharma, M., and Sharma, S., 2001, A model of alluvial megafan sedimentation: Ganga Megafan: Sedimentary Geology, v. 144, no. 3–4, p. 243–262, doi: 10.1016/S0037-0738(01)00060-4.

Sigleo, A., 1978, Organic geochemistry of silicified wood, Petrified Forest National Park, Arizona: Geochimica et Cosmochimica Acta, v. 42, p. 1397–1405, doi: 10.1016/0016-7037(78)90045-5.

Sigleo, A.C., 1979, Geochemistry of silicified wood and associated sediments, Petrified Forest National Park, Arizona: Chemical Geology, v. 26, no. 1–2, p. 151–163, doi: 10.1016/0009-2541(79)90036-6.

Singh, I.B., Parkash, B., and Gohain, K., 1993, Facies analysis of the Kosi megafan deposits: Sedimentary Geology, v. 85, p. 87–113.

Sinha, R., 1996, Channel avulsion and floodplain structure in the Gandak-Kosi interfan, north Bihar plains, India: Zeitschrift Fur Geomorphologie supplementband, p. 249–268.

Sinha, R., and Friend, P.F., 1994, River systems and their sediment flux, Indo-Gangetic plains, Northern Bihar, India: Sedimentology, v. 41, no. 4, p. 825–845, doi: 10.1111/j.1365-3091.1994.tb01426.x.

Sinha, R., Jain, V., Babu, G.P., and Ghosh, S., 2005, Geomorphic characterization and diversity of the fluvial systems of the Gangetic Plains: Geomorphology, v. 70, no. 3–4, p. 207–225, doi: 10.1016/j.geomorph.2005.02.006.

Smith, P.M.R., 1984, The use of fluorescence microscopy in the characterization of amorphous organic matter: Organic Geochemistry, v. 6, no. 0, p. 839–845, doi: 10.1016/0146-6380(84)90106-2.

Smith, N.D., Cross, T.A., Dufficy, J.P., and Clough, S.R., 1989, Anatomy of an avulsion: Sedimentology, v. 36, no. 1, p. 1–23, doi: 10.1111/j.1365-3091.1989.tb00817.x.

Soil Survey Staff, N., 1999, Soil Taxonomy: A Basic System of Soil Classification for Making and Interpreting Soil Surveys: Natural Resources Conservation Service.

Soil Survey Staff, 2011, Soil survey laboratory information manual, Soil Survey Investigations Report No. 5 (R. Burt, Ed.): USDA-NRCS, Washington, U.S. Government Printing Office.

Southard, R.J., Driese, S.G., and Nordt, L.C., 2011, Vertisols: Chapter 33.7, *in* Huang, P.M., Li, Y., and Sumner, M.E. eds., Handbook of Soil Science, 2nd Edition, CRC, Boca Raton, Florida, p. 33–82 to 33–97.

Stanistreet, I.G., and McCarthy, T.S., 1993, The Okavango Fan and the classification of subaerial fan systems: Sedimentary Geology, v. 85, no. 1, p. 115–133.

Stewart, J.H., 1969, Major Upper Triassic lithogenetic sequences in Colorado Plateau region: AAPG Bulletin, v. 53, no. 9, p. 1866–1879.

Stewart, J.H., Anderson, T.H., Haxel, G.B., Silver, L.T., and Wright, J.E., 1986, Late Triassic paleogeography of the southern Cordillera: The problem of a source for voluminous volcanic detritus in the Chinle Formation of the Colorado Plateau region: Geology, v. 14, no. 7, p. 567–570.

Stewart, J.H., Poole, F.G., and Wilson, R.F., 1972, Stratigraphy and origin of the Chinle Formation and related Upper Triassic strata in the Colorado Plateau region: US Geological Society Professional Paper, no. 690.

Stout, S.A., and Spackman, W., 1989, Notes on the compaction of a Florida peat and the Brandon lignite as deduced from the study of compressed wood: International Journal of Coal Geology, v. 11, no. 3–4, p. 247–256, doi: 10.1016/0166-5162(89)90117-1.

Surdam, R.C., and Boles, J.R., 1979, Diagenesis of volcanic sandstones: SEPM Special Publication 26.

Surdam, R.C., and Parker, R.D., 1972, Authigenic aluminosilicate minerals in the tuffaceous rocks of the Green River Formation, Wyoming: Geological Society of America Bulletin, v. 83, no. 3, p. 689, doi: 10.1130/0016-7606(1972)83[689:AAMITT]2.0.CO;2.

Tanner, L.H., 2003, Pedogenic features of the Chinle Group, Four Corners region; evidence of Late Triassic aridification: New Mexico Geological Society, Guidebook, 54th Field Conference, Geology of the Zuni Plateau,, p. 269–280.

Tanner, L.H., and Lucas, S.G., 2006, Calcareous paleosols of the Upper Triassic Chinle Group, Four Corners region, southwestern United States: Climatic implications: Geological Society of America Special Papers, v. 416, p. 53 –74, doi: 10.1130/2006.2416(04).

Taylor, T.N., Taylor, E.L., and Krings, M., 2008, Paleobotany, Second Edition: The Biology and Evolution of Fossil Plants: Academic Press.

Therrien, F., and Fastovsky, D.E., 2000, Paleoenvironments of Early Theropods, Chinle Formation (Late Triassic), Petrified Forest National Park, Arizona: Palaios, v. 15, no. 3, p. 194–211, doi: 10.1669/0883-1351(2000)015<0194:POETCF>2.0.CO;2.

Trendell, A.M., Atchley, S.C., and Nordt, L.C., 2012, Depositional and diagenetic controls on reservoir attributes within a fluvial outcrop analog: Upper Triassic Sonsela Member of the Chinle Formation, Petrified Forest National Park, Arizona: AAPG Bulletin, v. 96, no. 4, p. 679–707.

Vandenberghe, J., 2003, Climate forcing of fluvial system development: an evolution of ideas: Quaternary Science Reviews, v. 22, no. 20, p. 2053–2060, doi: 10.1016/S0277-3791(03)00213-0.

Vandenberghe, J., 2002, The relation between climate and river processes, landforms and deposits during the Quaternary: Quaternary International, v. 91, no. 1, p. 17–23, doi: 10.1016/S1040-6182(01)00098-2.

Vepraskas, M.J., 1992, Redoximorphic features for identifying aquic conditions: North Carolina Agricultural Research Service, Technical Bulletin, v. 301, p. 33.

Vepraskas, M.J., 1996, Redoximorphic features for identifying aquic conditions: N.C. Agricultural Research Service, N.C. State University.

Vepraskas, M.J., 2001, Morphological features of seasonally reduced soils, *in* Vepraskas, M.J. and Richardson, J.L. eds., Wetland soils: genesis, hydrology, landscapes, and classification, CRC Press, Boca Raton, p. 163–182.

Van der Voo, R., Mauk, F.J., and French, R.B., 1976, Permian-Triassic continental configurations and the origin of the Gulf of Mexico: Geology, v. 4, no. 3, p. 177 – 180, doi: 10.1130/0091-7613(1976)4<177:PCCATO>2.0.CO;2.

Weissmann, G.S., Hartley, A.J., and Nichols, G.J., 2011, Alluvial facies distributions in continental sedimentary basins - Distributive fluvial systems, *in* From River To Rock Record: The preservation of fluvial sediments and their subsequent interpretation, SEPM Special Publication No. 97, p. 327–355.

Weissmann, G.S., Hartley, A.J., Nichols, G.J., Scuderi, L.A., Olson, M., Buehler, H., and Banteah, R., 2010, Fluvial form in modern continental sedimentary basins: Distributive fluvial systems: Geology, v. 38, no. 1, p. 39 –42, doi: 10.1130/G30242.1.

Weller, J.M., 1959, Compaction of sediments: AAPG Bulletin, v. 43, p. 273–310.

Wells, N.A., and Dorr, J.A.J., 1987a, A reconnaissance of sedimentation on the Kosi alluvial fan of India, *in* Ethridge, F.G., Flores, R.M., and Harvey, M.D. eds., Recent Developments in Fluvial Sedimentology, Special Publication 39, Society of Economic Paleontologists and Mineralogists, SEPM, Tulsa, Oklahoma, p. 51–61.

Wells, N.A., and Dorr, J.A., 1987b, Shifting of the Kosi River, northern India: Geology, v. 15, p. 204–207.

Woody, D.T., 2006, Revised stratigraphy of the lower Chinle Formation (Upper Triassic) of Petrified Forest National Park, Arizona: Museum of Northern Arizona Bulletin, v. 62, p. 17–45.

Wright, V.P., 1992, Paleopedology, stratigraphic relationships and empirical models, *in* Martini, I.P. and Chesworth, W. eds., Weathering, soils and paleosols: developments in earth surface processes, Elsevier, Amsterdam, p. 475–499.

Wright, P.V., and Marriott, S.B., 1993, The sequence stratigraphy of fluvial depositional systems: the role of floodplain sediment storage: Sedimentary Geology, v. 86, no. 3–4, p. 203–210, doi: 10.1016/0037-0738(93)90022-W.

Zeigler, K.E., Kelley, S., and Geissman, J.W., 2008, Revisions to stratigraphic nomenclature of the Upper Triassic Chinle Group in New Mexico: Rocky Mountain Geology, v. 43, no. 2, p. 121 –141, doi: 10.2113/gsrocky.43.2.121.